

Nitrogen and phosphorus removal mechanisms in aerobic granular sludge sequencing batch reactor

By
SARVAJITH, M
LIFE 01201604006

Bhabha Atomic Research Centre, Mumbai, India

A thesis submitted to the
Board of Studies in Life Sciences
In partial fulfillment of requirements
for the Degree of
DOCTOR OF PHILOSOPHY
of
HOMI BHABHA NATIONAL INSTITUTE



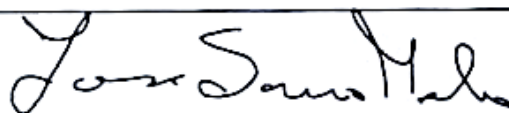
July 2021

Homi Bhabha National Institute¹

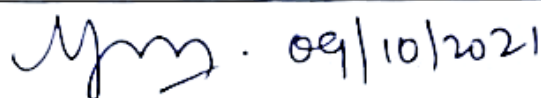
Recommendations of the Viva Voce Committee

As members of the Viva-Voce Committee, we certify that we have read the dissertation prepared by Mr. M. Sarvajith entitled "Nitrogen and phosphorus removal mechanisms in aerobic granular sludge sequencing batch reactor" and recommend that it may be accepted as fulfilling the thesis requirement for the award of Degree of Doctor of Philosophy.

Chairman – Prof. JS Melo



Guide / Convener – Prof. YV Nancharaiah

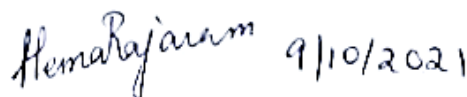
 . 09/10/2021

Examiner – Prof. S. Venkata Mohan



09/10/2021

Member 1- Prof. Hema Rajaram

 9/10/2021

Member 2- Prof. R Shashidhar

 9/10/21

Member 3- Prof. Celin Acharya

 09/10/2021

Final approval and acceptance of this thesis is contingent upon the candidate's submission of the final copies of the thesis to HBNI.

I/We hereby certify that I/we have read this thesis prepared under my/our direction and recommend that it may be accepted as fulfilling the thesis requirement.

Date: 09/10/2021
Place: Kalpakkam


Signature
Prof YV Nancharaiah

STATEMENT BY AUTHOR

This dissertation has been submitted in partial fulfillment of requirements for an advanced degree at Homi Bhabha National Institute (HBNI) and is deposited in the library to be made available to borrowers under rules of the HBNI.

Brief quotations from this dissertation are allowable without special permission, provided that accurate acknowledgement of source is made. Requests for permission for extended quotation from or reproduction of this manuscript in whole or in part may be granted by the Competent Authority of HBNI when in his or her judgment the proposed use of the material is in the interests of scholarship. In all other instances, however, permission must be obtained from the author.



Signature

Sarvajith, M

DECLARATION

I, hereby declare that the investigation presented in the thesis has been carried out by me. The work is original and has not been submitted earlier as a whole or in part for a degree / diploma at this or any other Institution / University.

A handwritten signature in black ink, appearing to read 'Sarvajith', written in a cursive style with a horizontal line through the middle.

Signature

Sarvajith, M

List of Publications arising from the thesis

Journal

1. “Granulation of the autochthonous planktonic bacterial community of seawater for saline wastewater treatment”, Sarvajith, M., Nancharaiah, Y. V. *RSC Environmental Science: Water Research & Technology*, **2020**, 6(7), 1902-1916.
2. “Biological nutrient removal by halophilic aerobic granular sludge under hypersaline seawater conditions” Sarvajith, M., Nancharaiah, Y. V, *Bioresource Technology*, **2020**, 318, 124065.
3. “Aerobic granular sludge for high-strength ammonium wastewater treatment: effect of COD/N ratios, long-term stability and nitrogen removal pathways”, Sarvajith, M., Reddy, G. K. K., Nancharaiah, Y. V. *Bioresource Technology*, **2020**, 306, 123150.
4. “Enhancing biological nitrogen and phosphorus removal performance in aerobic granular sludge sequencing batch reactors by activated carbon particles”, Sarvajith, M., Nancharaiah, Y. V. *Journal of Environmental Management*, **2021**, (under review).
5. “Differential enrichment of PAO clades: influence of carbon substrate and presence of charcoal particles”. Sarvajith, M., Nancharaiah, Y. V. *Bioresource Technology*, **2021**, (Submitted).

Chapters in books

1. “The EPS Matrix of Aerobic Granular Sludge”, Nancharaiah, Y. V., Sarvajith, M., Venugopalan, V. P. **2019**, *Microbial Biofilms in Bioremediation and Wastewater Treatment*, 33-65, ISBN 9781138626393.

Patent

1. “Method for bio-beads development for normal and saline wastewater treatment”. Nancharaiah, Y.V., Sarvajith, M., Reddy, G.K.K., Mohan, T.V.K., Venugopalan, V.P., Velmurugan, S. *Patent application 201921015793*, **2019**, India.

Conferences

1. Sarvajith. M., Y.V. Nancharaiah. “Beyond water reclamation: Prospective exploration of aerobic granular sludge microbes for novel metabolic functions”, Emerging applications of microbes, 2019, KU Leuven, Belgium, Europe. (Availed **HBNI international travel fund; IIM material endowment fund**).
2. Sarvajith. M., Y.V. Nancharaiah. “N- removal pathways of aerobic granular biomass”, Goldschmidt, 2018, Massachusetts, The United States of America. (Goldschmidt Abstracts, 2018, 1629). (Awarded **DST-ITS; Grant-USGS**).

3. Sarvajith. M., Y.V. Nancharaiah. "Aerobic granular biomass: an affluent stock of biopolymer", International Conference on Biotechnological Research and Innovation for Sustainable Development (BioSD), 2018, CSIR- ICT, Hyderabad, India.
4. Sarvajith. M., Y.V. Nancharaiah. "Selenium biomineralization in aerobic granular biomass", International Symposium on selenium Chemistry and Biology, 2017, Mumbai, India. (**ACS- Best Poster Award and SMC- Cash Award**).

Other publications

1. "Aerobic granular sludge for efficient biotransformation of chalcogen Se^{IV} and Te^{IV} oxyanions: Biological nutrient removal and biogenesis of Se⁰ and Te⁰ nanostructures". Nancharaiah, Y. V., Sarvajith, M., *Journal of Hazardous Materials*, **2022**, 422, 126833.
2. "Comparative performance of activated sludge and aerobic granular sludge sequencing batch reactors for removing metalloids Se^{IV/VI} oxyanions". Sarvajith, M., Nancharaiah, Y. V., *Journal of Hazardous Materials Letters*, **2021**, 100040.
3. "Development and performance of halophilic microalgae-colonized aerobic granular sludge for treating seawater-based wastewater". Rajitha, K*, Sarvajith*, M., Venugopalan, V.P., Nancharaiah, Y.V., *Bioresource Technology Reports*, **2020**, 100432. (*Equal contribution).
4. Aerobic granular sludge process: a fast-growing biological treatment for sustainable wastewater treatment. Nancharaiah, Y.V., Sarvajith, M., *Current Opinion in Environmental Science & Health*, **2019**, 12, 57-65.
5. Aerobic granular sludge: the future of wastewater treatment. Nancharaiah, Y.V., Sarvajith, M., Mohan, T.K., *Current Science*, **2019**, 117(3), 395.
6. Selenite reduction and ammoniacal nitrogen removal in an aerobic granular sludge sequencing batch reactor. Nancharaiah, Y. V., Sarvajith, M., Lens, P.N.L., *Water Research*, **2018**, 131, 131-141.
7. Textile dye biodecolourization and ammonium removal over nitrite in aerobic granular sludge sequencing batch reactors. Sarvajith, M., Reddy, G.K.K., Nancharaiah, Y.V., *Journal of Hazardous Materials*, **2018**, 342, 536-543.
8. 2,4-Dinitrotoluene removal in aerobic granular biomass sequencing batch reactors. Reddy, G.K.K., Sarvajith, M., Nancharaiah, Y.V., Venugopalan, V.P., *International Biodeterioration & Biodegradation*, **2017**, 119, 56-65.


Signature
Sarvajith, M

DEDICATIONS

न हि ज्ञानेन सदृशं पवित्रमिह विद्यते।


तत्स्वयं योगसंसिद्धः कालेनात्मनि विन्दति ॥

Translates as

In this world, there is nothing so sublime and pure as transcendental knowledge.

Such knowledge is the mature fruit of all mysticism.

The one who achieves, enjoys the eternal-self in passage of time.


Cheers to knowledge!

ACKNOWLEDGEMENTS

Finishing this thesis was in no means a one-man job. So many people have willingly or unwillingly contributed to my research, and wonderful discussions. I have had the pleasure to be surrounded by nice people. I hope that this writing will show how much I have been appreciating all your efforts!

Words aren't enough to describe the tenacious support and serenity. I owe it to you guys-my mom, dad, and sis who made it possible this far.

YV Nancharaiah, fantabulous PhD mentor, I really like, appreciate your enthusiasm, and energy. I'll miss our early morning meet-chat-discussions. I think we could borrow hours to 24. Cheers to you!

The doctoral committee (Prof. s'), VP Venugopalan, JS Melo, Hema Rajaram, R Shashidhar, and Celin Acharya. for their insightful comments and encouragement, but also for the hard question which incited me to widen my research perspectives. Special thanks to Hema Rajaram for being there always to support from administration.

I also need to thank all my colleagues over the years. There are too many to name you all, but I would like to thank Rajitha, Velraj, Saitya, Uday, my friends and batchmates, to whom I could rely on. A big part of my time I have spent on quality debates and culinary with Suman, who was always there for anything. I Always enjoy startling with Darpan, do cherish the moments with him & his family. I introduce these two as rare engineers, of course they are! both good by heart and best mates.

The timely support is critical & cannot be overlooked. A humble gratitude to (Prof. s') TV Krishna Mohan, R Rangarajan, S Velmurugan, Head, WSCD. A great thanks to bio-group (Prof. s'/Dr.s') TS Rao, Hiren (Specially), S Murthy, Kiran, Padma, Atif, Sudhir, Malathy. A big part of my time I spent working with pilot and full-scale SBR projects. So exclusive acknowledgements to George for all his help with big SBRs and Veeramani, from seawater to recent biofilter work. An extra mile with instrumentation facility is of great need. Thanks to (Dr. s') R. Pandian, Magadupathy, R Pushpalatha, (late) Sathyasheelan.

My stay at laboratory and at enclave have been always cherishing, I appreciate the support from staff, seniors, juniors, mentees (D Nandini, S Niveditha, J Shyni, G Sudharsan) from WSCD, BARC, Dean, student affairs and staffs from IGCAR, Abhinash-my roommate, friends from enclave.

I sincerely thank the department of Atomic Energy, for research fellowship. HBNI, IIM, DST, USGS for grants and ACS, RSC, SMC, Geochemical society for research recognition and awards.


Sarvajith, M

CONTENTS

Summary.....	x
List of figures.....	xii
List of tables.....	xiv
Chapter 1 General Introducton	1
1.1 Background.....	2
1.2 N and P biogeochemical cycles	3
1.3 Nitrogen and phosphorus: Current status and future trends	5
1.3.1 Phosphorus concern.....	7
1.3.2 Environmental significance	7
1.4 Prospects for removal and recovery of lost nutrients	8
1.4.1 Advancements in nutrient removal and recovery	9
1.4.2 Biological wastewater treatment	10
1.5 Aerobic granular sludge for wastewater treatment.....	12
1.5.1 Nitrogen and Phosphorus removal	13
1.5.2 Aerobic granular sludge formation.....	14
1.5.3 Effect of Salinity on granular stability and biological nutrient removal.....	16
1.6 Overall objectives of the thesis.....	17
1.6.1 Thesis outline	18
Chapter 2 Biological nutrient removal by AGS at high ammonium concentrations	21
2.1 Introduction	23
2.2 Materials and methods.....	24
2.2.1 Source of biomass	24
2.2.2 Synthetic wastewater.....	25
2.2.3 SBR setup and operation	25
2.2.4 High-strength ammoniacal-N removal	26
2.2.5 Microscopy	28
2.2.6 Genomic DNA extraction.....	28
2.2.7 Bacterial community analysis using 16S rRNA gene sequencing	28
2.2.8 Quantitative PCR.....	29
2.2.9 Analytical methods	29
2.3 Results and discussion	30
2.3.1 Cultivation of aerobic granular sludge from activated sludge inoculum	30
2.3.2 Nutrient removal performance	31
2.3.3 Nitrogen removal capabilities	32
2.3.4 Microbial community	36
2.3.5 Granular stability at lower COD/N ratios.....	39
2.3.6 Nitrogen removal mechanisms	41
2.4 Conclusions	44
Chapter 3 Granulation and enrichment of N and P removing organisms in the presence of charcoal particle	45
3.1 Introduction	47
3.2 Materials and methods.....	49
3.2.1 Source of biomass	49
3.2.2 Simulated wastewater.....	49
3.2.3 Coconut charcoal particles preparation	49

3.2.4 SBR setup and operation.....	50
3.2.5 Effect of carbon source on granulation.....	50
3.2.6 Effect of CSC particles on granulation.....	51
3.2.7 Analytical methods.....	51
3.2.8 Extracellular polymeric substances (EPS) matrix.....	53
3.2.9 Microbial community analysis.....	54
3.3 Results and discussion.....	55
3.3.1 Effect of carbon substrate on granulation and nutrient removal.....	55
3.3.2 Granulation and nutrient removal in the presence of CSC particles.....	60
3.3.3 Bacterial community composition of granules cultivated without and with CSC addition.....	65
3.3.4 Granulation mechanisms.....	70
3.4 Conclusions.....	72
Chapter 4.. Understanding the effect of charcoal-augmentation on biological N and P removal in aerobic granular sludge reactor.....	- 73 -
4.1 Introduction.....	75
4.2 Materials and methods.....	77
4.2.1 Source of biomass.....	77
4.2.2 Sorting of biomass based on size and type.....	77
4.2.3 Nutrient removal by different size groups.....	77
4.2.4 Nutrient removal by granule subtypes.....	78
4.2.5 P removal at different P/C ratios.....	78
4.2.6 Effect of salinity on nutrient removal.....	79
4.2.7 DNA extraction.....	79
4.2.8 qPCR.....	79
4.2.9 Polyphosphate staining using DAPI.....	80
4.2.10 Analytical methods.....	80
4.3 Results and Discussion.....	80
4.3.1 Prelude.....	80
4.3.2 Coexistence of granule subtypes.....	81
4.3.3 EBPR biochemical conversions.....	85
4.3.4 Effect of influent P/C ratios.....	89
4.3.5 Impact of salinity on PAO clades.....	90
4.3.6 Implications.....	92
4.4 Conclusions.....	93
Chapter 5 <i>De novo</i> granulation of native seawater microorganisms for biological Nitrogen and phosphorus removal under saline conditions.....	95
5.1 Introduction.....	97
5.2 Material and methods.....	98
5.2.1 Nutrient amended seawater.....	98
5.2.2 Cultivation of halophilic aerobic granular sludge (hAGS).....	98
5.2.3 Nutrient removal capabilities at different salinities.....	99
5.2.4 Characterisation of halophilic aerobic granular sludge.....	99
5.2.5 Genomic DNA extraction and bacterial community analysis.....	100
5.2.6 Nutrient analysis.....	101
5.3 Results and discussion.....	101
5.3.1 C, N and P removal from synthetic saline wastewater.....	101
5.3.2 C, N and P removal at different salinities.....	106
5.3.3 Bacterial community analysis.....	108
5.3.4 Granulation of autochthonous planktonic microbial community.....	111

5.4 Conclusions	117
Chapter 6 Evaluating biological nitrogen and phosphorus removal at hypersalinities.....	119
6.1 Introduction	121
6.2 Material and methods	122
6.2.1 Nutrient amended seawater	122
6.2.2 Cultivation of halophilic aerobic granular sludge (hAGS)	122
6.2.3 Nutrient removal from hypersaline seawater-based wastewater	122
6.2.4 Microscopy	123
6.2.5 Genomic DNA extraction and bacterial community	123
6.2.6 Extracellular polymeric substances (EPSs) matrix of hAGS	123
6.2.7 Analytical methods	124
6.3 Results and discussion	124
6.3.1 Nutrient removal from hypersaline seawater-based wastewater	125
6.3.2 Properties of halophilic aerobic granular sludge	133
6.3.3 EPSs matrix of hAGS	134
6.3.4 Bacterial community	135
6.3.5 Halotolerant <i>versus</i> halophilic granular sludge	138
6.4 Conclusions	139
Chapter 7 Major findings and future research directions	141
7.1 Major findings	142
7.2 Recommendations for future investigations	145
References	148
Epilogue.....	157
Appendix I.....	158
A1 Standard curve preparation	161
Appendix II.....	162
Published papers	163

SUMMARY

Aerobic granular sludge (AGS) process is increasingly considered for sustainable biological wastewater treatment. Cultivation of AGS, establishment of nitrogen (N) and phosphorous (P) removal pathways, long-term stability are key aspects for the successful implementation of AGS process in wastewater treatment plants. This study was focused on cultivation of AGS, establishment of effective N and P removal pathways under different process and tropical climate conditions while deciphering the mechanisms.

Aerobic granules were gradually exposed to increasing ammonium concentrations during 440 days of sequencing batch reactor (SBR) operation, to evaluate granular stability at lower COD/N ratios and to determine suitability for treating high-strength ammonium wastewater. Near complete removal of as high as 4000 mg L⁻¹ ammonium-nitrogen was efficiently achieved within 24 h batch comprising of anaerobic and aerobic phases, suggesting suitability for treating ammonium-rich wastewaters. A reduction in microbial diversity in the granules was observed with an increase in ammonium concentrations due to selection of certain bacterial groups. Nitrifying-, anammox- and denitrifying-bacteria were enriched in the granules. However, nitrite oxidizing bacteria were completely eliminated at lower COD/N ratios and tropical climate (>25 °C) conditions. This has resulted in occurrence of energy efficient nitrogen removal pathways like nitrification-denitrification and anammox. However, these pathways accounted partly for explaining ammonium removal mechanisms, indicating presence of unknown pathways. Moreover, phosphorus removal was found to be limited at 40% and achieved mainly by simple biological P (bio-P) removal for meeting cellular requirements.

In order to improve granulation and nutrient (especially P) removal, granulation of activated sludge was studied in the presence of charcoal particles in SBRs using different carbon sources, namely acetate, propionate, and acetate-propionate. The rate of granulation of activated sludge was higher in SBRs in the presence of charcoal particles using acetate or acetate-propionate. Enhancement of

granulation was facilitated by minimizing biomass washout, formation of particulate biofilms and increased inter-particle interactions. Addition of charcoal particles essentially decreased the start-up periods for appearance of granules and establishment of N and P removal pathways. Bio-P removal via enhanced bio-P removal (EBPR) was rapidly established in the biomass formed in the presence of charcoal. Both formation of granules and enrichment of functional N and P removing bacteria were shaped up by charcoal and carbon substrate. Differential enrichment of polyphosphate accumulating organism (PAO) clades was observed in the biomass developed using either acetate (PAO clade I) or acetate-propionate (PAO clades I and II). Interestingly, the biofilms contained higher abundance of PAO clades and performed EBPR, but not the co-existing granules, suggesting segregation of functional microorganisms. These findings were in support of attachment and growth of PAOs in the biofilms early on during granulation. But, the nutrient removal by EBPR biomass was severely inhibited at moderate salinities (2 to 10 ppt), necessitating development of alternative approaches for biological treatment under saline conditions.

For achieving nutrient removal under saline conditions, a completely different approach that is granulation of halophilic microbes present in the seawater was investigated without using inoculum. This new approach enabled rapid granulation of halophilic microorganisms of seawater (34 ppt) resulting in halophilic AGS (hAGS) which showed efficient ammonium, total nitrogen and phosphorus removal at 34 ppt. Subsequent studies revealed that hAGS was stable and performed efficient nutrient removal at salinities ranging from 17 ppt to 120 ppt. Under these saline to hypersaline conditions, ammonium and phosphorus were removed biologically via nitrification-denitrification and EBPR pathways, respectively. The developed hAGS matrix was dominated by acid-soluble exopolymer, likely responsible for conferring stability under saline conditions. Cultivation of hAGS from autochthonous halophilic microorganisms proves to be a promising approach for achieving biological N and P removals from hypersaline seawater-based wastewaters.

LIST OF FIGURES

Fig. 1.1. Major transformations in the nitrogen biogeochemical cycle.	3
Fig. 1.2. Schematic diagram showing biogeochemical cycle of phosphorus..	5
Fig. 1.3. Global phosphorus reserves and current status.....	7
Fig. 1.4. Schematic diagram of activated sludge process.	11
Fig. 1.5. Schematic representation of bioreactor and operational pahses in SBR	12
Fig. 1.6. Morphology of activated sludge and granular sludge.	13
Fig. 1.7. Proposed mechanism of aerobic granular sludge formation.	15
Fig. 1.8. Blueprint of the tailored approaches of saline wastewater treatment.....	17
Fig. 1.9. Thesis outline showing the connections between the individual chapters.	18
Fig. 2.1 Time course of granulation of activated sludge in SBR.....	30
Fig. 2.2 Time course of nutrient removal performace of AGS in SBR	32
Fig. 2.3 Nitrogen removal capabilities of AGS to high ammonium concentrations.....	34
Fig. 2.4. Ammonium removal kinetics in an SBR cycle at lower COD/N ratios.....	34
Fig. 2.5. Phosphorus removal performance at high ammonium concentrations	36
Fig. 2.6 Bacterial community structure of AGS at lower COD/N ratios.....	37
Fig. 2.7. qPCR results showing organisms involved in nitrogen metabolsim.	39
Fig. 2.8 Granular sludge propeties while treating at COD/N ratios (18.3 to 0.13).....	40
Fig. 2.9 Morphology of granular sludge at high and low COD/N ratios.....	40
Fig. 2.10 Proposed biological nitrogen removal pathways in AGS.....	44
Fig. 3.1. Granulation of activated sludge with different carbon substrate.....	56
Fig. 3.2. MLSS, settling properties (SVI) of AGS fed with different carbon sources.....	57
Fig. 3.3. Nutrient removal performance of AGS fed with different carbon sources.	59
Fig. 3.4. Nutrient removal kinetics of AGS fed with different carbon sources..	60
Fig. 3.5. Granulation of activated sludge in presence of CSC particles and with different carbon sources.....	61
Fig. 3.6. Changes in biomass properties in presence of CSC particles and carbon sources.	62
Fig. 3.7. Nutrient removal performance of AGS cultivated with CSC and fed with different carbon sources.....	63
Fig. 3.8. Nutrient removal kinetics of charcoal AGS AGS cultivated with CSC and fed with different carbon sources.....	64

Fig. 3.9. Changes in bacterial community composition of AGS with and without CSC and different carbon substrate.	67
Fig. 3.10. Prominent functional bacteria observed in AGS cultivated with CSC.	68
Fig. 3.11. Gelation properties of Alginate-like exopolymer (ALE) from AGS with CSC....	69
Fig. 3.12. Mechanism of formation of AGS in SBRs fed with different carbon substrate ...	71
Fig. 3.13. Schematics of formation of AGS with CSC.	72
Fig. 4.1. Phosphorus removal profiles of AGS cultivated with HAc and HAc-HPr.....	82
Fig. 4.2. Phosphorus removal profiles exhibited by granules and biofilms	83
Fig. 4.3. Abundance of PAO clades and microorganisms of nitrogen removal in AGS.....	84
Fig. 4.4. Kinetics of carbon utilization and phosphorus in biofilms.	86
Fig. 4.5. Microscopic visualization of DAPI stained poly-P in AGS.	88
Fig. 4.6. Proposed nitrogen and phosphorus removal mechanisms in co-existing granules and biofilms.....	89
Fig. 4.7. Phosphorus removal performance of biofilms at different influent P/C ratios.	90
Fig. 4.8. Nutrient removal performance of biofilms under saline conditions	92
Fig. 4.9. Abundance of PAO clade IA and clade IIE when subjected to different salinities.	92
Fig. 5.1. Nutrient removal performance of halophilic AGS under saline conditions.....	103
Fig. 5.2 Batch experiments to assess abiotic nutrient removal under saline condition	106
Fig. 5.3. Nutrient removal performance of hAGS at varying salinities from 34 to 17 ppt.	107
Fig. 5.4. Bacterial community of seawater and hAGS	108
Fig. 5.5. Microbial growth and retention during the initial days of granulation.....	111
Fig. 5.6. Microscopic observations of aggregate formation under saline conditions.....	109
Fig. 5.7. Time course granulation of hAGS using seawater microorganisms.....	110
Fig. 5.8. Morphological features and characterisation of hAGS for inorganic content.	116
Fig. 5.9. Proposed mechanism of <i>de novo</i> granulation.	117
Fig. 6.1. Nutrient removal performance of hAGS in presence of nitrate and ammonium ..	131
Fig. 6.2 Nutrient removal performance of hAGS at hypersalinity (34 to 120 ppt).	132
Fig. 6.3 Changes in morphology of hAGS at hypersalinity.....	133
Fig. 6.4 Bacterial community of hAGS treating hypersaline seawater-based wastewater..	137

LIST OF TABLES

Table 2.1 Nitrogen removal performance of AGS at different concentrations of influent ammonium.	33
Table 2.2 List of microorganisms related to nitrogen removal pathways identified in the AGS treating high strength ammonium concentrations.....	38
Table 4.1. Comparison of EBPR conversions observed in the biofilms with the published reports.	87
Table 5.1. Nutrient removal performance and properties of AGS at 34 ppt.....	102
Table 5.2 Functional bacteria detected in the hAGS formed from seawater microbes.	110
Table 5.3 Properties of hAGS formed from seawater microbes.....	113
Table 5.4 Concentration of metal ions in the influent, effluent and hAGS.....	115
Table 6.1 Nitrogen removal performance of hAGS at 34 ppt.....	125
Table 6.2 Nutrient removal performance of hAGS treating hypersaline seawater-based wastewater.....	126
Table 6.3 Characteristics of hAGS treating hypersaline seawater-based wastewater.	128

Chapter 1

General introduction

1.1 Background

Being components of building blocks of different biomolecules of intermediary metabolism, heredity (nucleotides and nucleic acids), cell membranes (phospholipids), and cytoplasmic solutes, nitrogen (N) and phosphorus (P) are essential for the growth and maintenance of all living organisms. Nitrogen and phosphorus play critical roles in plant growth and thus, important components of chemical fertilizers and heavily used in modern agriculture for securing food supply¹. Nitrogen is present abundantly (78%) in atmosphere in a highly stable form. But its content in soil is limited. In order to increase its availability in soil, nitrogen is fixed in the forms such as ammonia, nitrate and amino acids. The nitrogen required for making chemical fertilizers is met mainly by chemically converting N_2 to NH_3 using fossil fuel as energy source².

On the other hand, the phosphorus problem is more severe and related to its limited natural abundance due to its non-renewable nature. Igneous and sedimentary deposits in the Earth's crust are most common form of phosphorus. Mining of these rocks has been the most commercially viable method for meeting phosphorus demand of chemical fertilizers. Using the current rate of mining for meeting the phosphorus demand, the "readily exploitable" sources of phosphorus are likely to be depleted within the next 100 years³. Moreover, as these quality phosphorus reserves gets exhausted, it may be become necessary to shift to low-grade P sources.

1.2 N and P biogeochemical cycles

Nitrogen pools on Earth are distributed largely as atmospheric molecular nitrogen (N_2) and (biologically) reactive nitrogen such as NH_4^+ , NO_3^- , and organic nitrogen⁴. The biological nitrogen cycle mainly consists of transformations within the reactive nitrogen pool, with in- and out-flow between reactive nitrogen and atmospheric N_2 pools. Inter-conversions between these two large nitrogen pools are mainly controlled by two microbial processes, i.e., nitrogen fixation and denitrification⁴. Figure 1 depicts the five important stages in the nitrogen cycle such as (i) fixation ($N_2+8H^++8e^-\rightarrow 2NH_3+H_2$), (ii) ammonification (organic-N $\rightarrow NH_4^+$), (iii) nitrification ($NH_4^++2O_2\rightarrow NO_3^-+2H^++H_2O$), (iv) assimilation (proteins/nucleic acids), and (v) denitrification ($NO_3^-+10e^-+12H^+\rightarrow N_2+6H_2O$). The transformation of nitrogen in different oxidation states (-3 to +5) is key to productivity in the biosphere, mediated by the metabolic activities of diverse microbial assemblages (Fig. 1.1).

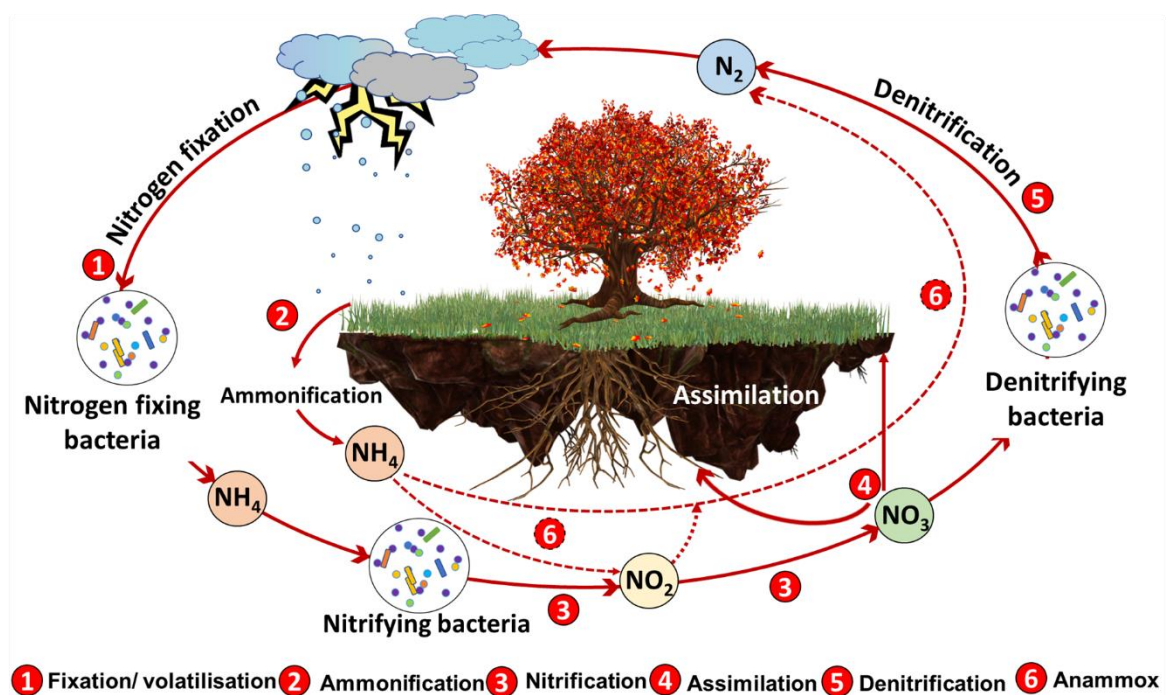


Fig. 1.1. Major transformations in the nitrogen biogeochemical cycle.

Increased urbanization and industrialization, however, forces intensive agriculture that locally distort the natural balance of the nitrogen cycle and causing accumulation of nitrogenous compounds (ammonia and nitrate) in rivers and lakes. Typical nitrogen-containing wastewaters include municipal wastewater, landfill leachate, abattoir wastewater, livestock farm wastewater and fertilizer industry effluents. To mitigate the anthropogenic influence on the N pool balance, biological processes of the nitrogen cycle are beneficially used to minimize the release and accumulation of ammonia and nitrate.

Phosphorus is a lithophile element present in the rocks⁵. The phosphate rock (PR) occurs in both sedimentary and igneous deposits in the Earth's crust. About 80 to 90% of PR used in chemical fertilizers is obtained from sedimentary deposits which are formed in marine continental shelf. Phosphorus biogeochemical cycle is a slow process compared to nitrogen cycling (Fig. 1.2). The inorganic P compounds used by living organisms include orthophosphate, pyrophosphate, and other condensed phosphates (phosphite, hypophosphite, and phosphine). The P forms are either used as P sources for synthesizing organic-P biomolecules, energy generation or forming metabolic by-products (e.g., phosphine (PH₃)). Organic P compounds contain C–O–P and C–P bonds which are formed by enzymes using inorganic P sources. Phosphorus, in general exists collectively with other elements due to its high-reactivity. Hence, microorganisms increase P bioavailability in environmental settings by solubilisation and releasing soluble phosphate (ortho-P).

Much of the phosphorus available in the Earth is tied up in PR and released by leaching, and mining. The released P passes through aquatic and terrestrial ecosystems *via* plants, predators to be returned back by death and decay (Fig. 1.2). Considerable amount of the released P is deposited in the shallow sediments, or in deep oceans, where it rarely wells up. Release and loss of P due to erosion or anthropogenic factors into surface waters affects the natural phosphorus cycle⁶. Of the 80% of the mined P applied to agricultural fields, only 40% is

utilised by crops. About 16% of this 40% fixed in the crops is only consumed by humans. However, all of the P consumed (16% of the mined P) by humans is released as waste and finds its way into sewers^{6,7}. The other largest flows of the lost P are in soil erosion and agricultural run-off (46% of mined P), which is a non-point source. Therefore, municipal wastewater represents a potential sink for lost P, a potential secondary P source.



Fig. 1.2. Schematic diagram showing biogeochemical cycle of phosphorus. Phosphorus is lost from mines (2) to fertilizers (3) to livestock (4) and humans (4). Soil erosion and runoff are the major non-point sources (46% of the mined P). Whereas animal waste and domestic wastewater (40% and 16% of total mined P) are major point sources.

1.3 Nitrogen and phosphorus: Current status and future trends

Most of the naturally occurring reactive **nitrogen** (100–300 Tg (teragram) N/year globally) originates from biological fixation (98%) and to a lesser extent from lightning (2%)⁸. However, reactive nitrogen generated by natural processes is insufficient to meet the food production demand of increasing population. Therefore, anthropogenic production of ammonia-nitrogen became essential for fertilizers. Haber-Bosch process that converts atmospheric N₂ to NH₃ using fossil fuel as the energy source is a major source for meeting

the nitrogen requirement of chemical fertilizers⁶. Annually 4 Tg (out of 170 Tg) of the applied reactive nitrogen is accumulated in the plants and the rest is lost to the environment⁹. About 2% of global reactive nitrogen escapes as N₂O contributing to the global warming⁹. About 12% of total nitrogen escapes as NO_x and NH₃¹¹. Hence, the climate change pattern and nitrogen interactions may impact agricultural productivity due to the elevated ozone levels, and changing environmental conditions like extreme rainfall, flooding, drought, and heat.

The major source of **phosphorus** from PR is mined by open pit or open cast mining techniques. Majority of PR deposits are processed by underground mining in China, Russia and other countries. Currently, the world PR reserves accounts to 69 BT (billion tonne) PR, of which, Morocco and western Sahara holds 72% reserves¹² (Fig. 1.3A). China currently holds about 3200 MT (metric tonne) PR reserve (4.6% of the world P). Though the total global P resources are estimated to be 300 BT, a major part of it is not attractive for extraction with current economic and technological conditions. North Africa (Morocco and Western Sahara), from its huge amount of reserves, has the highest PR exports (up to 60%) to other regions in the world (Fig. 1.3B). South Asia, including India meets up to 86% of its P demand from imports (Fig. 1.3B), due to lower mining, high consumption, or poor-quality reserves¹².

The future trend of PR production and consumption is highly debated. The world's population has been increasing exponentially over the last 50 years, adding between 70 and 87 million people annually¹⁴. Thus, requirement of chemical fertilizers is steadily increasing for meeting food production demand (Fig. 1.3C). Since 1990s, the population rate has been more stable, between 77 and 81 million people annually. However, UN forecasted a decline in the annual population growth rate in the coming years. If the current level of per capita PR production rate is applied to the UN projected population, the reserves would last until 2315 and not 2035 (*peak phosphorus*) as predicted by Cordell¹⁵ (Fig. 1.3D). However, if the population growth rate continues to stay similar, then it is expected to last until 2170¹⁶.

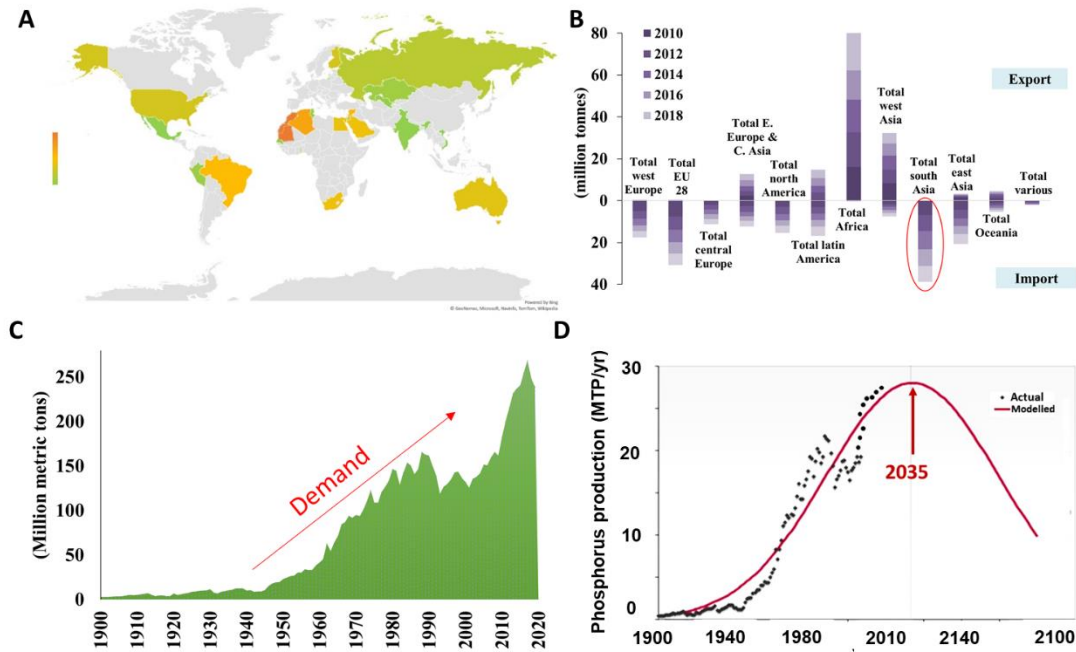


Fig. 1.3. Global phosphorus reserves as on 2020 (China not shown) (A), historic phosphorus regional import/export (B) and demand (C). Phosphorus peak curves illustrating global peak phosphorus after which production will be significantly reduce. Data D is adapted from Cordell et al.¹³

1.3.1 Phosphorus concern

There are reasons to be concerned due to (i) limited availability of PR deposits, (ii) non-renewable nature of PR deposits, (iii) uneven distribution, and (iv) geopolitical issues. The uneven global distribution of reserves, and population growth may induce unprecedented international tensions. Therefore, society must modify the current wasteful practices of P resources and manage P to avoid environmental problems.

1.3.2 Environmental significance

Wastage of nutrients from chemical fertilizers creates unwanted environmental problems, demanding proper use coupled to mitigation approaches for sustainable development. The nitrogen and phosphorus released to the aquatic ecosystems causes increased algal growth manifesting “eutrophication” and dead zones due to lack of oxygen¹⁷.

Amount of P released into the water bodies is expected to reach about 50 million tons per year by 2050¹⁸. The P requirement is expected to be highest in regions like Latin America, the

Caribbean, Southern Asia, North Africa and West Asia, leading to higher P levels in their water bodies. High rates of P loss to water bodies may continue in East and Southeast Asia. It is estimated that very high application of P fertilizers to several agricultural areas may impact the biogeochemical planetary boundary for P in high-risk zones³. Currently, high risk areas with high P levels include the US mid-West, Western Europe, the Ganges Valley and East Asia.

Therefore, further degradation of water resources is likely in the absence of appropriate mitigation measures for containing P pollution³. Due to increasing P load, frequent occurrence of eutrophication can be expected in the Gulf of Mexico, **the Ganges Valley and coastal regions of Bay of Bengal**. The P issue not only concerns environmental implications, but also impact the economy and livelihoods of coastal communities. In addition, an increase in PR processing and fertilizer production demand increases rates of water extraction for the chemical processes, augmenting water stress issues especially in the arid regions³.

1.4 Prospects for removal and recovery of lost nutrients

Since a large fraction of the applied fertilizer escapes into the atmosphere and surface water bodies⁹, recovery of lost nutrients holds promise in mitigating the problems. Nutrient recovery reduces the burden on reactive nitrogen and phosphorus levels, in turn ensuring limited environmental complications. However, the first step towards recovery is to remove the nutrients from the nutrient-containing streams.

The municipal wastewater contains phosphorus in the range of 4–16 mg L⁻¹ PO₄³⁻-P. About 20–30% of this P present in the wastewater is removed during conventional biological aerobic treatment for meeting cellular needs without using any specific P-removal processes^{19,20}. This would still leave sufficient P concentrations (3 to 12 mg L⁻¹ P) in treated effluents. However, due to recent environmental regulations, removal of P by conventional wastewater treatment

is not satisfactory. Based on the EU Water Framework Directive²¹, P discharge concentrations to the environment from WWTP is limited to 1-2 mg L⁻¹. Estimations have revealed that P recovery and recycling from wastewater can only provide about 10% of the total global supply²². This estimate is based on 10% of the applied P fertilizer reaching WWTP considering the P digested by humans.

The concentration of nitrogen compounds varies in wastewater and is dependent on wastewater origin. For instance, municipal wastewater contains 20-85 mg L⁻¹ N, abattoir runoff between 160 and 280 mg L⁻¹ N, whereas landfill leachate may contain as high as 3000 mg L⁻¹ N²³. The conventional treatment systems for municipal wastewater effectively remove ammonia via nitrification and denitrification²⁴. These processes are dependent on supply of oxygen and electron donor (e.g., carbon substrate). The removal of nitrogenous compounds from wastewater by biological processes becomes limiting when carbon to nitrogen ratio is too low. Keen attention is needed to provide optimum oxygen for nitrification but not to exhaust organic matter (electron donor for denitrification). This is essential for achieving total nitrogen removal in wastewater treatment plants. Hence, novel and efficient processes are required to handle low carbon and high ammonium containing wastewater (**Problem 1**).

1.4.1 *Advancements in nutrient removal and recovery*

The phosphorus is clearly a double-edged issue: it alarms with phosphorus resource depletion, as well as environmental pollution concerns. There are several intervention points (e.g., mining, fertilizer production and use, livestock, and municipal wastewater) that could conserve phosphorus, reduce its discharge to the environment, or both. Municipal wastewater is an important point source for nitrogen and phosphorus. Chemical precipitation of phosphorus by the addition of metal cations (Al³⁺, Fe³⁺, or Ca²⁺) has been successfully implemented at some wastewater treatment plants (WWTPs) in developed countries²⁵.

Chemical precipitation is simple to implement, and achieves required discharge limits for phosphorus. However, the disadvantages include sludge production and cost of chemicals.

The issue of reactive nitrogen compounds (ammonia, and nitrate) is also similar to phosphorus, as environmental discharge is linked to environmental pollution and recovery is of importance in agriculture. Recently, bioelectrochemical systems have attracted interest for recovering ammonium from concentrated waste streams like human urine^{6,26}. Chemical precipitation of both ammonium and phosphorus in the form of struvite (NH_4MgPO_4) has been implemented at some treatment facilities. However, these methods are suitable for treating concentrated wastewaters. These methods do not appear economically and technologically feasible for dilute waste streams like municipal wastewater. On the other hand, biological processes are most environmental friendly, cost effective and suitable for removing nutrients from dilute waste streams like municipal wastewater⁶.

1.4.2 Biological wastewater treatment

'Modern' biological wastewater treatment is largely depending on conventional activated sludge process (ASP) which was developed in the early 20th century. Conventional ASP is used worldwide for treating municipal and industrial wastewaters²⁷. ASP relies on microbial metabolism for removing biochemical oxygen demand²⁸. The microorganisms oxidise the organic matter using O_2 to CO_2 and H_2O . The conventional ASP has been modified for integrating nitrogen and phosphorus removal as required to meet discharge guidelines. Nitrogen removal typically involves nitrification and denitrification processes performed by nitrifying bacteria (e.g., ammonium oxidising bacteria (AOB), and nitrite oxidising bacteria (NOB)) and denitrifying bacteria, respectively. However, separate tanks or partition in the treatment tank is needed for maintaining aerobic and anoxic environments for nitrification and denitrification, respectively. Establishment of biological P removal *via* enhanced biological phosphate removal (EBPR) also needs alternating anaerobic-aerobic conditions

and selection of polyphosphate accumulating organisms (PAOs). Thus, integration of N and P removal requires introduction of multiple unit processes and recirculation flows (Fig. 1.4).

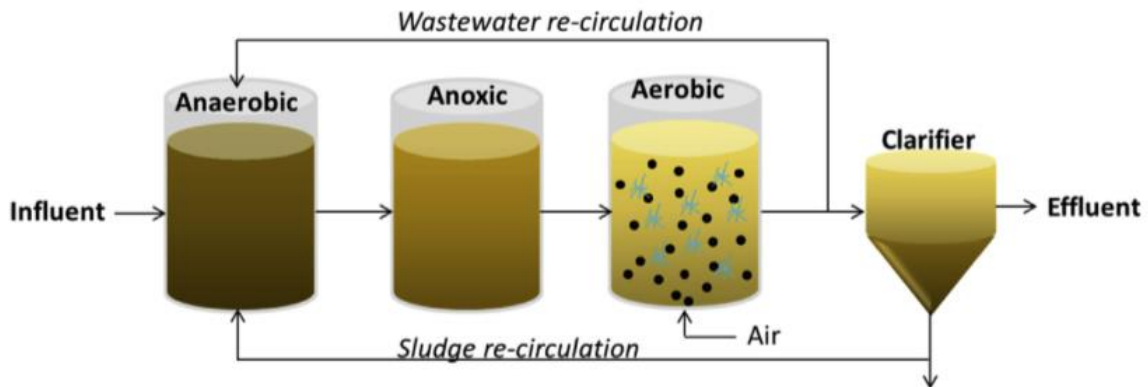


Fig. 1.4. Schematic diagram showing main unit processes and re-circulation flows in ASP for achieving organic carbon, nitrogen and phosphorus removal from wastewater. (Adapted from Nancharaiah and Sarvajith. 2019)²⁹.

Due to continuous process type and poor sludge settling properties, separate clarifier tanks are used for activated sludge-treated wastewater separation in conventional ASP. Secondary clarifier tanks are avoided by shifting from continuous plug flow to fill-and-draw type treatment systems. Fill-draw treatment by sequencing batch reactors (SBRs) is extensively considered for wastewater treatment due to operational flexibility, efficient nutrient removal and smaller footprint. But conventional SBRs are still dependent on activated sludge which exhibit poor settling properties and prone to bulking under changing environmental conditions.

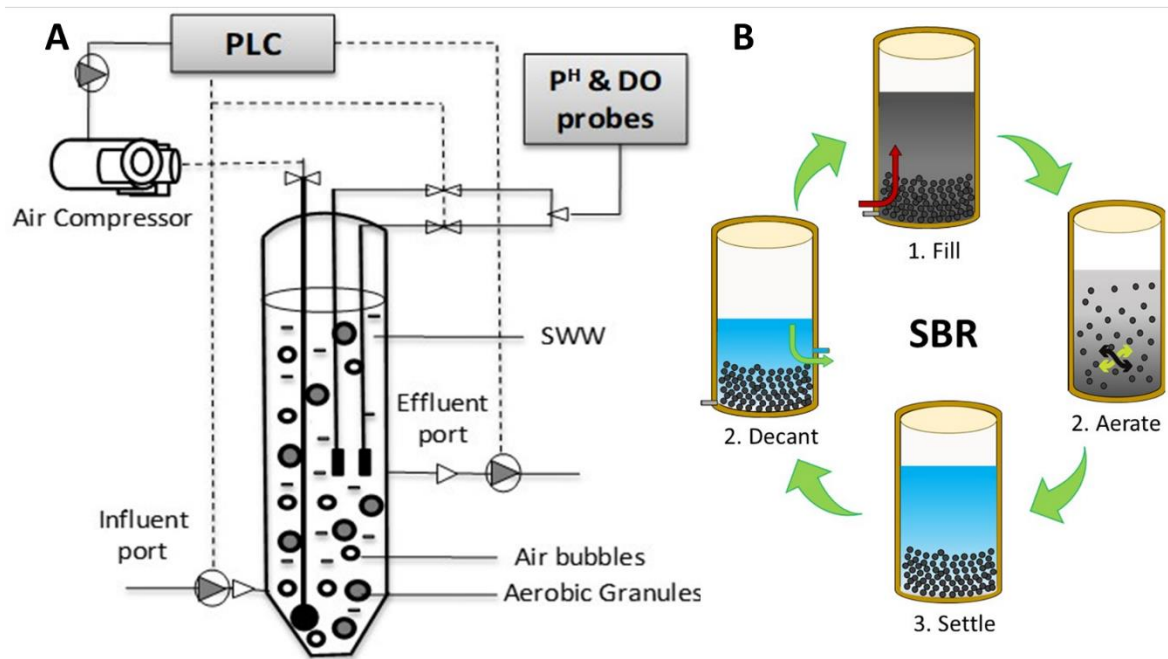


Fig. 1.5. Schematic representation of bioreactor (A), and operational phases in each batch of bioreactor operation (B).

1.5 Aerobic granular sludge for wastewater treatment

AGS represent bacteria and archaea laden granules that are characterized with large particle size, compact microstructure and superior settling velocities than activated sludge flocs. Due to advantages like excellent settling properties, effective nutrient removal, efficient biodegradation capabilities, and higher tolerance to toxic pollutants, AGS attracted interest for its application in WWTPs^{27,31}. Moreover, AGS process offers significant reduction in land foot print (up to 75%), costs (up to 50%) as compared to other biological treatment methods^{32,33}.

For cultivating AGS from AS flocs, SBR is typically operated with anaerobic, aerobic and short settling phases in the cycle. The SBR operating conditions facilitate enrichment of slow-growing microorganisms such as nitrifying bacteria, polyphosphate accumulating organisms (PAOs) and glycogen accumulating organisms (GAOs) as dense granules.

The settling velocity of aggregates is higher than that of flocs, thus, allowing their retention in the SBR. The growth of these microbial aggregates results in formation of millimetre-sized

granules (Fig. 1.6). Due to larger particle size and oxygen consumption, the granules contain aerobic, anoxic, and anaerobic microenvironments across depth³⁴. The different redox conditions in granules are useful for simultaneously removing organic carbon, nitrogen, and phosphorus from wastewater. The important attributes of granules include higher density, higher biomass retention, effective nutrient removal, and superior biomass-treated wastewater separation. Reliable cultivation of granules, enrichment of functional microorganisms, and long-term stability are important for successful implementation in WWTPs. It emphasizes better understanding and development of strategies for improving granulation, enrichment of functional microorganisms, stability and evaluating these aspects under varied process conditions. Hence, this thesis was focused on investigations for understanding and improving cultivation of AGS and establishment of nitrogen and phosphorus removal pathways.

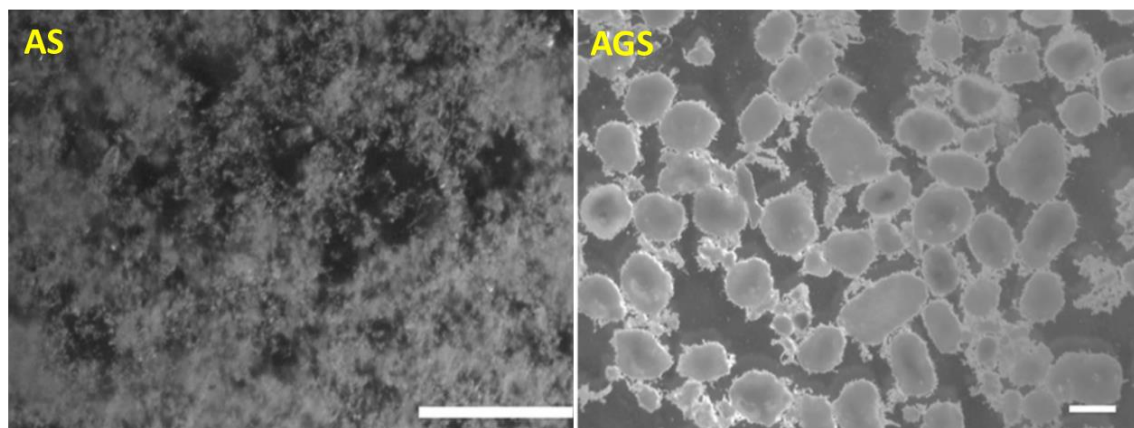


Fig. 1.6. Morphology of activated sludge and granular sludge. (Nancharaiyah et al., 2019)³². Scale bar=1mm.

1.5.1 Nitrogen and Phosphorus removal

AGS is suitable for performing simultaneous COD, nitrogen, and phosphorus removal from wastewater. One of the key advantages of AGS is its efficient nitrogen and phosphorus removal capabilities. This requires proper enrichment of desired microorganisms and right environmental operating conditions. Effective oxidation of ammonium coupled with accumulation of nitrate was reported in some studies³⁵. Accumulation of either nitrite or nitrate is not desirable and compromises total nitrogen removal efficiencies. Establishment of

biological P removal by EBPR is influenced by the substrate type, concentrations of nitrite/nitrate (formed during ammonium removal) and operating conditions (e.g., dissolved oxygen, temperature). There is limited information on the AGS stability, and nutrient removal capabilities under tropical climate conditions. Data on structural stability of granules, operating nitrogen and phosphorus removal pathways is needed for implementing AGS systems for treating municipal wastewaters in tropical climates. Development of alternative strategies for minimizing nitrate/nitrite build-up and to decrease start-up periods for establishing EBPR are of technological importance for considering AGS process in municipal wastewater treatment.

AGS can effectively oxidize the ammonium present in the low-strength wastewaters such as municipal wastewater³⁶, but not in high-strength wastewaters³⁷. High strength ammonium wastewaters containing up to 5000 mg L⁻¹ ammonium-N are generated from municipal solid waste disposal, and industrial (fertilizer, petrochemical, etc.) activities³⁸. Apart from high ammonium concentration, these wastewaters are also characterized with low COD/N ratios. Some studies have reported deterioration in granular stability, and nitrogen removal capabilities at lower COD/N ratios^{39,40}. However, these studies were not in line with the proposition that selection of slow-growing nitrifying bacteria that promotes AGS formation and stability. Thus, deeper in-sights into stability and nutrient removal of AGS at lower COD/N ratios requires thorough investigation.

1.5.2 Aerobic granular sludge formation

In the last decade, numerous hypotheses have been proposed for formation of aerobic granules^{27,41}. Although these models have identified distinct events during granulation, only few events are supported by the experimental evidence. Some of the unifying concepts that are common to granulation include selection pressures by shear force and short settling times, substrate loading rate, extracellular polymeric substances (EPSs) production, and cell-cell

interactions. Interactions among cells, microbial attachment and formation of aggregates, enhanced EPS production and finally shaping of granules are the key events observed during granulation (Fig. 1.7).

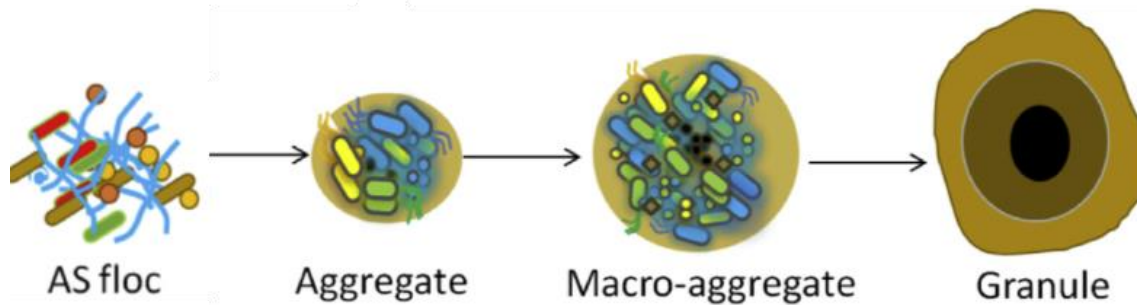


Fig. 1.7. Proposed mechanism of aerobic granular sludge formation in sequencing batch reactors. (Modified from Nancharaiah and Sarvajith 2019).

Development of granules is the key to achieving effective nutrient removal and biomass-treated wastewater separation. Although granules can be reliably and rapidly cultivated under well-defined conditions, some studies have reported that requirement of several months (up to 10 months) for cultivation of granules while treating real municipal wastewaters. Also, there are concerns on the long-term stability of granules. This is because cultivation of granules is dependent on wastewater characteristics, type and concentration of organic substrate and environmental conditions. This necessitates development of alternative strategies for enhancing granulation and stability. In this context, external agents such as crushed granules, micro powder, zeolite, magnet powder, and granular activated carbon on granulation have been added to SBRs for increasing the rate of granulation⁴². These studies have shown improvements in granulation of activated sludge. However, the role of external agents on selection of functional microorganisms involved in nutrient removal, if any, is not known. Moreover, detailed studies on understanding the role of external agents on granulation are desirable before contemplating their application in treatment systems (**Problem 2**).

1.5.3 Effect of Salinity on granular stability and biological nutrient removal

Salinity is another important wastewater-characteristic that can influence the structure, stability, and function of aerobic granules. Previous studies indicated decrease in granule size⁴³, formation of irregularly shaped granules^{44,45,46} and even disintegration of granules upon exposure to saline conditions.

Inhibition in nitrogen and phosphorus removal by AGS was observed at higher salinities. Impact on nitrogen removal was characterized by nitrite accumulation under saline conditions. The effects of salinity on the EBPR process are inconclusive and inconsistent because (i) often the employed growth conditions were not suitable for PAO's, and (ii) the impact of salinity on nitrogen removal leading nitrite accumulation causing indirect effects on P removal.

Previous studies have focused on development of salt-tolerant AGS by (i) cultivating AGS from AS under saline conditions, and (ii) acclimation of pre-formed AGS to saline conditions^{43,44,45,46} (Fig. 1.8). These approaches not only require long acclimation periods, but establishing inefficient nutrient removal is primarily related to lower abundance of salt-tolerant organisms in the inoculum. **(Problem 3)** (Fig. 1.8). Hence, there is a need for systematic and novel approach for development of granules which can perform efficient nitrogen and phosphorus removal under saline conditions. Considering autochthonous halophilic microorganisms is one such approach for cultivation of granules for performing biological treatment of saline wastewaters (Fig. 1.8).

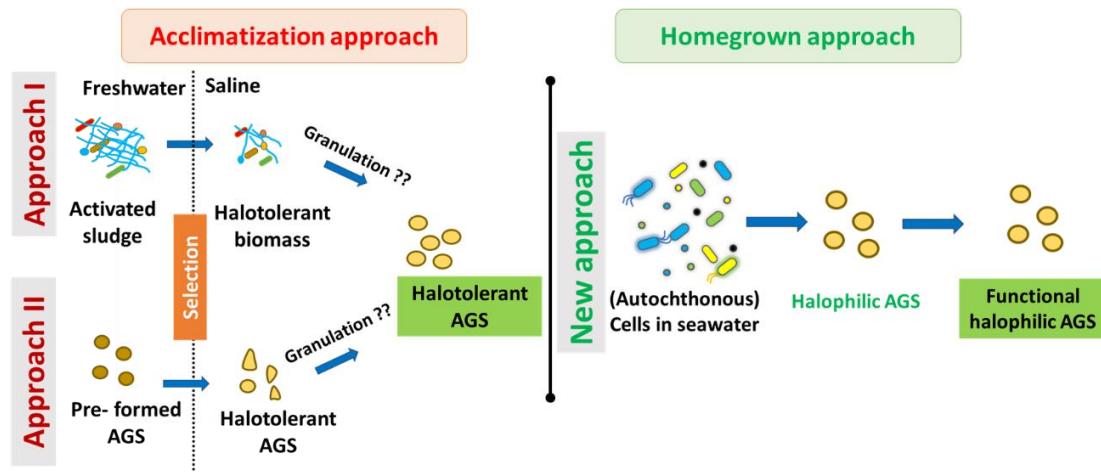


Fig. 1.8. Blueprint of the tailored approaches of saline wastewater treatment (acclimatization approach), and the novel homegrown *de novo* approach described in this thesis.

1.6 Overall objectives of the thesis

AGS is an emerging and novel microbial consortium for achieving biological treatment for sustainable wastewater treatment. Although AGS is very attractive as replacement of activated sludge in wastewater treatment plants, there are limited studies on cultivation of granules, nutrient removal capabilities, granular stability, and salinity tolerance under tropical climate conditions. A deeper understanding of the AGS on complex interactions between key the microorganisms, the mechanisms involved in enrichment of selected microorganisms in the community, strategies for improving granulation and enrichment of functional microorganisms, granular stability and life cycle, and response to harsh wastewater conditions is helpful in considering AGS process in wastewater treatment plants.

For understanding and improving granulation, and establishment of nutrient removal pathways, the following objectives were investigated during this thesis work.

- Granulation and biological nutrient removal mechanisms in sequencing batch reactors
- Enrichment of nitrogen and phosphorus removing microorganisms in aerobic granular sludge under different process conditions
- *de novo* granulation of native microorganisms of seawater for saline wastewater treatment

- Nitrogen and phosphorus removal at different ammonium and COD/N ratios.

1.6.1 Thesis outline

The thesis was divided into 7 chapters on the basis of the research work carried out to fulfil the thesis objectives as outlined in Fig. 1.9.

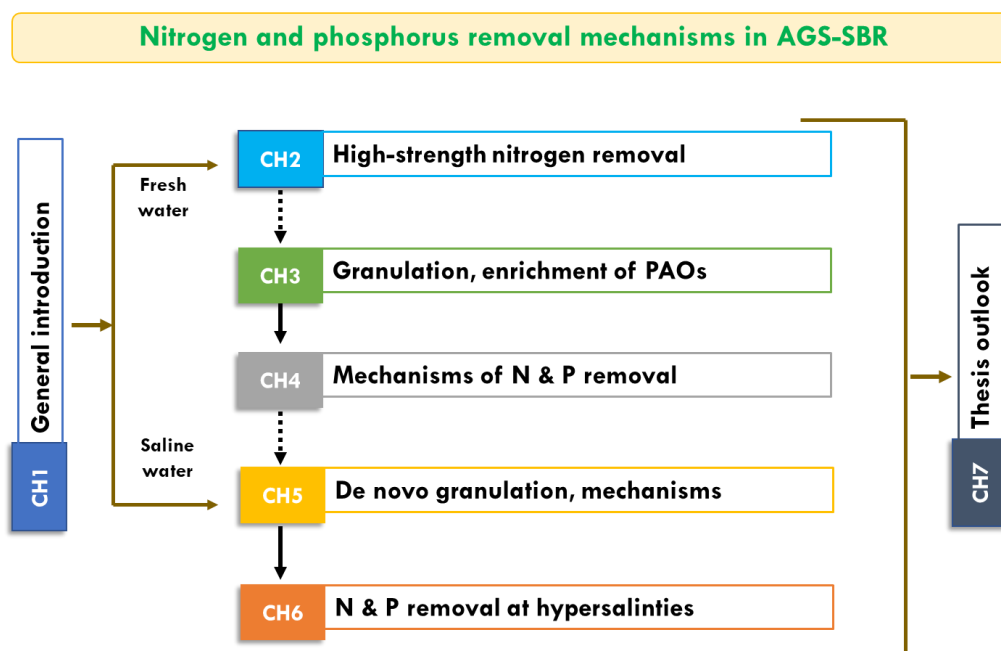


Fig. 1.9. Thesis outline showing the connections between the individual chapters.

Chapter 1 provides current knowledge-state on nitrogen and phosphorus removal, and advancements in biological wastewater treatment and identifies the objectives for this thesis work. Chapters 2 to 6 constitute independent chapters, each containing the materials used, experimental methodology, results, and discussion. **Chapter 2** focuses on the ammonium removal capabilities, nitrogen and phosphorus removal pathways under high ammonium conditions and COD/N ratios. **Chapter 3** describes the experimental results obtained on granulation, nutrient removal and enrichment of PAOs under different conditions. Granulation of activated sludge was studied in bench scale SBRs with and without coconut shell charcoal (CSC) particles and in the presence of different carbon sources (i.e., acetate, propionate, and acetate-propionate combination). **Chapter 4** includes experimental results on fractionation of the biomass developed in SBRs in the presence of CSC particles. The biomass

was fractionated based on particle size and type (e.g., biofilms, granules) for understanding nutrient (N and P) removal capabilities, and elucidation of functional organisms. This chapter also includes results on the effect of salt stress on biological nutrient removal. **Chapter 5** describes a novel method for cultivation of halophilic granular sludge for saline wastewater treatment. Here, cultivation of halophilic autochthonous microorganisms of seawater was investigated for establishing efficient nitrogen and phosphorus removal under saline conditions. **Chapter 6** includes biological nutrient removal, characteristics of halophilic granules and microbial community changes at hypersalinity (34 to 120 ppt). Finally, **Chapter 7** concludes with the major findings and guidelines for future research.

Chapter 2

Biological nutrient removal by aerobic granular sludge at high ammonium concentrations

Abstract

Aerobic granular sludge (AGS) process is increasingly considered for simultaneous COD, nitrogen and phosphorus from domestic and industrial wastewaters. High ammonium containing wastewaters are generated in anaerobic digestion, municipal solid waste disposal, fertilizer production and aquaculture. These wastewaters are typically characterized with lower COD/N ratios. The nutrient removal capabilities and stability of AGS are not well understood especially at high ammonium concentrations. This study evaluated biological nutrient removal and granular stability at different influent ammonium concentrations (30 to 4000 mg L⁻¹ NH₄⁺-N; loading rates of 0.03 to 4 kg NH₄⁺-N m⁻³ d⁻¹), and varied COD/N ratios (0.13 to 18.3) in a sequencing batch reactor operated for 440 days. Ammoniacal and total nitrogen removals were found to be high at 99.9% and 99.3%, respectively, even at higher ammonium concentrations. Phosphorus was stabilized at ~50% and mediated by normal bio-P removal. A reduction in bacterial diversity along with enrichment of ammonia oxidizing bacteria (AOB), anammox and denitrifying bacteria was noticed at higher influent ammonium concentrations. Quantitative PCR showed enrichment of AOB, anammox bacteria, *Nitrospira* and denitrifiers. Chemical data and bacterial community supported occurrence of nitrification and anammox pathways. AGS had stable granular structure with excellent settling properties at lower COD/N ≤ 1. Experimental data suggests that AGS process is suitable for treating high ammonium wastewaters.

Keywords: Aerobic granules; Ammonium-rich wastewater, Anammox, COD/N ratio, Nitrification, Nutrient removal.

2.1 Introduction

Ammoniacal nitrogen is a principal contaminant in both municipal and industrial wastewater, causes toxicity to aquatic organisms and eutrophication in water bodies^{47,48}. High-strength ammonium wastewaters (200 to 5000 mg L⁻¹ NH₄⁺-N) are generated in municipal solid disposal activities and industrial processes like petrochemical, pharmaceutical and fertilizer production³⁸. Biological treatment methods are widely applied for removing ammonium from wastewaters due to environmental friendliness and low-cost operations as compared to physiochemical methods like ammonia stripping, breakpoint chlorination, ion exchange and electro dialysis⁴⁹. Biological treatment of high-strength ammonium wastewater typically depends on aerobic nitrification (NH₄⁺-N to NO₃⁻-N) and anoxic denitrification (NO₃⁻-N to N₂), performed by slow-growing nitrifiers and fast-growing denitrifiers, respectively. It is possible to combine these two distinct processes in a single bioreactor tank using biofilms which allows longer sludge retention times⁵⁰. Immobilization of nitrifying consortia (or activated sludge) avoided the inhibitory effect of free ammonia (NH₃) formed in high-strength ammonium wastewaters and also improved the biological nitrogen removal (BNR)⁵¹.

Aerobic granular sludge (AGS) represents bacteria laden granules formed by self-immobilization of microorganisms without a carrier material attracting numerous interests for effective and simultaneous removal of organic and inorganic pollutants⁵². However, instability of granular structure is a major impediment for widespread implementation of AGS process in wastewater treatment plants^{53,54}. This is because instability of granular structure can lead to high suspended solids in the treated wastewater, deterioration in settling characteristics, loss of biomass and functionality^{55,56}. The COD/N ratio of wastewater is a key parameter influencing the granular stability⁵⁵. AGS process has proven for effective oxidation of ammonium ions and for implementing energy efficient BNR pathways like partial nitrification (nitritation: conversion of NH₄⁺-N to NO₂⁻-N) and anaerobic ammonium

oxidation (anammox) which are attractive for treating high-ammonium wastewaters^{23,57,58,59} as compared to autotrophic nitrification ($\text{NH}_4^+\text{-N}$ to $\text{NO}_2^-\text{-N}$ and $\text{NO}_2^-\text{-N}$ to $\text{NO}_3^-\text{-N}$) and heterotrophic denitrification ($\text{NO}_3^-\text{-N}$ to N_2). Poor ammonium or TN removals were observed while treating high-strength ammonium wastewaters^{36,37,39}. Ammonium and TN removals were lower at 35% and 39.3%, respectively, while treating landfill leachate containing $1105 \text{ mg L}^{-1} \text{ NH}_4^+\text{-N}$ ⁶⁰. Yu et al.⁵⁸ observed lower TN removals of 71.3% and 59.6%, respectively, from synthetic medium containing 600 mg L^{-1} and $2000 \text{ mg L}^{-1} \text{ NH}_4^+\text{-N}$. Luo et al.¹⁵¹ reported poor ammonium removal and disintegration of AGS when the COD/N ratio lowered to 1. Due to limited understanding, further research is essential to evaluate BNR potential and long-term stability of AGS under high $\text{NH}_4^+\text{-N}$ loadings and lower COD/N ratios.

This study was designed to evaluate BNR capabilities of AGS for removing high-strength ammoniacal nitrogen (up to 4000 mg L^{-1}) and long-term stability of AGS at different COD/N ratios. For this, a laboratory scale sequencing batch reactor (SBR) was operated for granulation of activated sludge. The formed granules were harvested and subjected to different influent ammoniacal nitrogen ranging from 30 to 4000 mg L^{-1} during 440 days. The COD/N ratio was gradually decreased from 18.3 to 0.13. Bacterial community was determined by Illumina MiSeq sequencing and quantitative polymerase chain reaction. Chemical data and bacterial community were analysed to decipher BNR pathways that are operating at high influent ammonium levels and different COD/N ratios.

2.2 Materials and methods

2.2.1 Source of biomass

Activated sludge was collected from the aeration tank of an operating municipal wastewater treatment plant at Kalpakkam Township, Tamil Nadu, India. Activated sludge was added to

the bioreactors at 3.5 g L^{-1} at the beginning. Activated sludge acted as the source of microorganisms for cultivating bacterial granules in the bioreactors.

2.2.2 Synthetic wastewater

Synthetic wastewater containing $0.05 \text{ g L}^{-1} \text{ K}_2\text{HPO}_4 \cdot 2\text{H}_2\text{O}$, $0.041 \text{ g L}^{-1} \text{ KH}_2\text{PO}_4$, $0.01 \text{ g L}^{-1} \text{ CaCl}_2 \cdot 2\text{H}_2\text{O}$, $0.01 \text{ g L}^{-1} \text{ MgSO}_4 \cdot 7\text{H}_2\text{O}$, $0.04 \text{ g L}^{-1} \text{ NaHCO}_3$ and 0.1 ml L^{-1} trace elements stock was prepared in demineralized water. The trace elements stock solution contained the following (g L^{-1}): FeSO_4 (0.54), ZnSO_4 (0.4), MnCl_2 (0.1), $\text{CuSO}_4 \cdot 5\text{H}_2\text{O}$ (0.25), $\text{CoCl}_2 \cdot 6\text{H}_2\text{O}$ (0.5), $\text{NiCl}_2 \cdot 6\text{H}_2\text{O}$ (0.19), $\text{NaMoO}_4 \cdot 2\text{H}_2\text{O}$ (0.22), and H_3BO_4 (0.014). Sodium acetate was added directly to the simulated wastewater to provide organic carbon at a chemical oxygen demand (COD) of 500 mg L^{-1} . Ammonium-N and phosphate-P concentrations were kept at 30 and 10 mg L^{-1} , respectively. The initial concentrations of nutrients mentioned in the graphs refer to the concentrations in the bioreactor immediately after filling.

2.2.3 SBR setup and operation

Transparent polycarbonate columns (height: 62 cm; diameter: 9 cm) were used as bioreactors for studies on granulation. Each column having 3 L working volume was operated in SBR mode with 6 h cycle and 4 cycles a day. The 6 h cycle contained static plug-flow filling (60 min), aeration (270 min), settling (10 to 4 min), decant (10 min), and idle (10 to 6 min) periods. Cycle operation (switching on/off of feed pump, aeration pump, and drain pump) was controlled by electronic timers and programmable logic controllers (PLC). Air was supplied from the bottom of the SBRs at an air flow rate of 2 L min^{-1} corresponding to 0.5 cm s^{-1} superficial air velocity (SAV). Dissolved oxygen (DO) was not controlled but found to be low ($<0.08 \text{ mg L}^{-1}$) during filling phase and reach saturation concentrations ($\sim 7 \text{ mg L}^{-1}$) during aeration phase. The treated water (effluent) was withdrawn through an outlet port located at 17 cm from bottom of the SBR resulting in a volumetric exchange ratio of 66%. The pH was not controlled but was observed to vary between 7.6 and 8.0 during SBR

operation. The experiments were performed at an ambient temperature of 31 ± 5 °C and relative humidity of $>85\%$. The liquid samples collected regularly from the SBRs were centrifuged at 10000 g for 10 min and stored at 4 °C.

2.2.4 High-strength ammoniacal-N removal

2.2.4.1 Inoculum and synthetic ammonium wastewater

AGS was harvested from an operating laboratory scale SBR treating acetate-containing synthetic wastewater on day 70 and used as the seed biomass for the high strength ammonium removal experiments. Synthetic wastewater was prepared in demineralized water as explained above. Sodium lactate (60% w/v, Merck) and ammonium chloride were used as the sole sources of carbon and nitrogen, respectively. Sodium lactate was added directly to synthetic wastewater to give a final chemical oxygen demand (COD) of 550 mg L^{-1} . Ammonium concentration was increased stepwise during SBR operation. Concentrations of nutrients (COD, ammonium, nitrate, nitrite, and phosphorus) mentioned at 0 time in the graphs refer to concentrations in the reactor after filling.

2.2.4.2 Bioreactor configuration and operational strategy for ammonium wastewater

A glass cylinder (height: 46 cm, diameter: 7 cm) with 1 L working volume was used for studying ammoniacal nitrogen removal. It was inoculated with 1.98 g VSS L^{-1} AGS and fed with synthetic wastewater (section 2.2.3). It was operated in fill-and-draw mode with 24 h cycle. Each 24 h cycle contained filling (15 min), anaerobic (8 h), aeration (15 h), settling (5 min), decant (10 min) and idle (30 min) phases. At the end of each cycle, 80% of the treated liquid was removed and replaced with freshly prepared synthetic wastewater. The hydraulic retention time (HRT) was 34.2 h. Aeration was provided at 1 litre per minute (LPM) through an air diffuser placed at the bottom. Superficial air velocity during the aeration phase was determined to be 0.4 cm s^{-1} . Filling, aeration and decant operations were performed by

operating the pumps automatically using pre-programmed electronic timers. The bioreactor was operated at an ambient temperature of 31 ± 5 °C.

2.2.4.3 Ammonium removal in AGS sequencing batch reactor

AGS bioreactor was operated at different initial ammonium concentrations to determine nitrogen removal capabilities. For the initial 20 cycles, SBR was fed with synthetic wastewater containing $30 \text{ mg L}^{-1} \text{ NH}_4^+\text{-N}$ to condition the biomass with lactate as carbon source. Subsequently, ammoniacal nitrogen concentration was gradually increased up to $4000 \text{ mg L}^{-1} \text{ NH}_4^+\text{-N}$. At each concentration, the bioreactor was operated for a minimum of 20 cycles to ensure stable BNR. The bioreactor was operated for a period of 440 days and evaluated removal of $4000 \text{ mg L}^{-1} \text{ NH}_4^+\text{-N}$. Liquid samples were collected regularly for determining removal performance and profiles during the cycle. The biomass was monitored regularly for morphology, size and settling characteristics.

2.2.4.4 Batch experiments on nitrogen removal mechanisms

Batch tests were performed in 100 mL serum bottles with 80 ml synthetic wastewater. AGS was harvested from AGS reactor treating synthetic wastewater containing $600 \text{ mg L}^{-1} \text{ NH}_4^+\text{-N}$ and used for batch experiments. About 1.21 g of AGS was transferred to serum bottle containing 80 mL synthetic wastewater. The serum bottles were closed with butyl rubber stoppers, crimp-sealed with aluminium caps and purged with argon for 10 min to establish anaerobic condition. Then, serum bottles were incubated in an orbital shaker at 160 rpm and 30 °C. Serum bottles were setup in duplicates without AGS, with AGS, and with heat-killed AGS. Heat-killed AGS was prepared by transferring AGS to serum bottles and autoclaving twice at 121 °C and 15 psi for 20 min. Batch experiments were repeated in fed-batch mode for 5 cycles. For this, the treated synthetic wastewater was replaced (100% exchange) with fresh synthetic wastewater at the end of every 24 h. Liquid samples were collected at regular time intervals for monitoring concentration of ammonium, nitrate and nitrite.

2.2.5 Microscopy

Stereo microscope was used for determining the morphology and size of granules performing BNR at different ammonium concentrations. Images of granules were taken using Olympus DP70 camera coupled to SMZ1000 stereomicroscope (Nikon, Japan). Particle size was determined using *ImageJ* software³¹. Surface morphology of the granules performing BNR at different ammonium concentrations of 500 and 4000 mg L⁻¹ NH₄⁺-N was determined using scanning electron microscope. For this, granules were suspended in 2.5% (v/v) glutaraldehyde solution prepared in phosphate buffer saline (pH 7.4) for 4 h at 30 °C⁶². Fixed granules were dehydrated by immersing for 5 min each in ethanol series (50, 60, 70, 80, 90 and 100% ethanol). The dehydrated granules were imaged using Zeiss supra 55 scanning electron microscope, SEM, (Carl Zeiss, Germany). Electron dispersive X-ray spectrum (EDX) of AGS was recorded at energies up to 10 keV with Zeiss supra-55.

2.2.6 Genomic DNA extraction

Genomic DNA was extracted from AGS sample collected from the bioreactor on day 203 and 440 using QIAGEN® DNA extraction mini kit following the manufacturer's protocol.

2.2.7 Bacterial community analysis using 16S rRNA gene sequencing

The 16S rRNA based metagenomics sequencing was performed by amplifying V3-V4 regions with specific primers (Forward: 5'-TCGTCGGCAGCGTCAGATGTGTATAAGAGACAG-3'; Reverse: 5'-GTCTCGTGGGCTCGGAGATGTGTATAAGAGACAG-3') and sequencing using MiSeq platform at Genotypic Technology Pvt. Ltd., Bangalore, India. 20 ng of genomic DNA was amplified to generate ~550 bp amplicons using KAPA HiFi Hot Start PCR Kit (Boston, MA USA) The amplicons were sequenced again to add 120 bp Illumina sequencing barcoded adaptors (Nextera XT v2 Index Kit, Illumina, U.S.A) to obtain a size ~600 bp. The constructed libraries were validated, pooled and cleaned for sequencing on Illumina. Only high-quality sequences were selected using FastQC for further processing.⁶³ Following this,

the reads were stitched and analysed using Fastq-join and QUIME pipeline. The query sequences were clustered using UCLUST5 method and the taxonomy of clusters were assigned based on $\geq 97\%$ sequence similarity against the curated chimera free 16S rRNA database (Greengenes6v 13.8) for generating biom file which was used for statistical analysis.

2.2.8 Quantitative PCR

Quantitative PCR (qPCR) was performed using LightCycler Instrument (Roche, Germany) with powerUp SYBR Green mastermix (Thermo Fisher Scientific, the USA) following the manufacturer's protocol and previously established protocols (Appendix I). qPCR was carried out in 20 μL total reaction volume containing 10 μL SYBR Green mastermix, 100 ng template and 0.5 μL of 1.25 mM concentrations of forward and reverse primers. Primers specific for ammonium oxidising bacteria (AOB), nitrite oxidising bacteria (NOB), anammox, Nitrospira and denitrifiers were used. The complete details on primer sequence and conditions are detailed in Appendix I. qPCR data was evaluated using the LightCycler data analysis software ver 4.0.

2.2.9 Analytical methods

Liquid samples collected were subjected to centrifugation at 8000 g for 10 min to remove the suspended cells. Cell-free supernatant samples were analysed for soluble chemical oxygen demand (COD) using closed reflux method. Ammonium, nitrite and phosphate was measured using Nessler's, N-(1-Naphthyl) ethylenediamine, and molybdenum reagent-based methods, respectively⁶⁴. Nitrate was measured by UltiMate™ high performance liquid chromatograph (Dionex, USA) with acclaim organic acid column and variable wavelength detector (VWD 3000) using 3 mM H_2SO_4 as eluent⁶². Total organic carbon (TOC) was analysed using TOC analyser (Shimadzu, Japan). Sludge volume index (SVI), mixed liquor suspended solids (MLSS), and mixed liquor volatile suspended solids (MLVSS) were determined following standard methods⁶⁴. Dissolved oxygen and pH were monitored online using LDO and pH

probes (Hach, Germany), respectively. Turbidity was measured using portable turbidimeter (Hach, Germany). The morphology of seed sludge flocs and granular sludge was observed under stereo microscope equipped with a digital camera (Jenoptik, Nikon). Particle size was analysed using *ImageJ* freeware software.

2.3 Results and discussion

2.3.1 Cultivation of aerobic granular sludge from activated sludge inoculum

The appearance of aerobic granules was observed within 20 days of SBR operation. Concomitantly, the SVI values decreased. At the beginning of the SBR operation, the SVI₅/SVI₃₀ ratio was already around 2.8 (Fig. 2.1), which eventually reduced to 1.4 by day 20, indicating formation of granules⁶⁵.

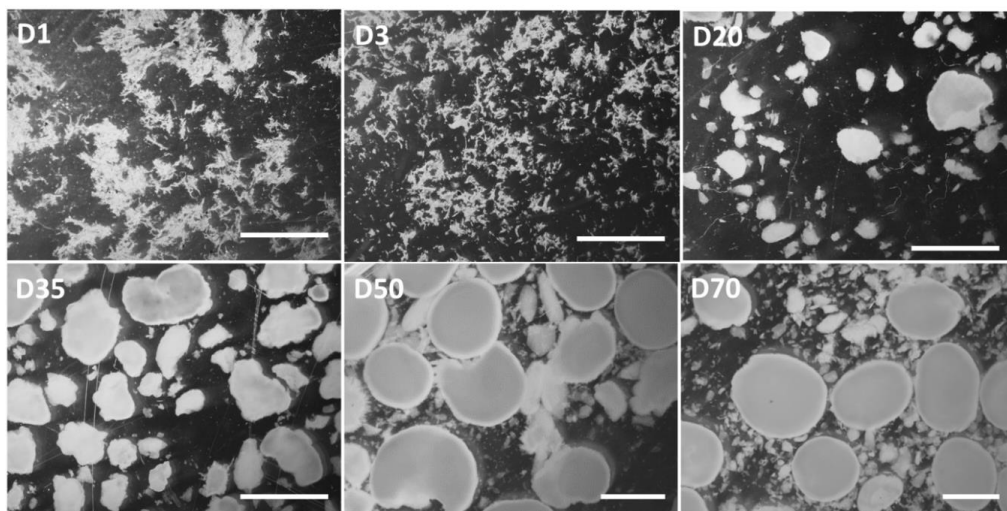


Fig. 2.1 Time course development of aerobic granular sludge from activated sludge inoculum in sequencing batch reactor fed with acetate (HAc)-containing synthetic wastewater. Scale bar=1 mm.

The MLSS increased from 3.5 g L⁻¹ on day 1 in SBR to 7.6 g L⁻¹ by day 70. The settling velocity of cultivated sludge also increased to 90 m h⁻¹, suggesting formation of well settling granules. The granular size steadily increased up to 1.3±0.3mm by day 40 and stabilized thereafter. During the course of experiment the flocs were completely washed out from the SBR and granules with regular surface morphology dominated (Fig. 2.1).

2.3.2 Nutrient removal performance

SBR Performance in removing COD, ammonium, and phosphorus were shown in Figure 2. COD removal was observed from the initial days of SBR (Fig. 2.2A) and remained stable throughout the experiment. About 40% of the influent COD (500 mg L^{-1}) was consumed in the anaerobic phase of the SBR cycle. Remaining COD was removed completely within 2 h of aeration phase (Fig. 2.2B).

Ammonium removal was observed from the beginning, but complete removal of 30 mg L^{-1} was established by day 20 of start-up (Fig. 2.2C). The effluent nitrite and nitrate concentrations were maintained below 2 mg L^{-1} , resulting in high TN removals of above 95%. Removal profiles revealed near complete removal of ammonium within 5 h of cycle (Fig. 2.2D). Although ammonium removal was corroborated with formation of nitrite and nitrate, their concentrations were below 2 mg L^{-1} indicating occurrence of their utilization. Effective ammonium removal along with appearance of low levels of nitrite and nitrate and their subsequent utilization suggests operation of simultaneous nitrification and denitrification and/or nitrification-denitrification pathways.

Phosphorus removal was steadily increased to ~50% by day 30 and remained stable thereafter (Fig. 2.2E). Phosphorus removal was not having any distinct anaerobic-aeration patterns, rather a simple consumption profile for meeting the cellular demand (Fig. 2.2F). Hence, the AGS cultivated was suitable for effectively removing COD/BOD and nitrogen removal. However, P removal was partial and ineffective due to non-establishment of enhanced biological phosphorus removal pathway.

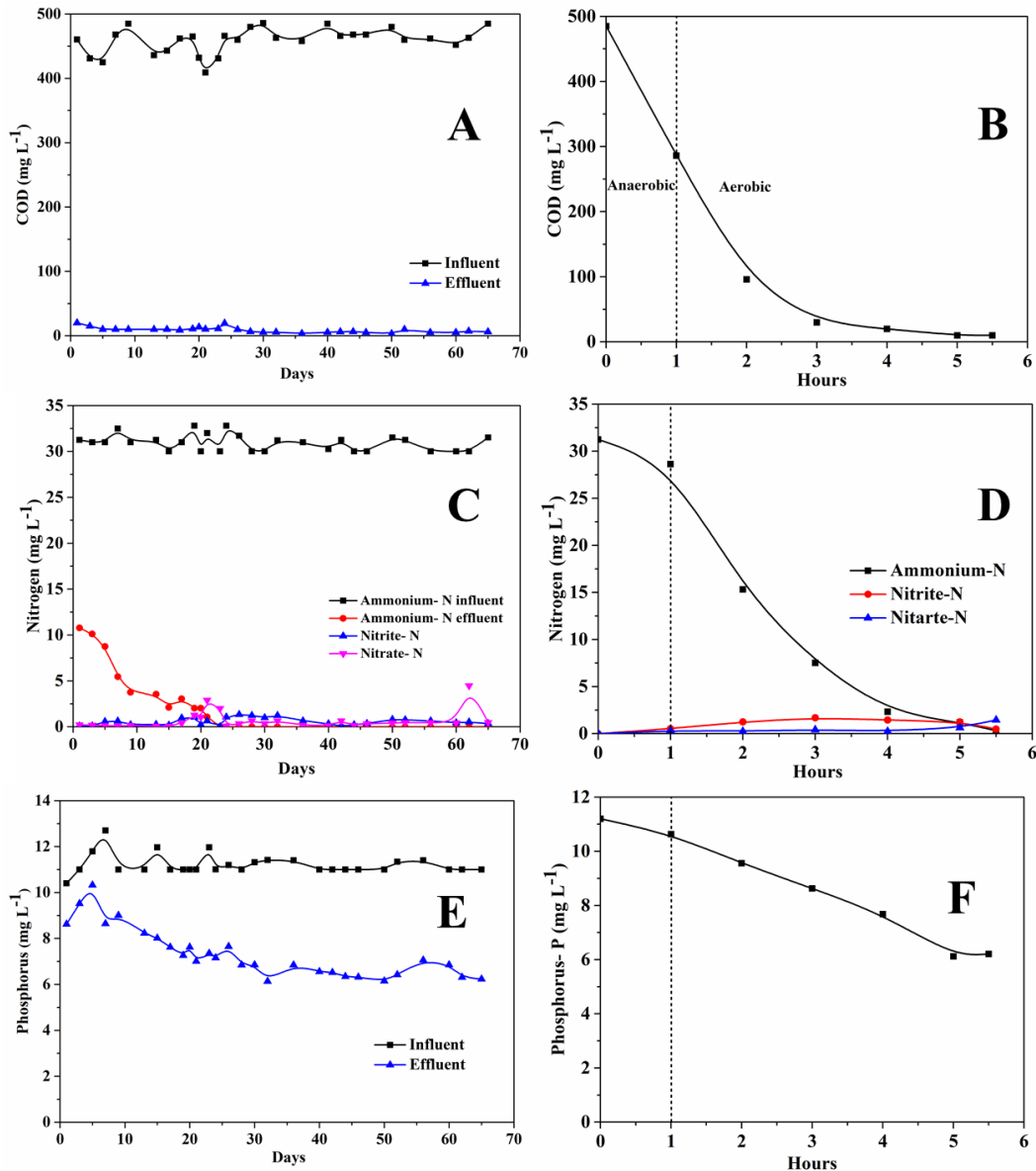


Fig. 2.2 Time course variations of influent and effluent COD (A, B), nitrogen (NH_4^+ -N, NO_2^- -N, NO_3^- -N) (C,D) and phosphorus (E,F) concentrations. Removal profiles of COD (B), ammonium (D), and phosphorus (F) in a single SBR cycle.

2.3.3 Nitrogen removal capabilities

Nitrogen removal performance at different ammonium concentrations was shown in Fig. 2.3.

Ammonium removal was observed from the beginning. Removal of $30 \text{ mg L}^{-1} \text{ NH}_4^+$ -N was near complete during the cycle and stable during multiple cycles. Removal of 30 mg L^{-1} of NH_4^+ -N removal was accompanied with the formation of only tiny quantities of nitrite (0.9 mg L^{-1}) and nitrate (1.6 mg L^{-1}) (Fig. 2.3). NH_4^+ -N, NO_3^- -N and NO_2^- -N concentrations

were found to be lower in the effluent indicating efficient ammonium and TN removal (Fig. 2.3). Ammonium and TN removal efficiencies were close to 100 and 96.2%, respectively, in the first 20 days. After achieving stable and sustained BNR, ammoniacal nitrogen concentration was gradually increased up to 4000 mg L⁻¹ during 440 days (Fig. 2.3). Ammonium ion removal was successfully achieved at all the tested NH₄⁺-N concentrations. NH₄⁺-N, NO₃⁻-N and NO₂⁻-N concentrations were found to be lower at ≤ 7, 3 and 5 mg L⁻¹, respectively, at the end of cycle even at higher influent ammonium concentrations (Fig. 2.3). Previous studies indicated an inverse relationship between influent ammonium concentration and BNR efficiency. For example, Wei et al.,³⁹ reported nitrogen removal efficiencies of 92.3%, 61.9% and 39.3%, respectively, at influent concentrations of 366, 788 and 1105 mg L⁻¹ NH₄⁺-N. Yu et al.⁴⁰ observed reduction in TN removal efficiency from 71.3% to 59.6% with an increase in NH₄⁺-N from 600 to 2000 mg L⁻¹. Ammonium and TN removals observed in this study are far more superior to previous studies on high strength ammonium wastewaters and related to the establishment of efficient N removal organisms/pathways.

Table 2.1 Nitrogen removal performance of 1 L aerobic granular sludge SBR operated at different ammonium nitrogen concentrations.

Ammonium-N (mg L ⁻¹)	Ammonium-N removal (%)		Total N removal (%)
	Anaerobic (8 h)	Aeration (15 h)	
30	86.2 ± 11.2	13.7 ± 8.2	97.1 ± 1.4
00	87.1 ± 2.0	11.5 ± 2.3	99.6 ± 0.4
500	88.1 ± 1.5	10.6 ± 0.8	99.4 ± 0.3
1000	84.9 ± 2.3	14.2 ± 1.6	99.8 ± 0.1
2000	83.5 ± 1.3	16.0 ± 1.8	99.9 ± 0.4
3000	86.5 ± 2.0	14.2 ± 0.8	99.4 ± 0.1
4000	88.2 ± 1.0	13.4 ± 0.4	99.9 ± 0.4

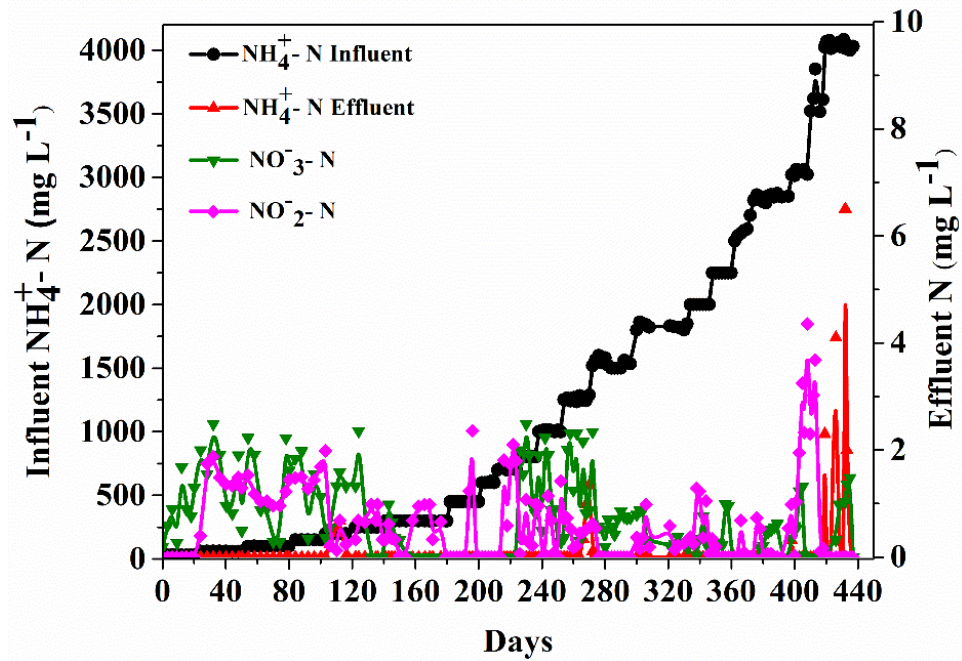


Fig. 2.3 Time course nitrogen removal performance of 1 L aerobic granular sludge sequencing batch reactor operated at different influent ammonium concentrations.

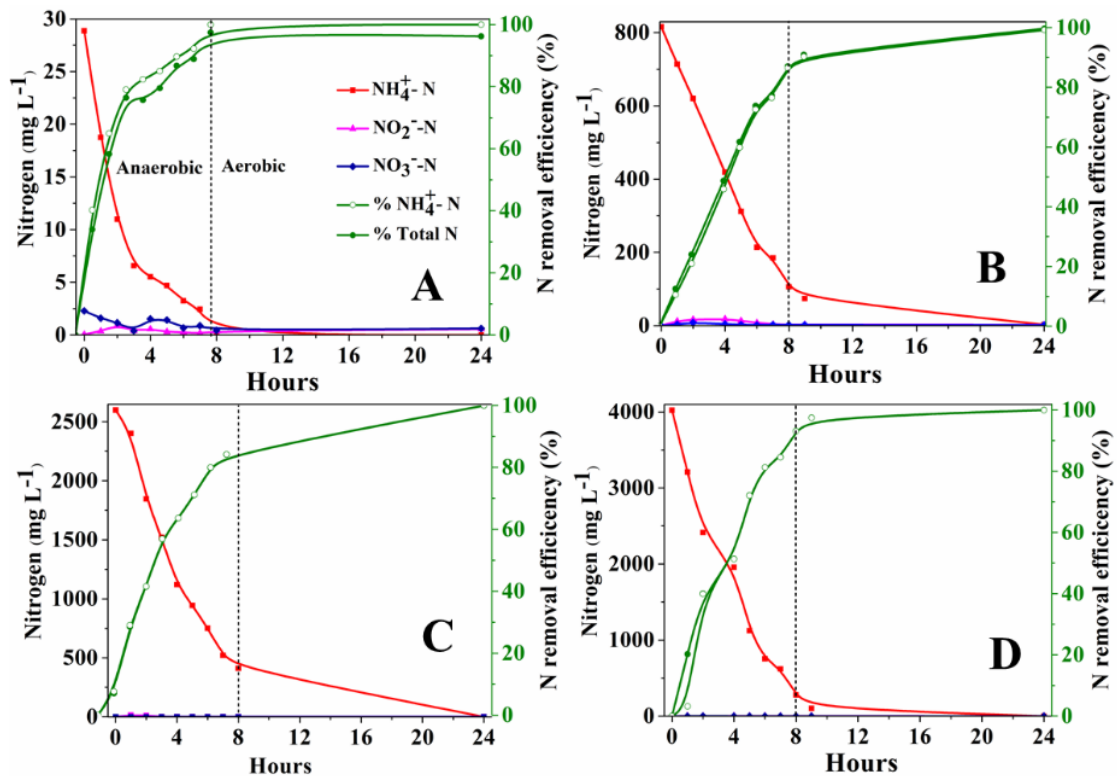


Fig. 2.4. Ammonium, nitrate and nitrite removal kinetics in SBR individual cycles at different $\text{NH}_4^+\text{-N}$ concentrations of 30 mg L^{-1} (A), 800 mg L^{-1} (B), 2500 mg L^{-1} (C), 4000 mg L^{-1} (D).

The distinct features of this study include: (i) efficient and complete nitrogen removal process for up to 4000 mg L⁻¹ NH₄⁺-N, (ii) removal of majority of the influent ammonium (and nitrogen) in the non-aeration phase (first 8 h of cycle), (iii) ammonium and TN removal efficiencies at varied and lower COD/N ratios, (iv) release of only minor quantities of nitrite and nitrate during ammonium ion removal and (v) long-term stability of granular structure and BNR activity at lower COD/N ratios (≤ 1). NH₄⁺-N and TN removal efficiencies were approximately 99.9% and 99.3%, respectively, and stable during long term SBR operation. A stepwise increase in NH₄⁺-N concentration from 30 to 4000 mg L⁻¹ with a fixed lactate concentration in the influent led to a substantial decrease in the COD/N ratio from 18.3 to 0.13. Interestingly, lower COD/N ratios had no detrimental impact on AGS performance in removing NH₄⁺-N or TN.

The kinetics of reactive nitrogen compounds (NH₄⁺-N, NO₃⁻-N and NO₂⁻-N) during individual cycles at different initial NH₄⁺-N concentrations were shown in Fig. 2.4. Typically, ammonium removal profiles could be distinguished into a logarithmic removal phase followed by a slow removal phase. Lag phases were not evident in the NH₄⁺-N removal profiles, irrespective of higher initial ammonium concentrations. Notably, ammonium removal followed similar patterns at different initial NH₄⁺-N concentrations. No major increase in the concentration of nitrate or nitrite was evident at higher ammonium concentrations (Fig. 2.4). Phosphorus removal was ~50% and remained stable (Fig. 2.5). Phosphorus removal was not having any distinct anaerobic-aeration profile, rather a simple consumption profile for meeting the cellular demand (Fig. 2.5B). Hence, the AGS cultivated was not suitable for effective P removal.

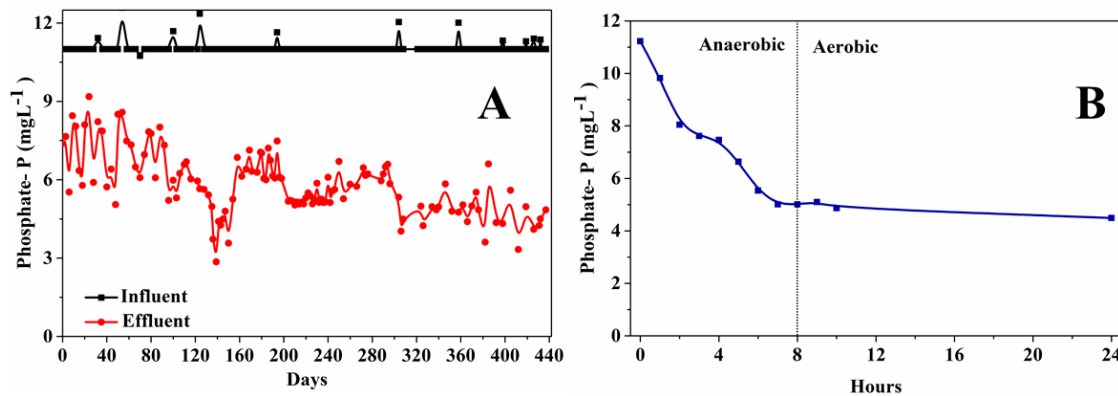


Fig. 2.5 Time course phosphorus removal performance at different influent ammonium concentrations (A). Phosphorus removal kinetics in a single SBR cycle while treating 4000 mg L⁻¹ ammonium (B).

2.3.4 Microbial community

MiSeq sequencing of 16S rRNA gene from sludge treating 500 and 4000 mg L⁻¹ NH₄⁺-N were presented in Fig. 2.6. The number of OTUs decreased with the increase in influent ammonium concentration from 500 to 4000 mg L⁻¹ NH₄⁺-N (Fig. 2.6A). These results clearly revealed that increasing NH₄⁺-N concentrations from 500 to 4000 mg L⁻¹ was related to lower bacterial diversity and species richness (Fig. 2.6A). Shannon, Chao and Simpson indices showed decreased bacterial species richness as NH₄⁺-N increased from 500 to 4000 mg L⁻¹ (Fig. 2.6A). Proteobacteria (57.7%), Firmicutes (16%), Bacteroidetes (7.4%), Planctomycetes (4.5%), Chloroflexi (3.9%), and Nitrospirae (3.38%) were the main phyla found in the AGS treating 500 mg L⁻¹ NH₄⁺-N. The changes in the relative abundance of Proteobacteria (53.2%), Firmicutes (4%), Bacteroidetes (17.5%), Planctomycetes (5.5%), Chloroflexi (4.4%), and Nitrospirae (4.6%) was observed 4000 mg L⁻¹ NH₄⁺-N (Fig. 2.6B). A major shift from γ -Proteobacteria (27 to 0.002%) to β -Proteobacteria (15 to 49%) was observed while treating 4000 mg L⁻¹ NH₄⁺-N. Several members of Nitrospirales, Chitinophagales, Rhodocyclales, Competibacterales, and Xanthomonadales are known for performing ammonium oxidation and denitrification were enriched in the AGS (Fig. 2.6B).

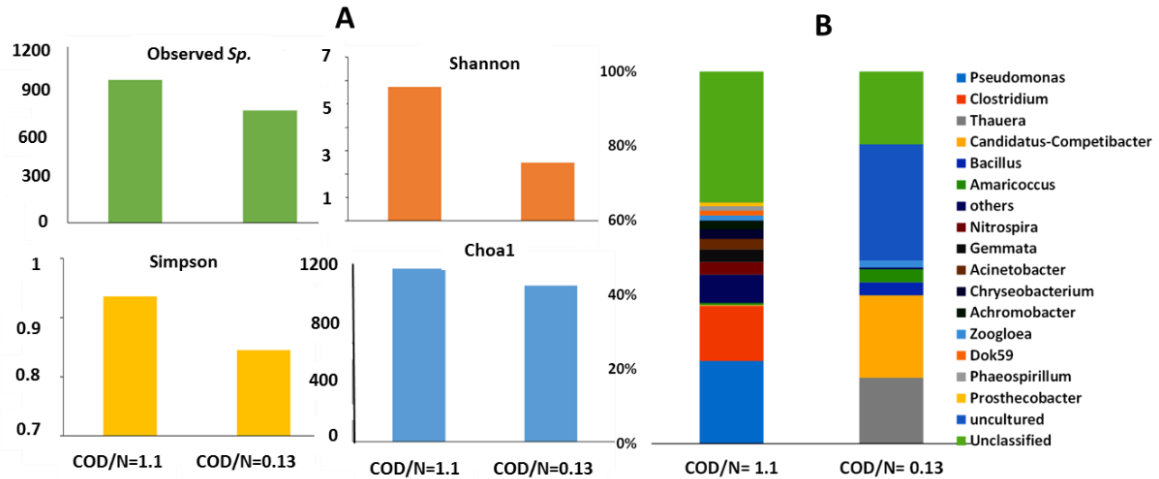


Fig. 2.6 Number of bacterial species and diversity indices (A), Bacterial community structure at genus level observed in the aerobic granular sludge performing biological nitrogen removal from synthetic wastewater containing 500 and 4000 mg L⁻¹ NH₄⁺-N at lower COD/N ratios of 1.1 and 0.13, respectively. Abundance of sequences representing >1% of the total annotated sequences was considered.

Bacteria that could be classified up to species level along with their role in nitrogen cycle were listed in Table 2.2. Organisms of Gemmatimonadetes phylum and *Nitrospira* genus which can perform anaerobic ammonia oxidation and complete ammonia oxidation, respectively, are enriched in the community. Organisms of *Pseudomonas* genus which can perform heterotrophic denitrification dominating at 500 mg L⁻¹ NH₄⁺-N was eventually eliminated from the community. Interestingly, *Candidatus* Competibacter, a glycogen accumulating organism (GAO) and competitor to polyphosphate accumulating organisms (PAOs) and *Thauera* were enriched in the community up to 20% and 16%, respectively, at the genus level while treating 4000 mg L⁻¹ NH₄⁺-N (Fig. 2.6B). Previous reports suggest that *Competibacter* sp. can utilize lactate anaerobically and perform denitrification^{66,67}. *Thauera* is also known for denitrification and nitrogen accumulation⁶⁸.

Table 2.2 List of microorganisms related to nitrogen removal pathways identified in the aerobic granular sludge treating high strength ammonium concentrations

Microorganism	Prominent function
<i>Methylobacterium adhaesivum</i>	Ammonium oxidation
<i>Stenotrophomonas geniculata</i>	-do-
<i>Novosphingobium capsulatum</i>	-do-
<i>Nannocystis exedens</i>	Ammonium oxidation and Denitrification
<i>Agromyces mediolanus</i>	Aniline assimilation
<i>Gemmata obscuriglobus</i>	Anammox
<i>Methanobreibacter arboriphilus</i>	AOA metabolism
<i>Pseudomonas mexicana</i>	Denitrification
<i>Acidovorax delafieldii</i>	-do-
<i>Nostocida limicola</i>	-do-
<i>Erythobacter nanhaisediminis</i>	-do-
<i>Brevidomonas diminuta</i>	-do-
<i>Anoxybacillus kestanbolensis</i>	-do-
<i>Prostheco bacter debontii</i>	-do-
<i>Pseudomaonas citronellosis</i>	-do-
<i>Stenotrophomonas acidaminiphila</i>	-do-
<i>Desulfovibrio putealis</i>	-do-
<i>Pseudomonas nitroreducens</i>	-do-
<i>Roseibium denhamense</i>	-do-
<i>Paracoccus aminovorans</i>	-do-
<i>Pseudoxanthomonas indica</i>	-do-
<i>Pseudoclavibacter bifida</i>	-do-
<i>Staphylococcus haemolytica</i>	-do-
<i>Aeromonas taiwanensis</i>	-do-
<i>Azotobacter armeniacus</i>	Nitrogen fixation
<i>Bosea genosp</i>	Nitrogen fixation
<i>Aquicola tertiaricarbonis</i>	GAO metabolism
<i>Blastomonas natatoria</i>	Phototroph
<i>Burkholderia tuberum</i>	Symbiotic nitrogen fixation
<i>Pseudomonas carboxydohydrogena</i>	Uses CO as carbon source

Quantitative PCR data supported enrichment of AOB, ammonia oxidizing archaea (AOA), anammox bacteria, *Nitrospira* and denitrifiers at $\text{NH}_4^+\text{-N}$ concentrations of 1000 and 4000 mg L^{-1} as compared to 500 mg L^{-1} (Fig. 2.7). Enrichment was significant in terms of a 5-fold increase in AOB, *Nitrospira* and 2- to 3-fold increase in anammox, denitrifying and AOA communities. However, a decrease in AOA was reported while treating wastewater containing 262 mg L^{-1} $\text{NH}_4^+\text{-N}$ than low-strength ammonium wastewaters⁶⁹. Although both

AOA and AOB were detected, AOB were the dominant at higher ammonium concentrations. In contrast, no major change in AOA was observed at higher ammonium concentrations in the present study.

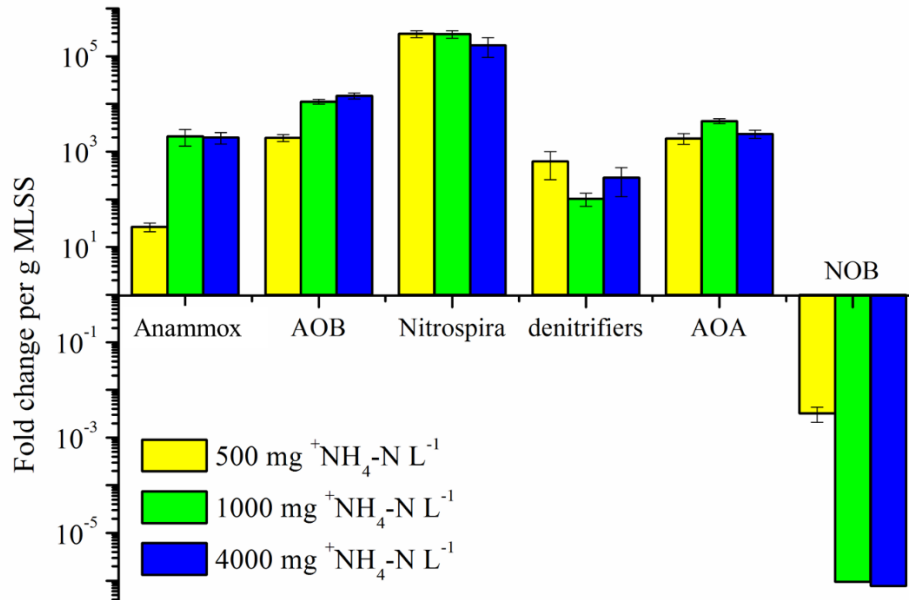


Fig. 2.7. Quantitative PCR for detecting BNR performing organisms in aerobic granular sludge removing ammonium and total nitrogen from synthetic medium containing 500, 1000 and 4000 mg L⁻¹ NH₄⁺-N.

2.3.5 Granular stability at lower COD/N ratios

Due to the changes in HRT (from 9 h to 34 h) and substrate (from acetate to lactate), granules have initially developed irregular fluffy growth on the edges. However, aerobic granules quickly got rid of the fluffy growth and became denser. During SBR operation, the biomass concentrations increased to about 8.4 g L⁻¹ (Fig. 2.8A). Size of the granules also increased and stabilized between 1.3 and 1.5 mm (Fig. 2.8B). SVI decreased steadily and stabilized at <15 ml g⁻¹, indicating compact microbial structure (Fig. 2.8A). SEM images also revealed compact microbial structure in the aerobic granules (Fig. 2.9). SEM-EDX did not show any signatures of ammonium precipitates like struvite in AGS. The structure of aerobic granules was stable while achieving ammonium and nitrogen removal at higher NH₄⁺-N concentrations during 440 days. The settling characteristics of aerobic granules were not significantly

affected when COD/N ratio was ≤ 1 . Disintegration of granular sludge was not evident at lower COD/N ratios. Granules were compact and exhibited superior settling properties during steady-state reactor operation (Fig. 2.8; Fig. 2.9).

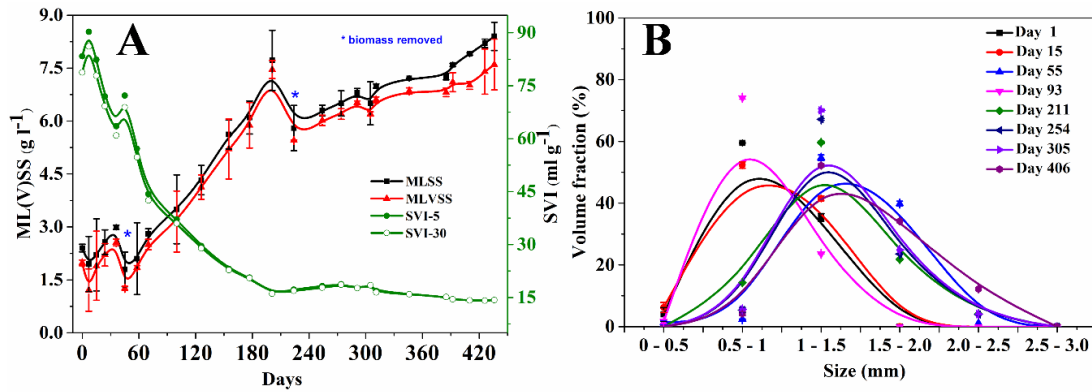


Fig. 2.8 MLSS and SVI (A) and particle size distribution (B) of sludge treating different influent $\text{NH}_4^+\text{-N}$ (30 to 4000 mg L^{-1}) and COD/N ratios (18.3 to 0.13) in 1 L aerobic granular sludge SBR.

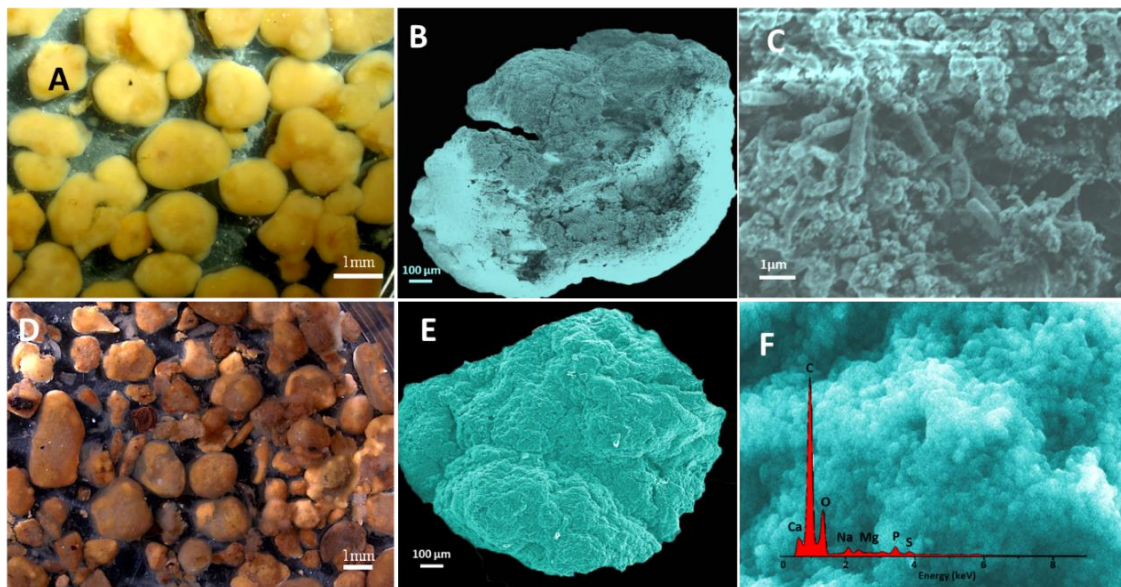


Fig. 2.9 Stereomicroscopic and scanning electron microscopic images of aerobic granular sludge performing nitrogen removal from synthetic wastewater containing 500 mg L^{-1} (A, B and C) and 4000 mg L^{-1} (D, E and F) $\text{NH}_4^+\text{-N}$ at different COD/N ratios. Inset (F) shows EDX spectrum of single microbial granule treating 4000 mg L^{-1} .

This contrasts with previous study that, a decrease in COD/N ratio from 4 to 1 was detrimental to the settleability of aerobic granules⁶⁰. Stability of ammonium removing granules observed in the present study could be related to the operational conditions which are conducive for

selection of slow-growing AOB and anammox bacteria. This was also evident from the reduction in bacterial diversity at $4000 \text{ mg L}^{-1} \text{ NH}_4^+\text{-N}$. These results strongly suggest that AGS technology is suitable for treating ammonium-rich wastewaters typically characterized with lower COD/N ratios.

2.3.6 Nitrogen removal mechanisms

Majority of the ammonium was removed in the first 8 h (Fig. 2.4) which did not receive aeration. The DO present in the feed gradually decreased and reached to 0.08 mg L^{-1} in the first 60 min and stabilized thereafter. Based on DO levels, cycle could be distinguished into anaerobic (non-aerated) and aeration phases. The phase immediately after filling was considered anaerobic wherein the DO was found to be at 0.08 mg L^{-1} due to microbial respiration. Batch experiments also showed that AGS was able to remove ammonium completely under anaerobic conditions. Ammonium removal from the medium was negligible in the absence of AGS under the experimental conditions. Removal of ammonium was decreased to marginal at 3.2% when AGS was killed by autoclaving. However, ammonium removal of up to 18% was reported by autoclaved granules⁷⁰. In long term reactor experiments, adsorption is not considered important for the nitrogen balance calculations since the adsorbed ammonium will be desorbed and/or available for biological conversions⁷¹. A close relation between the DO profile and COD removal pattern was observed during the cycle. COD removal pattern was corroborated with low DO in the liquid phase. Majority (70%) of the COD was removed during the first 8 h. Consumption of DO in the oxidation of COD and NH_4^+ in the first one hour led to anaerobic condition in the AGS reactor. In the subsequent aeration phase, the DO reached to about 2 mg L^{-1} and stabilized at this concentration for the next 2 h. Afterwards, DO increased and stabilized at 7 mg L^{-1} till the end of aeration phase. This DO saturation period was coincided with negligible COD in the SBR. The COD profiles followed similar trend irrespective of initial $\text{NH}_4^+\text{-N}$ concentration.

Low DO and mesophilic temperature (30 °C) are favourable for AOB enrichment in the microbial community^{35,69}. These experimental conditions impose selection for AOB in the AGS and washout of NOB from the bioreactor. The reason for detection of low nitrite could be due to its consumption in other parallel metabolic reactions such as further oxidation to nitrate or reduction to N₂. However, negligible quantities of nitrate were detected in the SBR indicating the possibility of short-cut BNR (nitrification and denitrification). Electron donor availability is a crucial parameter that determines selection of microorganisms and BNR removal pathways. COD removal was consistent and stable at different influent NH₄⁺-N concentrations. Measurements of reactive nitrogen compounds during 24 h cycle showed that (i) most of the ammonium-nitrogen (~86%) was removed in the anaerobic phase (first 8 h) and (ii) ammonium ion removal was associated with release of minimal amounts of nitrite and nitrate (Fig. 2.4). SEM-EDX analysis did not show ammonium precipitates (i.e., struvite), if any, in the granules. Possible BNR pathways for removing ammonium were depicted in Fig. 2.10. Lower COD/N ratio (< 1) was encountered in this study when influent contained 500 mg L⁻¹ or higher NH₄⁺-N. At these higher NH₄⁺-N levels, the electron donor (lactate) supplied at 5.26 mM was insufficient as compared to the electrons required for complete reduction of nitrite or nitrate emanating from NH₄⁺-N oxidation. For example, complete reduction of nitrate and/or nitrite emanating from 4000 mg L⁻¹ NH₄⁺-N oxidation via classical nitrification-denitrification (ND) and short-cut BNR pathways, respectively, requires about 100 and 50 mmoles of lactate. Thus, ND or short-cut BNR pathways cannot fully account for the observed BNR efficiencies especially when influent NH₄⁺-N was 500 mg L⁻¹ and higher. At lower COD/N ratios, anammox can be other major operating BNR pathway which generates nitrate in trace amounts. The electron requirement for the denitrification of nitrate formed via anammox cannot be met by the available lactate. Therefore, existing nitrogen pathways cannot fully explain the removal of high-strength ammonium at lower COD/N

ratios. Though presence of several groups of denitrifying organisms in the community, experimental conditions (i.e., low DO and low COD/N ratio) and measured profiles of nitrogen compounds suggest division of metabolic labour through partial nitrification (nitritation) followed by anammox pathway, it cannot completely account for high-strength ammonium used in this study. Therefore, ammonium removal by other novel pathways is predicted because of stable removal, no accumulation of intermediates, no possibilities for stripping and significant removal under non-aerated condition.

Free ammonia (FA) and free nitrous acid (FNA) generated at high ammonium concentration can be inhibitory to AOB and NOB. The concentrations of FA and FNA are influenced by effects of temperature and pH on the equilibrium between $\text{NH}_4^+ \rightleftharpoons \text{NH}_3$ and $\text{NO}_2^- \rightleftharpoons \text{HNO}_2$ ⁷². Moreover, susceptibility of AOB and NOB species to FA and FNA differ from each other⁷². The reported levels of FA concentrations that can inhibit AOB activity were 10 to 50 mg L⁻¹ NH₃-N⁷³ and 4.06 to 22.4 mg L⁻¹ NH₃-N⁵³. However, activity of *Nitrobacter* was reported to be diminished at 0.1 to 1.0 mg L⁻¹ NH₃-N^{70,72}. FNA is a known antibacterial agent and can disrupt respiration in *Pseudomonas aeruginosa* at a concentration as low as 0.1 mg L⁻¹ HNO₂-N⁷⁴. Under the experimental conditions of this study, FNA formation was estimated to be at 1.94 mg L⁻¹ at 4000 mg L⁻¹ NH₄⁺-N. Therefore, FNA formation was very minor as compared to previous studies⁷⁴. Disappearance of *Pseudomonas* genus and NOB at 4000 mg L⁻¹ NH₄⁺-N could be related to production of minor concentrations of FNA or FA which exceeded the reported threshold concentrations for inhibition. These results were in agreement with previous work that NOB is inhibited in the presence of 1.5 mg L⁻¹ FA⁷⁰. The changes in microbial community supported this contention and revealed the presence of AOB, anammox bacteria, comammox bacteria and heterotrophic denitrifying bacteria in the aerobic granules. NOB was not detected in the community performing high-strength ammoniacal nitrogen

removal at lower COD/N ratios. Overall, a significant reduction in common core of genes led to a new set of microbial genera capable of performing BNR at lower COD/N ratios.

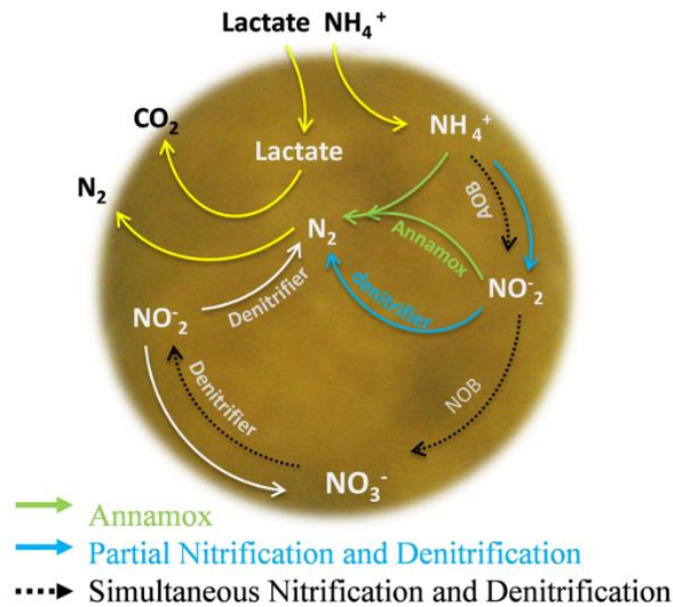


Fig. 2.10 Proposed biological nitrogen removal pathways operating in aerobic granular sludge reactor removing high-strength ammonium at lower COD/N ratios. The proposed existing mechanisms cannot fully account for ammonium removal by AGS under low COD/N condition, suggesting possibilities for novel nitrogen removal pathways.

2.4 Conclusions

This study demonstrated effective nitrogen removal in AGS reactor operated with alternating anaerobic-aerobic phases at different loadings rates of 0.3 to 4 kg $\text{NH}_4^+\text{-N m}^{-3} \text{d}^{-1}$. High ammonium and total nitrogen removals were achieved even at COD/N ratios <1. Removal of up to 4000 mg L^{-1} $\text{NH}_4^+\text{-N}$ from synthetic wastewater was accompanied by formation of subtle quantities of nitrite and nitrate. Stable biological nitrogen removal was recorded while treating 4000 mg L^{-1} $\text{NH}_4^+\text{-N}$ and long term SBR operation (440 days). Enrichment of AOB, anammox bacteria and denitrifying bacteria and washout of NOB was observed at lower COD/N ratios. Nitrification and anammox were the major BNR pathways operating at lower COD/N ratios.

Chapter 3

Granulation and enrichment of nitrogen and phosphorus removing organisms in the presence of charcoal particles

Abstract

Cultivation of aerobic granular sludge and nutrient removal were investigated in sequencing batch reactors (SBR) with and without coconut shell charcoal (CSC) particles by using acetate (HAc), propionate (HPr) or acetate-propionate (HAc-HPr) as carbon source. Short-term experiments showed that addition of CSC particles to activated sludge increases the aggregation index and settleability. This has aided in minimizing washout of activated sludge inoculum from the SBR during initial days of operation. By acting as substratum for bacterial attachment and growth of particulate biofilms, addition of CSC particles hastened the formation of granules. Formation of biofilms and granules has led to effective biomass retention and rapid establishment of biological nutrient removal (BNR) pathways. HAc and HAc-HPr were found to be suitable over HPr for both granulation and establishment of BNR pathways. COD, ammonium, total nitrogen (TN), and phosphorus removals were stabilized at >94%, >95% and >90%, respectively, in CSC-augmented SBR. Removal of phosphorus was achieved through enhanced biological phosphorus removal (EBPR) pathway by phosphorus accumulating organisms (PAOs). Sequencing of 16S rRNA gene revealed higher enrichment of PAOs, denitrifying PAOs, and ammonia oxidizers in CSC-augmented SBR. Addition of CSC particles to SBRs appears to be simple strategy for improving granulation and rapidly establishing BNR pathways in granular reactors.

Keywords: Aerobic granulation, Carbon substrate, Charcoal particles, EBPR, Nitritation-denitritation.

3.1 Introduction

Aerobic granular sludge (AGS) process is an emerging biological wastewater treatment technology that relies on bacteria-laden granules for removing organic carbon, nitrogen, and phosphorus and other contaminants from wastewater^{24,27}. AGS is cultivated by operating the bioreactor in sequencing batch reactor (SBR) mode that allow selection of fast settling biomass over slow settling biomass⁷⁶. The conditions that allow selection of slow-growing bacteria is important for cultivating stable AGS^{6,75}. For instance, SBR is primarily operated with a cycle consisting of an initial anaerobic (filling) and subsequent aeration phases. The readily biodegradable organic substrate supplied during anaerobic filling phase is taken up inside the cells and converted to storage polymers (e.g., glycogen, and polyhydroxyalkanoate) by specialist organisms called polyphosphate accumulating organisms (PAOs). In the subsequent aerobic phase, these organisms utilize endogenous stored polymers for accumulating inorganic phosphate as polyphosphate inside the cells. This kind of microbial metabolism is useful for selecting relatively slow-growing bacteria and developing stable granules⁷⁵.

Reliable cultivation of granules, maintenance of granular stability and efficient biological nutrient removal (BNR) are important to the successful implementation of AGS in wastewater treatment plants. Apart from other factors, type of organic substrate and addition of nucleating agents (substratum for bacterial attachment) have received attention for improving granulation and nutrient (i.e., nitrogen and phosphorus) removal capabilities. Defined carbon sources such as acetate (HAc), propionate (HPr), ethanol and xenobiotic compounds have been used for developing granules from activated sludge²⁷. HAc and HPr account for about 50-70% and 24-33% of volatile fatty acids (VFAs), respectively, in municipal wastewaters⁷⁷. The intracellular uptake of VFAs under anaerobic conditions and their conversion to storage polymers intracellularly is important for granulation and granular stability. Although early

studies have evaluated several organic substrates on cultivation of granules, there are limited to no studies on the effect of carbon source on granulation and BNR pathways under tropical climate conditions. Hence, the effect of different VFAs such as HAc, HPr, and HAc-HPr combination was investigated on granulation of activated sludge and BNR in SBRs.

For cultivating AGS, SBRs are often inoculated with activated sludge and operated with short settling time. But, application of short settling times is associated with loss of biomass from the SBR during initial cycles. Loss of biomass can cause long start-up periods for establishment of BNR pathways. Moreover, long start-up periods of up to 10 months have been reported for cultivating AGS while treating real domestic wastewaters⁷⁸. Therefore, novel strategies aimed at minimizing biomass loss, selection of BNR organisms, and enhancing granulation are desired. Addition of materials including granular activated carbon (GAC), yellow earth, biochar, and magnetite have been proposed for enhanced granulation of activated sludge^{42,79,80}. Among these external agents, GAC or biochar addition appears to be technically suitable for application in large scale wastewater treatment systems. However, their role in minimizing biomass washout, selection and retention of BNR organisms, particularly PAOs is lacking. Thus, the other objective of this study was to investigate the effect of charcoal particles addition on granulation of activated sludge, nutrient removal and underlying mechanisms.

The study was focussed mainly on the role of type of organic carbon source, and charcoal particles addition on granulation of activated sludge, BNR and probable mechanisms. Experimental results on granulation and BNR in parallel SBRs by using different carbon sources such as HAc, HPr, and HAc-HPr were presented in this chapter. Subsequently, granulation of activated sludge and BNR were investigated in the presence of charcoal particles by feeding HAc and HAc-HPr as carbon sources.

3.2 Materials and methods

3.2.1 Source of biomass

Activated sludge was collected from the aeration tank of an operating municipal wastewater treatment plant at Kalpakkam Township, Tamil Nadu, India. Activated sludge (3.5 g L^{-1} , dry weight) was added at the beginning of experiment to each of the SBR. Activated sludge acted as the source of microorganisms for cultivating bacterial granules in the bioreactors.

3.2.2 Simulated wastewater

Simulated wastewater containing $0.05 \text{ g L}^{-1} \text{ K}_2\text{HPO}_4 \cdot 2\text{H}_2\text{O}$, $0.041 \text{ g L}^{-1} \text{ KH}_2\text{PO}_4$, $0.01 \text{ g L}^{-1} \text{ CaCl}_2 \cdot 2\text{H}_2\text{O}$, $0.01 \text{ g L}^{-1} \text{ MgSO}_4 \cdot 7\text{H}_2\text{O}$, $0.04 \text{ g L}^{-1} \text{ NaHCO}_3$ and 0.1 mL L^{-1} trace elements stock was prepared in demineralized water. The trace elements stock solution contained the following (g L^{-1}): FeSO_4 (0.54), ZnSO_4 (0.4), MnCl_2 (0.1), $\text{CuSO}_4 \cdot 5\text{H}_2\text{O}$ (0.25), $\text{CoCl}_2 \cdot 6\text{H}_2\text{O}$ (0.5), $\text{NiCl}_2 \cdot 6\text{H}_2\text{O}$ (0.19), $\text{NaMoO}_4 \cdot 2\text{H}_2\text{O}$ (0.22), and H_3BO_4 (0.014). Sodium acetate, and sodium propionate were added directly to the simulated wastewater to provide give a chemical oxygen demand (COD) of 500 mg L^{-1} . Ammonium-N and phosphate-P concentrations were kept at 30 and 5 mg L^{-1} , respectively. The initial concentrations of nutrients mentioned in the graph refer to the concentrations in the reactor immediately after filling.

3.2.3 Coconut charcoal particles preparation

Coconut shell charcoal (CSC) particles were used for studying the effect of external materials on granulation. CSC particles was prepared from commercial coconut shells which were prepared through pyrolysis. The coconut charcoal shells were made into smaller particles by grinding. These particles were then fractionated into three size groups, (i) $>0.5 \text{ mm}$, (ii) $0.25\text{--}0.5 \text{ mm}$, and (iii) $0.125\text{--}0.25 \text{ mm}$ by sieving. The obtained CSC particles were suspended in demineralised water with bubble aeration for about 5 h to remove the dissolved gases, if any, and dredge blocked pores prior to use. CSC particles with an average particle size of

0.33±0.06 mm (fraction 0.25-0.5 mm) were mostly suspended in the water column during bubble aeration. Hence, this size fraction was used for study. The surface area and pore volume of CSC particles was determined to be 1250 m² g⁻¹ and 0.59 cm³ g⁻¹, respectively.

3.2.4 SBR setup and operation

Transparent polycarbonate columns (working height: 62 cm; diameter: 9 cm) were used as bioreactors for studies on granulation. Each column having 3 L working volume was operated in SBR mode with 6 h batch and 4 batches per day. The 6 h cycle contained static plug-flow filling (60 min), aeration (270 min), settling (10 min), decant (10 min), and idle (10 min) periods. After 2 days, settling time was decreased to 4 min. Unit operations such as switching on/off of feed pump, aeration pump, and drain pump during each batch was controlled by electronic timers and programmable logic controllers (PLC). Air was supplied from the bottom of the SBRs at an air flow rate of 2 L min⁻¹ corresponding to 0.5 cm s⁻¹ superficial air velocity (SAV). Dissolved oxygen (DO) was not controlled but found to be low (<0.08 mg L⁻¹) during filling phase and reached saturation concentrations (~7 mg L⁻¹) during aeration phase. The treated wastewater (effluent) was withdrawn through an outlet port located at a height of 17 cm from bottom of the SBR resulting in a volumetric exchange ratio of 66%. The pH was not controlled but was observed to vary between 7.6 and 8.0 in 6 h batch. The experiments were performed at an ambient temperature of 31±5 °C and relative humidity of >85%. The liquid samples collected regularly from the SBRs were centrifuged at 10000 g for 10 min, and stored at 4 °C.

3.2.5 Effect of carbon source on granulation

The 3-litre volume SBRs as described above were operated in parallel using HAc (R1), HPr (R2) and HAc-HPr (R3) as carbon sources. The SBRs were inoculated with 3.5 g activated sludge and fed with synthetic wastewater containing 500 mg L⁻¹ COD (HAc, HPr or HAc-HPr), 30 mg L⁻¹ NH₄⁺-N and 5 mg L⁻¹ PO₄³⁻-P. The SBRs were operated for 70 days at

ambient room temperature ($31\pm 5^{\circ}\text{C}$) and humidity ($>85\%$) to evaluate granulation and nutrient removal performance. Biomass was sampled once a week for monitoring granulation. Liquid samples were collected regularly and monitored for nutrients.

3.2.6 Effect of CSC particles on granulation

3.2.6.1 Granulation in the presence of different amounts of CSC particles

Four 3-litre volume SBRs (A1 to A4) were inoculated with activated sludge and operated for 30 days. A1 was operated without CSC particles. While A2, A3 and A4 were augmented onetime at the beginning with 3 g, 6 g and 9 g CSC particles, respectively. All the four SBRs were operated under identical conditions using HAc as the sole carbon source. The SBRs were operated with 6 h batch and 4 batches per day as detailed above. Granulation and nutrient removal were monitored.

3.2.6.2 Granulation in the presence of CSC particles and different carbon sources

Two 3 litre volume SBRs (CR1 and CR2) as described above were inoculated with 3.5 g L^{-1} activated sludge and augmented with 9 g CSC particles. CR1 was fed with HAc containing synthetic wastewater. While CR2 was fed with HAc-HPr containing synthetic wastewater. This experiment was continued for 70 days for determining granulation and biological nutrient removal in the presence of different carbon sources. Biomass and liquid samples were collected regularly for monitoring granulation and nutrient removal, respectively.

3.2.7 Analytical methods

Liquid samples were subjected to centrifugation at 10000 g for 10 min to remove the suspended cells. Cell-free supernatant samples were analysed for soluble chemical oxygen demand (COD) using closed reflux method. Ammonium, nitrite and phosphate was measured using Nessler's, N-(1-Naphthyl) ethylenediamine, and molybdenum reagent-based methods, respectively⁶⁴ Nitrate was measured by UltiMate™ high performance liquid chromatograph

(Dionex, USA) with acclaim organic acid column and variable wavelength. Sludge volume index (SVI), mixed liquor suspended solids (MLSS), and mixed liquor volatile suspended solids (MLVSS) were determined following standard methods⁶⁴. Dissolved oxygen and pH were monitored online using LDO and pH probes (Hach, Germany), respectively. Turbidity was measured using turbidimeter (Hach, Germany). The morphology of seed sludge flocs and granular sludge was observed under stereo zoom microscope equipped with a digital camera (Jenoptik, Nikon). Particle size was analysed using *ImageJ* freeware software³¹.

For relative hydrophobicity measurement, 1 g of biomass was collected, washed and suspended in water. The suspension was homogenised using glass bead homogenizer. The suspension was mixed with 8 mL hexadecane, allowed to stand for 30 minutes. After separation, the aqueous phase was carefully transferred for measuring biomass concentration. MLSS was in the aqueous phase before and after emulsification⁸¹. The relative hydrophobicity was calculated by taking the ratio of biomass concentration in the aqueous phase before (MLSS_b) and after emulsification (MLSS_a)⁸².

For settling velocity, biomass particles were dropped at the top of water column in a glass cylinder (dimensions 24.02" L x 24.02" W x 12.99" H). The time taken for reaching these particles to the bottom point was recorded using a stopwatch for calculating settling velocities.

Biomass density was determined by volume displacement technique⁸³. A 100 mL of biomass sample was filtered through 0.45 mm Millipore filter and the wet biomass retained by the filter was transferred to 20 mL of demineralized water. The increase in the liquid volume was determined. Then the dry weight of biomass was determined incubating in hot air oven at 105 °C for 24 h. The biomass density (g cm⁻³) was calculated by dividing the dry weight of the biomass by the volume occupied by wet biomass.

For aggregation test, 10 mL sludge was collected, washed with 1 mM potassium nitrate solution and re-suspended in the same solution. Then 5 mL of sludge suspension ($A_{600\text{nm}}$: 0.45-0.5) was carefully transferred to a cuvette. The changes in the absorbance of the suspension were measured at 600 nm for 40 min. The aggregation capability was measured as, aggregation index (%) = $100 \times ((OD_{t=0} - OD_{t=30}) / OD_{t=0})$.

For flocculation test, 50 mL of biomass was collected in a glass beaker. Absorbance (A_a) was measured at 540 nm. Then it was subjected to homogenization by ultrasonication (20 KHz 40% for 15 sec) in a cold ice bath. Subsequently, the suspension was centrifuged at 1200 g for 2 min. Supernatant was collected immediately, and the absorbance was measured at 540 nm (A_b). The contents along with the pellet after centrifugation was transferred to a glass beaker, and stirred with the aid of magnetic stirrer at the lowest speed (rpm) for 30 min. The contents were subjected for 2nd round of centrifugation at 1200 g for 2 min. The supernatant after 2nd centrifugation step was collected and measured absorbance at 540 nm (A_c) for calculating re-flocculation ability⁸². Flocculation and re-flocculation experiments were carried out in three replicates with different amount of CSC addition.

3.2.8 Extracellular polymeric substances (EPS) matrix

EPS extraction was carried out using sodium carbonate method⁸⁴ with minor modification. The sludge was collected on day 10, 30 and 70 from the SBRs (R1, R3, CR1, and CR2) for determining the EPS content. Activated sludge inoculum was also used for EPS extraction. Briefly, 1 g (dry weight) sludge was added to 250 mL flask containing 100 mL 0.5% (w/v) Na_2CO_3 , stirred at 400 rpm in a water bath for 3 hat $80 \pm 1^\circ\text{C}$. After cooling, the extract was centrifuged at 4000 g, and 4°C for 20 min. Supernatant was collected in a glass bottle and the pH was adjusted to 2.2 with 1 M HCl under stirring. It was subjected to second centrifugation step (4000 g, at 4°C , 20 min) for recovering alginate like exopolysaccharide

(ALE) in the pellet. The amount of sludge used for extraction was quantified in terms of total solids (TS) and volatile solids (VS) according to standard methods⁶⁴.

3.2.9 Microbial community analysis

Bacterial community was determined by performing 16S rRNA based V3-V4 amplicon sequencing on Illumina MiSeq system. Biomass samples collected on day 68 from R1, R3, CR1, and CR2 were used. The genomic DNA was isolated following manufacturers protocol (Qiagen QIAamp DNA Mini Kit). Sequencing was performed at MedGenome Labs Ltd. (Bangalore, India). Briefly, the amplicons were subjected to a sequence of enzymatic steps. The enzymatic steps repair the ends and tailing with dA-tail. Subsequently, the sequences are ligated with adapters, cleaned using SPRI beads and indexed during limited cycle PCR. This generates the final libraries for paired-end sequencing for further processing. The resulting Libraries are quantified before loading on the cBot for cluster generation and sequencing on Illumina MiSeq system to generate 2×250 bp sequence reads. Prepared library was quality checked (below Q30 discarded), Sequenced data was processed to generate FASTQ files. Chimeric sequences generated in PCR was removed using usearch and uchime algorithm. Sequences with similarity (>97%) were grouped using *de novo* method as a single operational taxonomic unit (OTU). A typical sequence from each OTU was used for classification (RDP classifier) against green gene database at 97% similarity. The taxonomy classification of sequences was done at phylum, class, order, family and genus level.

3.3 Results and discussion

3.3.1 Effect of carbon substrate on granulation and nutrient removal

3.3.1.1 Granulation of activated sludge

Time course development of granules in the SBRs operated with HAc, HPr and HAc-HPr is shown in Fig. 3.1. The activated sludge used for inoculation was greyish brown in colour, and comprised of irregular and loosely-structured flocs. During the course of SBR operation, the activated sludge flocs have gradually developed into granules (Fig. 3.1). Granules appeared on day 17 in R1 (HAc) and R3 (HAc-HPr). After day 30, the granules became smooth and round-shaped (Fig. 3.1A). The colour of the granules changed to off-white, and then to light yellow in the end of SBR operation. Among the three reactors, formation of granules was slower in R2 which received HPr as the sole carbon source. The granules formed in HPr-fed reactor had hairy structures (Fig. 3.1B). It corroborates with a previous study that granulation with HPr takes longer time than HAc or mixed carbon substrate⁸⁵. It could be related to HPr toxicity and metabolism. Enrichment of microorganisms capable of metabolizing HPr as carbon and energy source via propionyl-CoA^{86,87} and 2-methylcitric acid cycle⁸⁵ is needed for granulation.

The time course changes in biomass concentration, settling properties and particle size during SBRs operation was shown in Fig. 3.2. At the beginning, the loss of activated sludge from the SBRs was observed and ranged from 1.7 to 2 g L⁻¹ (Fig. 3.2A to 1C). The loss of biomass during the initial days was attributed to lower settling velocities of activated sludge and the applied short settling periods. However, the MLSS values started to increase after a week due to growth and retention of biomass having good setting properties. No major deviation between the MLSS and MLVSS indicated minimal inorganic content in the SBRs. The biomass concentrations steadily increased and reached to 4.5, 3 and 4.8 g L⁻¹ MLSS, respectively, in R1, R2 and R3 by day 70 (Fig. 3.2A and C). A gradual decrease in the SVI

values indicated development of sludge with good settling properties. The sludge developed in the R1 and R3 had lower SVI values of $<50 \text{ mL g}^{-1}$ by day 70, indicating superior settling properties typical of granular sludge. The minimal difference between the SVI_{30} and SVI_5 also indicated smaller fraction of flocs in the system. These changes in the SVI values were also corroborated by a gradual increase in the particle size. Whereas, the SVI values were higher in R3 and ranged from 60 to 100 mL g^{-1} indicating lower settling properties. Although granules were formed in HPr-fed reactor (R2), the granules were smaller in size and had hairy structures.

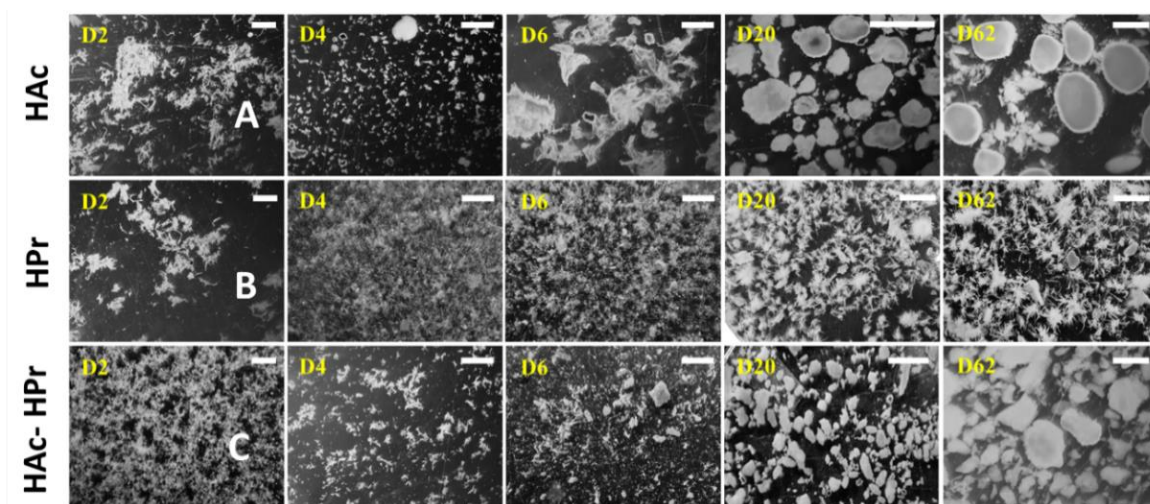


Fig. 3.1. Time course changes in the morphology of sludge and formation of granules in SBRs fed with acetate (HAc) (A), propionate (HPr) (B) and acetate-propionate (HAc-HPr) (C) as carbon substrates. D in D2, D4...D62 refers to day of sampling from the SBRs. Scale bar=1mm.

Apart from SVI values, particle size is a direct parameter for monitoring granulation. A gradual increase in particle size was observed in all three reactors. The particle size has increased and stabilized at 0.9 to 1.2 mm in R1 and R3 that were fed with HAc, and HAC-HPr, respectively. In R2, the particle size was stabilized at about 0.9 to 1 mm.

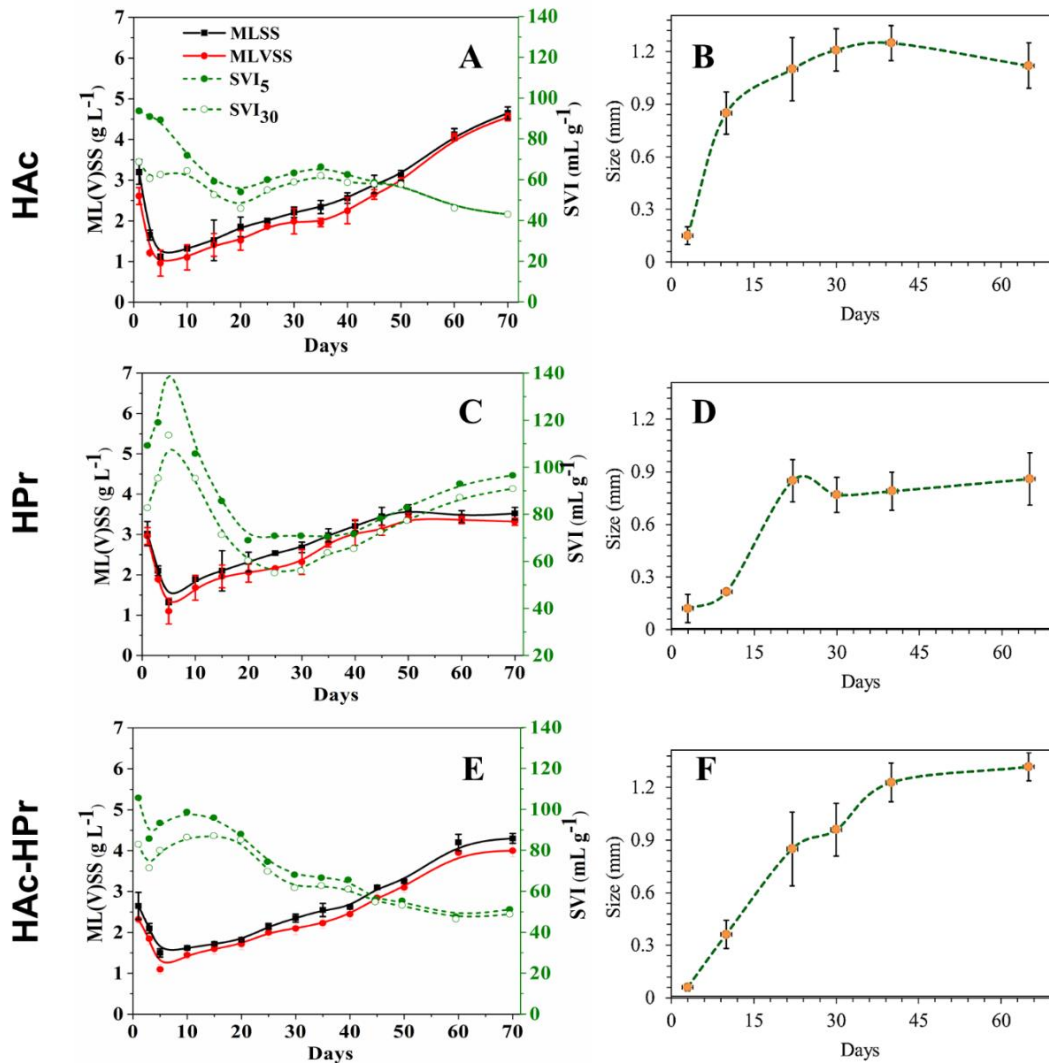


Fig. 3.2. Change in biomass (MLSS, MLVSS), settling properties (SVI₃₀, SVI₅) and particle size in SBRs fed with acetate (A, B), propionate (C, D) and acetate-propionate (E, F) as carbon substrates.

3.3.1.2 SBR performance

Fig. 3.3 shows COD, reactive nitrogen ($\text{NH}_4^+\text{-N}$, NO_3^- , and NO_2^-) and phosphate in the influents, and effluents of three SBRs operated with HAC, HPr, and HAC-HPr containing synthetic wastewater. COD removal has gradually improved and reached to about ~80% by day 15 in all three SBRs (Fig. 3.3A to C). After that, COD removal performance was almost stable until the end (70 days) of the experiment. Ammonium removal was gradually established in the SBRs (Fig. 3.3D to F). Near complete removal of influent ammonium ($30 \text{ mg L}^{-1} \text{ NH}_4^+\text{-N}$) was established by day 38 and 25 in R1 and R3, respectively. After that, the

ammonium concentrations in the effluents of R1 and R2 were maintained below 0.1 mg L^{-1} . In contrast, removal of ammonium was inefficient in R2 fed with HPr as the sole carbon substrate. Although ammonium removal performance was improved during the first 15 days, it was stabilized at 75% resulting residual $8 \text{ mg L}^{-1} \text{ NH}_4^+\text{-N}$ in the effluents of R2 until the end of experiment. Removal of ammonium through nitrification was indicated by release of nitrite and nitrate. Formation of nitrite and nitrate was evident in effluent's concentrations during start-up and in the ammonium removal profiles (Fig. 3.4E). Profiles of reactive nitrogen during 6 h cycle indicated that ammonium removal was accompanied by formation of subtle quantities of nitrite and nitrate (Fig. 3.4D and 4E). Nitrite and nitrate were also removed during the cycle contributing to effective total nitrogen (TN) removals. Minimal effluent nitrite and nitrate concentrations suggest occurrence of nitrification-denitrification and nitrification-denitrification.

Near complete removal of ammonium during cycles resulting $<1 \text{ mg L}^{-1} \text{ NH}_4^+\text{-N}$ in the effluents of SBRs fed with HAc and HAc-HPr (Fig. 3.4D and F) by day 30. Among all three SBRs, R3 fed with HAc-HPr had negligible $\text{NO}_2^-\text{-N}$ and $\text{NO}_3^-\text{-N}$ in the effluents for the whole experimental period. In R1, the effluents had lower levels of $\text{NO}_2^-\text{-N}$ and $\text{NO}_3^-\text{-N}$ only during start-up period. Comparatively, R2 effluents had higher levels of $\text{NO}_2^-\text{-N}$ and $\text{NO}_3^-\text{-N}$ during start-up. However, the effluent $\text{NO}_2^-\text{-N}$ and $\text{NO}_3^-\text{-N}$ concentrations became significantly lower ($<1 \text{ mg L}^{-1}$) in R1 and R2, coinciding with formation of granules. Ammonium and TN removals were highest at 88% and 86%, respectively, in the R3 received mixed carbon substrate (HAc-HPr). HAc fed SBR (R1) also achieved higher ammonium and TN removals of 84% and 80%, respectively. Poor ammonium and TN removals of 35% and 30%, respectively, were recorded in R2 receiving HPr. The poor nitrogen removal performance of R2 was mainly related to incomplete ammonium removal.

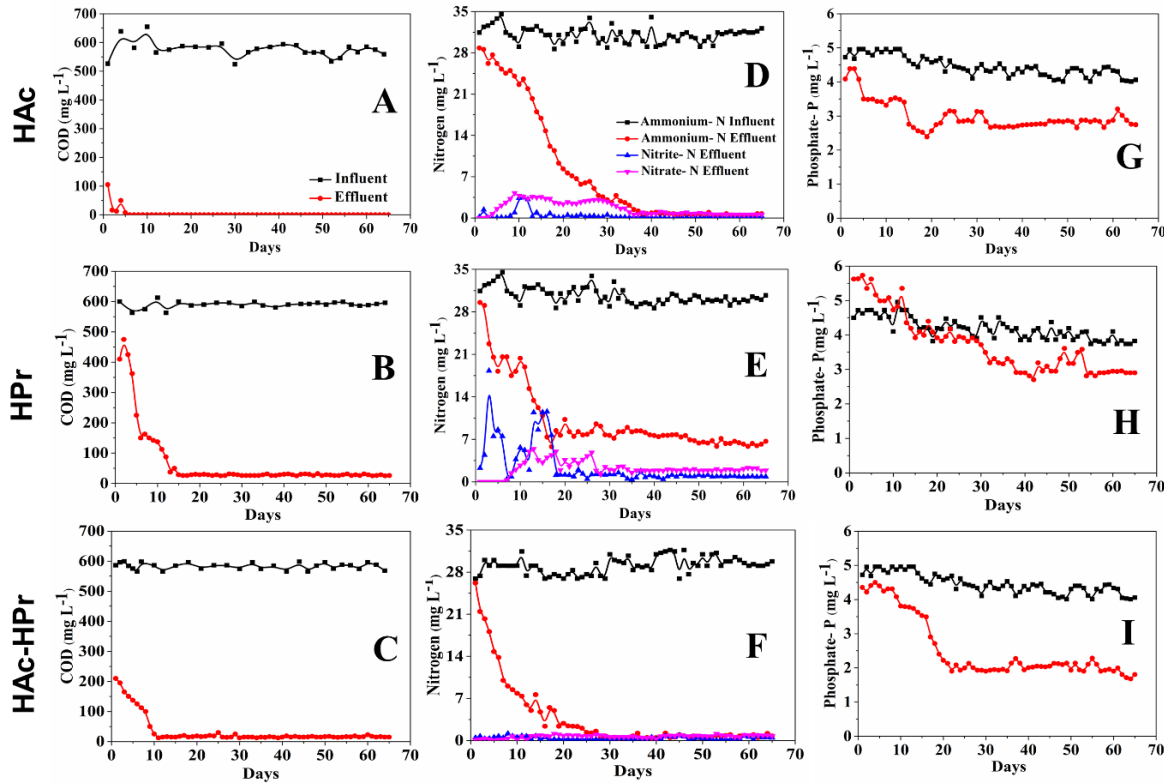


Fig. 3.3. Time course measurements of COD (A to C), nitrogen (D to F), and phosphorus (G to I) in the influents and effluents of SBRs fed with HAC, HPr and HAC-HPr.

A gradual increase in phosphorus removal was observed during the start-up phase of all three SBRs (Fig. 3.3G to I). Later, phosphorus removal was stabilized at about 30% and 40% in R1 (HAC) and R3 (HAC-HPr), respectively. In R2, phosphorus was not removed during the initial days. Due to this, the effluent phosphorus concentrations were higher than the influent phosphorus concentrations until day 10. Afterwards, phosphorus concentration in the effluents became lower than the influents due to establishment of bio-P removal. Comparatively, phosphorus removal was more stable in HAC and HAC-HPr fed SBRs. However, phosphorus removal efficiencies were lower at 30 to 40% of $10 \text{ mg L}^{-1} \text{ PO}_4^{3-}\text{-P}$.

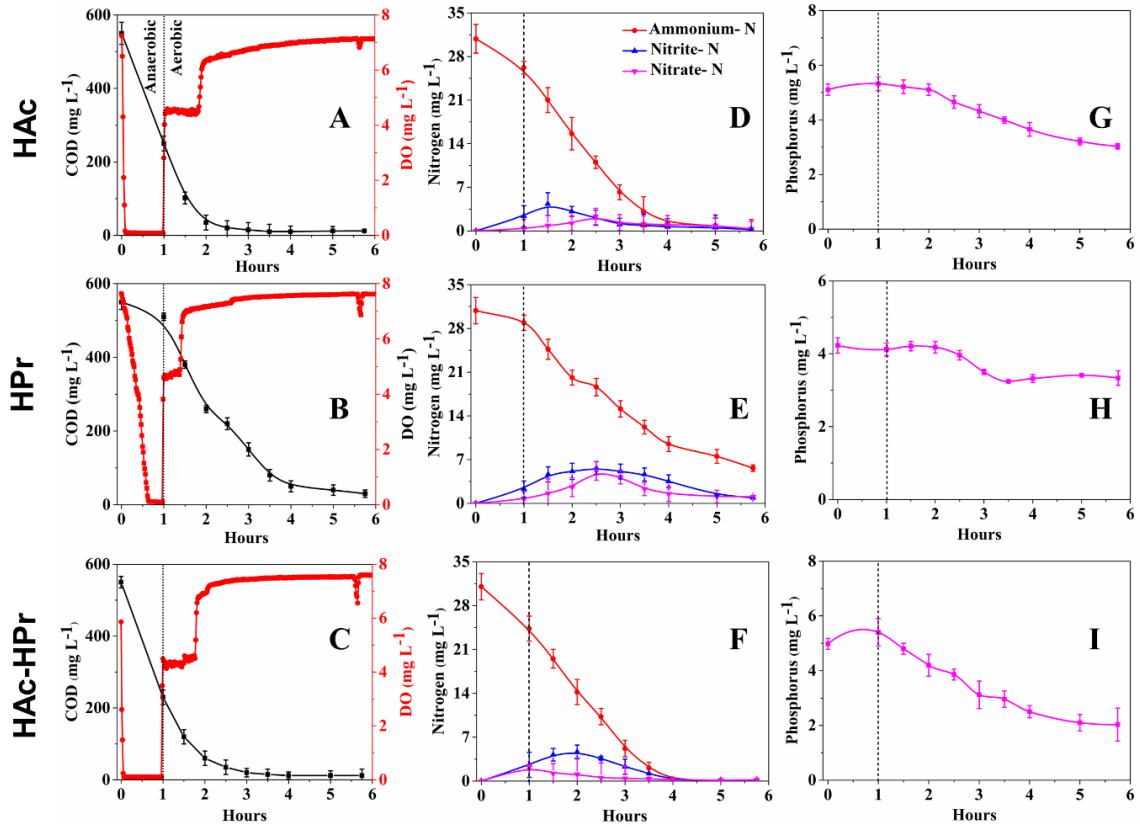


Fig. 3.4. Nutrient removal profiles in individual SBR cycles. Profiles of COD (A,B,C), nitrogen (D,E,F), and phosphorus (G,H,I) in SBRs fed with HAC (A, D, and G), HPr (B, E, and H), or HAC-HPr (C, F, and I).

3.3.2 Granulation and nutrient removal in the presence of CSC particles

3.3.2.1 Granulation of activated sludge

Fig. 3.5 shows time course development of granular sludge in the presence of CSC particles in the SBRs fed with either HAC or HAC-HPr. Within a week, visible microbial growth was seen as aggregates and on the surface of CSC particles. These particles grew in size to macro-scale particles by day 20. Stereomicroscope images clearly depicted microbial growth as distinct particles. CSC particles were clearly seen at the core and surrounded by microbial growth. Microbial growth without the CSC particles was co-existing with growth supported by CSC particles. Thus, sludge growth in the CSC-augmented SBRs could be distinguished into particulate biofilms (biofilm growth on CSC particles) and aggregates/granules. Moreover, the sludge was dominated by biomass particles and devoid of activated sludge

flocs. Fig. 3.6 shows changes in biomass concentrations, settling properties and particle size during 70 days of SBRs operation. Loss of sludge from the CSC-augmented SBRs was observed during the first few days. However, sludge loss was comparatively minimal in the presence of CSC particles. For example, CSC-augmented SBRs had 2 g L^{-1} MLSS as compared to 0.98 g L^{-1} in SBRs without CSC particles on day 10, indicating a role for CSC particles in minimizing activated sludge loss. After that, MLSS values have gradually increased and reached to about 6 to 7 g L^{-1} by day 70. SVI values decreased to $<40 \text{ ml g}^{-1}$ in both the CSC-augmented SBRs, indicating excellent settling properties. The average particle size increased to about 1.2 mm on day 30, corroborating stereomicroscopic images. The settling velocities of the sludge were found to be higher at 80 m h^{-1} .

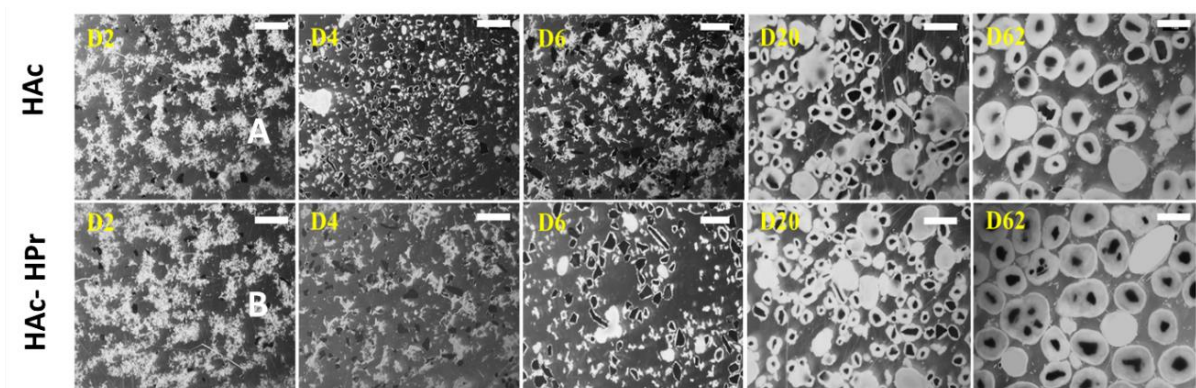


Fig. 3.5. Changes in morphology of activated sludge during granulation with CSC augmentation and using acetate (HAc) (A), and acetate and propionate (HAc-HPr) (B) as carbon substrate. Corresponding MLSS, SVI (C and D) and size distribution (E and F) during 70 days of SBR operation are shown. D in D2, D4...D62 refers to day of sampling from the SBRs. Scale bar=1mm.

Previous studies reported that addition of granular activated carbon or biochar aids in development of aerobic granules in SBRs^{79,88}. The charcoal particles are coarse, with irregular surfaces, and highly porous⁸⁹ structure, allows bacterial attachment and growth of colonies^{79,89}. The rapid microbial attachment/aggregation increased the effective collisions among CSC-biofilms, aggregates and CSC particles facilitating faster granulation⁹⁰. This

process increased the density and sludge settling properties resulting in higher biomass retention.

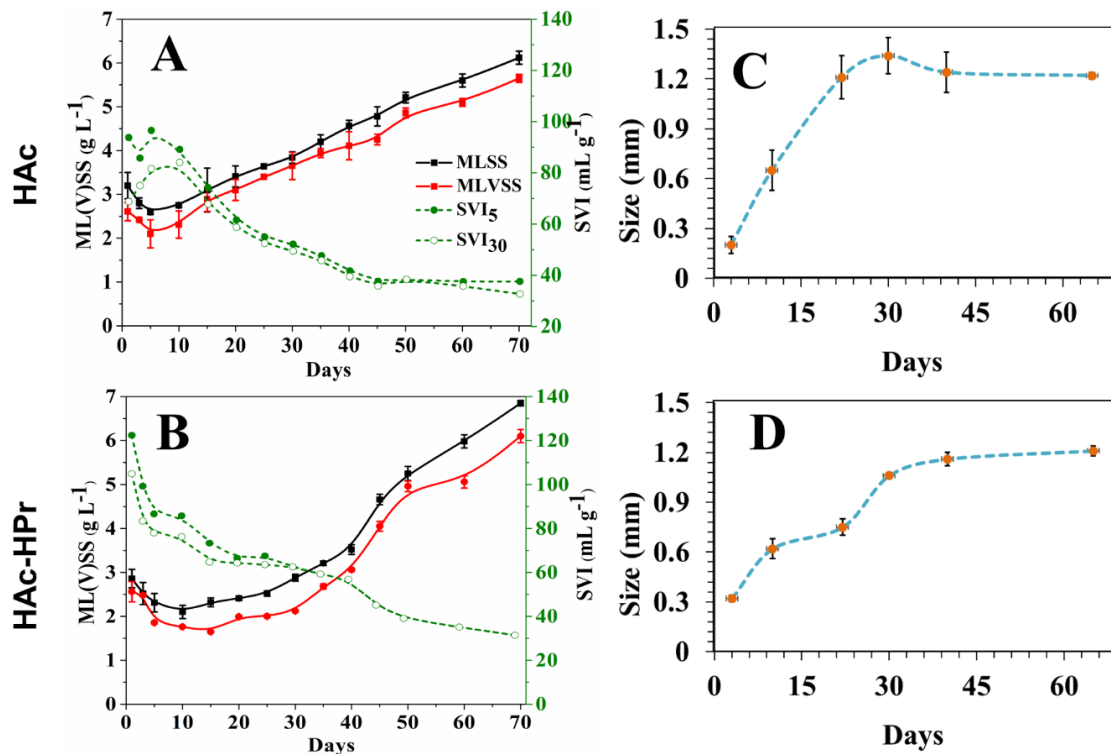


Fig. 3.6. Change in biomass (MLSS, MLVSS), settling properties (SVI₃₀, SVI₁₅) and particle size in SBRs fed with acetate (A, B), and acetate-propionate (C, D) as carbon substrates.

3.3.2.2 Nutrient removal performance of CSC-augmented SBRs

Fig. 3.7 shows time course measurements of COD, nitrogen and phosphorus in the influents and effluents of CSC-augmented SBRs fed with HAc or HAc-HPr. COD removal was very rapidly established with a very short start-up period of one week in both the SBRs. In fact, the COD removal was very efficient and stable at >94% from day 10 onwards. Ammonium removal was complete and stable from day 22 onwards in HAc fed CSC-augmented SBR. While, complete removal of ammonium was seen from day 16 in HAc-HPr fed CSC-augmented SBR. The effluents of HAc-fed SBR had nitrite during start-up, indicating ammonia nitrification and incomplete TN removal. However, neither nitrite nor nitrate were found in the effluents during later part of HAc-fed SBR. The concentrations of nitrite and

nitrate were not significant in the effluents of HAC-HPPr fed SBR, contributing to effective TN removals. A sharp increase in P removal was noticed after 10 days. The P removal seemed to stabilize after 35 days at 64% in HAC fed SBR. But, the P removal performance of HAC-HPPr fed SBR continued to improve during 65 days. The P removal performance of HAC-HPPr fed SBR was ranged from 80 to 85% during 35 to 65 days. P removal efficiencies were 2- and 1.7-fold higher, respectively, in HAC and HAC-HPPr SBRs augmented with CSC as compared to corresponding SBRs operated without CSC particles.

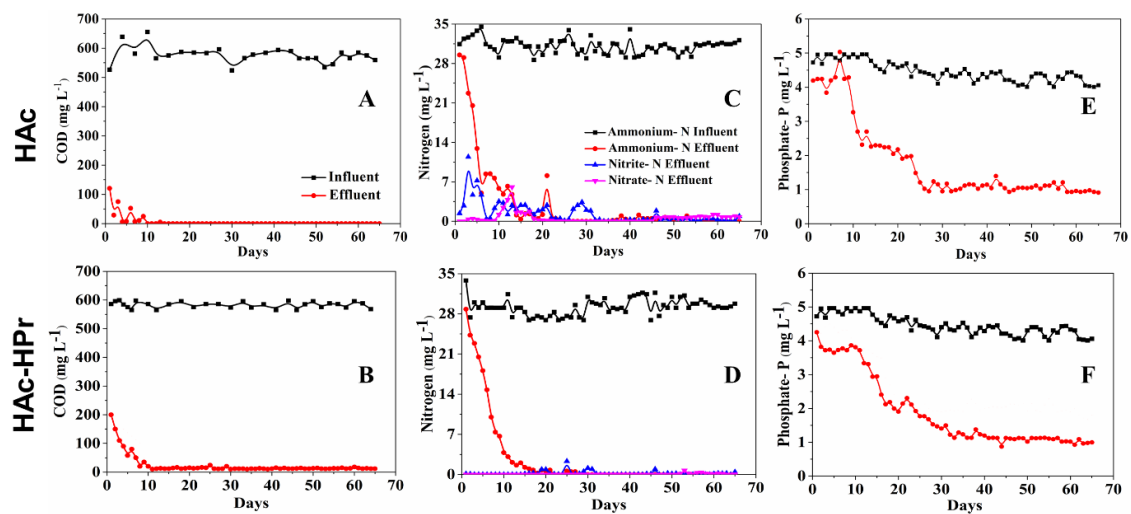


Fig. 3.7. COD (A and B), nitrogen (C and D) and phosphorus (E and F) removal performance of CSC-augmented SBRs fed with HAC (A, C and E) and HAC-HPPr (B, D and F).

Fig. 3.8 shows the profiles of COD, DO, nitrogen, and phosphorus in representative 6 h cycles. COD removal profiles were comprised of rapid decline phase followed by a steady removal phase. A significant fraction of COD was consumed in the static fill period (60 min). COD removal was near complete within the first 3 h, corroborated with the measured DO profiles. Influent ammonium (30 mg L^{-1}) was near complete within 4 h. At steady stage, release of nitrite and nitrate into the bulk liquid was found to be insignificant during ammonium removal. P removal profiles typically comprised of release and uptake phases corresponding to anaerobic and aeration phases, respectively. Amount of P released and

removed varied among the SBRs. About 0.98 and 1.5 mg of P was released in HAC and HAC-HPr fed SBRs, respectively. About 3 and 6 mg of P was removed in the aeration phase of cycle in HAC and HAC-HPr fed SBRs.

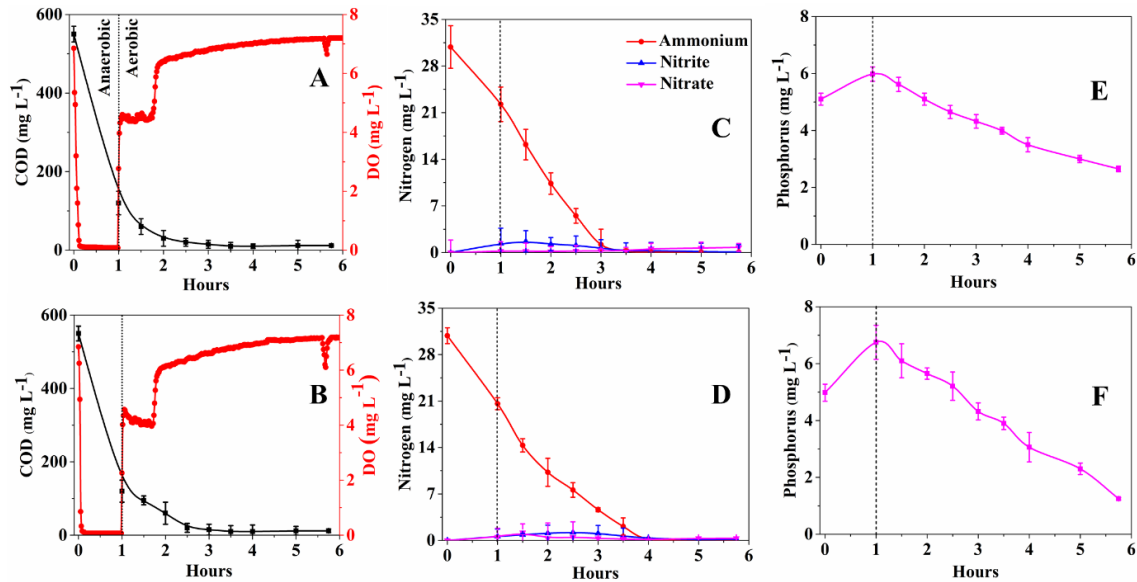


Fig. 3.8. Profiles of COD, DO (A and B), nitrogen (C and D) and phosphorus (E and F) in CSC-augmented SBRs fed with HAC (A, C and E) and HAC-HPr (B, D and F)-containing synthetic wastewater.

The amount of CSC particles was varied from 3 to 9 g in for evaluating performance. Nutrient removal was found to be higher in all the three SBRs (A2 to A4) that received CSC particles than control SBR (A1) operated without CSC particles. Among the CSC particle-augmented SBRs, nutrient removal was higher in SBRs augmented with 6 g and higher. Ammonium, TN and phosphorus removals were 86 ± 2 , 82 ± 3 and 49 ± 3 , respectively. Abiotic removal through adsorption of ammonium (<2%) and phosphorus (not detected) by CSC particles was found to be insignificant. Thus, CSC particles contributed to enhancement of nutrient removal by taking part in biofilm formation and granulation.

3.3.3 Bacterial community composition of granules cultivated without and with CSC addition

Variations in bacterial taxonomic groups in the SBRs operated with and without CSC, are shown in Fig. 3.9. A decrease in the number of OTUs and diversity indices was evident in the biomass developed in SBRs as compared to activated sludge inoculum. A total of 1348 OTUs were detected in the activated sludge. The OTUs were lower at 378 and 492, respectively, in HAc and HAc-HPr fed SBRs, indicating selection of certain bacterial groups during granulation. Shannon diversity index decreased from 7.25 in activated sludge to 5.462 and 5.630, respectively, in HAc and HAc-HPr fed SBRs. However, granular sludge developed in the presence of CSC particles had higher OTUs and diversity, but lower than that of activated sludge. The granules developed using HAc-HPr substrate had higher OTUs and diversity than developed using HAc.

Lower bacterial diversity was related to washout during start-up and selection of certain bacterial groups during granulation process. Reduction in bacterial diversity in granules as compared to activated sludge was consistent with previous studies^{91,92} and related to the SBR operating conditions like anaerobic filling, short settling time, and feast-famine feeding regime.

Proteobacteria, Bacteroidetes, and Planctomycetes have accounted for 82% total bacterial community in the activated sludge (Fig. 3.9B). Thiotrichales and Burkholderiales were abundant in activated sludge at 24% and 15%, respectively. However, Thiotrichales was washed out from the SBRs. While the abundance of Burkholderiales was decreased to 2% and 7.5%, respectively, in HAc and HAc-HPr fed SBRs. Rhodocyclales and Clostridiales sp. were dominant at 23% and 16%, respectively, in the granules formed in HAc fed SBR. The other abundant organisms in HAc fed SBR belonged to orders Pseudomonadales (9.2%), Rhizobiales (6.3%), and Rhizospirillales (6.6%).

In HAc-HPr fed SBR, Thiotrichales was completely washed out. Abundance of Burkholderiales was reduced from 24% to 7.5%. Other abundant bacteria belonged to orders Pseudomonadales (8.5%), Xanthomonadales (12%), Rhodospirillales (7%), and Nitrospirales (5.8%). PAOs or DPAOs were detected. But *Candidatus* Competibacter, a known competitor of PAOs was enriched in AGS at 35% and 29%, respectively, in HAc and HAc-HPr fed SBRs (Fig. 3.9E).

Proteobacteria, Bacteroidetes and Planctomycetes together accounted for 77 and 87% of the total genome, respectively although at a different degree of individual enrichment (Fig. 3.9D). The heatmap of order (Fig. 3.9E), and genus (Fig. 3.10) level classification revealed a distinct bacterial community in the granules formed in HAc and HAc-HPr SBRs as compared to seed sludge. For instance, Thiotrichales which was dominant in AS at 24% was below <1% in AGS. Rhodocyclales was dominant in granules formed in HAc fed SBR. While, Xanthomonadales, and Pseudomonadales were dominant in the granules formed in HAc-HPr fed SBR. Abundance of *Thauera sp.*, was at 9.8% and 13.2%, respectively, in HAc and HAc-HPr fed SBRs. *Thauera sp.* was previously reported as hydrophobic bacterium in HPr fed SBRs. Cell surface hydrophobicity and hydrophobic interactions are important in bacterial aggregation and co-aggregation during granulation⁹³. Several bacteria capable of performing anammox, aerobic ammonium oxidation, and denitrification reactions were also detected (Fig. 3.10). *Candidatus*-Kapabacteria, a known denitrifying PAO was enriched up to 27.7% in HAc fed SBR. However, *Rhodobacter sp.*, a PAO was enriched in the granules formed in HAc-HPr fed SBR. The population of PAOs and DPAOs were about 18% and 31%, respectively, in HAc fed SBR. Whereas PAOs and DPAOs were at 42% and 0.08%, respectively, in the granules developed using HAc-HPr. However, GAO population (2%) was found only in the granules formed using HAc-HPr. Thus, differential enrichment of PAOs in the granules was related to carbon source.

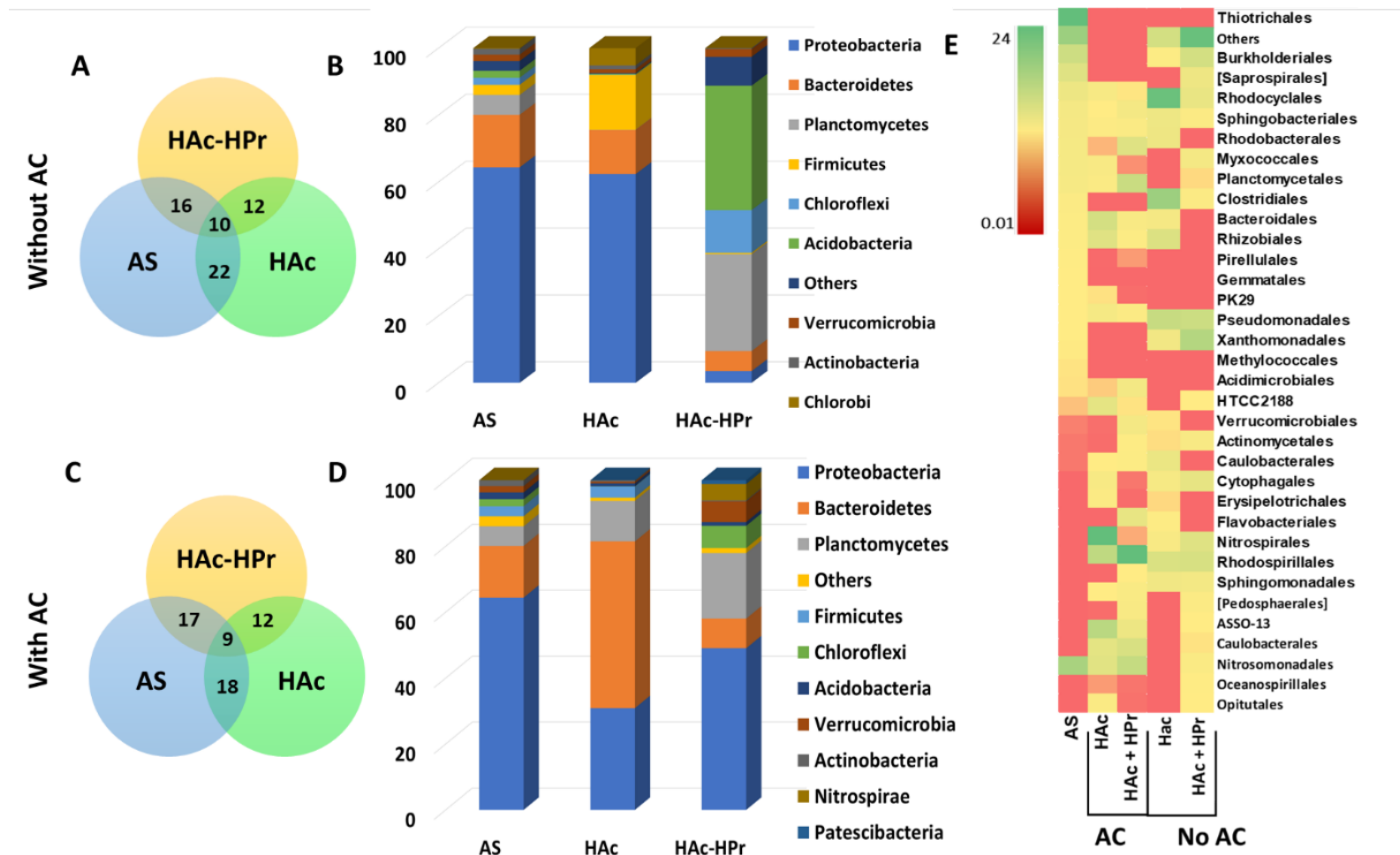


Fig. 3.9. Bacterial community composition of activated sludge and granules formed in SBRs without and with CSC particles and different carbon sources. Phylum level classification in granules formed with different carbon substrates in without (A, and B) and with CSC particles (C, and D). Venn diagram (A, C) showing overlap in phyla among activated sludge and granules. Heat map analysis of bacterial population at order level (E). Abundance of sequences representing >1% of the total annotated sequences was only considered.

Genus	HAc	HAc-HPr	Function
<i>Pirellula</i>	6.0281	0.425600	Anammox
<i>Paludisphaera</i>	2.4308	2.473300	Anammox
<i>uncultured-Planctomycetaceae-bacterium</i>	0.0154	1.300891	Anammox
<i>Aquisphaera</i>	0.0103	1.485586	Anammox
<i>Lacunisphaera</i>	0	1.935277	Anammox
<i>Nitrospira</i>	0	4.930539	Commamox
<i>Singulisphaera</i>	0	1.903156	dissimilatory nitrate reducer
<i>Candidatus-Kapabacteria</i>	27.751	0.008030	DPAO
<i>Brevundimonas</i>	1.9425	0.016060	DPAO
<i>Labrenzia</i>	1.3413	0.064242	DPAO
<i>Candidatus-Competibacter</i>	0.0206	2.200273	GAO
<i>Aquimonas</i>	1.367	0.160604	N & P- metabolism
<i>Haliangium</i>	0	1.011804	N & P- metabolism
<i>Ensifer</i>	2.6569	0.088332	N- fixer
<i>Allorhizobium-Neorhizobium-Pararhizobium-Rhizobium</i>	1.1871	0.064242	N- fixer
<i>Azoarcus</i>	0.0925	1.646190	N- fixer
<i>Reyranella</i>	1.4698	0.072272	N-metabolism
<i>Thauera</i>	9.8566	13.298000	PAO
<i>Prostheco bacter</i>	0.4368	3.067534	PAO
<i>Rhodobacter</i>	0.3186	21.666426	PAO
<i>Zoogloea</i>	0.0771	5.307958	PHA producers
<i>Bdellovibrio</i>	0.7092	1.557858	Predator
<i>Azospira</i>	0	1.405284	Predator
<i>Persicitalea</i>	5.7043	3.123745	putative PAO
<i>Exiguobacterium</i>	1.2693	0.008030	putative PAO
Unclassified	35.315	50.678551	unknown

Fig. 3.10. Bacterial community composition at genus level along with prominent function of AGS formed in SBRs augmented with CSC particles and fed with different carbon substrates. Abundance of genera representing >1% of total genome were only included.

The EPSs content of sludge was monitored during granulation using sodium carbonate extraction method. Sodium carbonate method has been found to be suitable for extracting the structural EPSs similar to commercial alginate in gelation properties, hence, it is referred to as alginate-like polymer (ALE). The ALE content was low in activated sludge at 48 mgALE/gVSS (Fig. 3.11). However, the ALE content of sludge increased during SBRs operation with or without CSC particles (Fig. 3.11A and B). The increase in ALE was found to be similar in SBRs fed with either HAc or HAc-HPr. However, the amount of ALE was higher at 636 mgALE/gVSS in the granules with CSC particles as compared to 500±40 mgALE/gVSS without CSC particles, indicating a positive role for CSC on EPSs production.

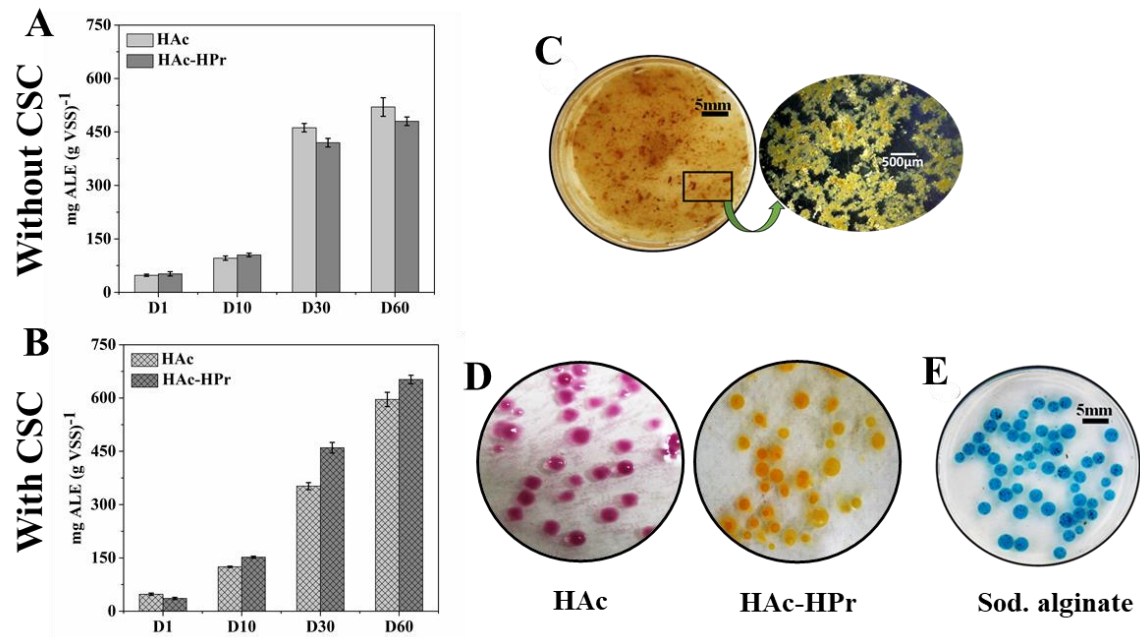


Fig. 3.11. Gelation properties of alginate-like exopolymer (ALE) in 2% (w/v) extracted from AS (A) and AGS (B). For reference commercial sodium alginate was used stained with Alcian blue (C).

Furthermore, the ALE extracted from the seed AS did not form beads in 2% CaCl_2 (Fig. 3.11C). In contrary, ALE extracted from granules formed beads (0.74 ± 0.08 mm) in 2% CaCl_2 (Fig. 3.11D), similar to those formed by commercial alginate (Fig. 3.11E). These results suggested that the EPSs obtained from the granules exhibited good gelation properties *in vitro*. The gelation properties of EPSs are considered important for formation and stability of granules⁹⁴. The gel-forming capability of ALE is dependent on amount of GG, MG and MM blocks. The content of GG blocks in the ALE of AS was determined to be at 38%. The ALE recovered from the AGS had higher amount of GG blocks at 68% to 70%. However, the MG blocks were lower in the ALE at 14 to 20% % in the granules. This was in agreement with previous study that the ALE recovered from the AGS cultivated while treating real sewage contained 69.1% GG blocks and 14.6% MG blocks⁹⁴. Higher amount of homopolymer (GG) blocks than heteropolymer (MG) blocks in the extracellular matrix confers more structural stability to granules.

3.3.4 Granulation mechanisms

The microbial community of granules was dependent on type of carbon source. HAc feeding enriched organisms of order Rhodocyclales in the granules. However, HAc-HPr enriched organisms of Planctomycetes and Acidobacteria in the granules. Granules formed using HAc were compact and had clear boundaries. But, the granules formed using HPr or HAc-HPr had hairy outgrowth/boundaries. Thus, morphology of granules developed in the SBRs was related to the available carbon substrate type, its uptake and utilization patterns. Major portion of HAc was accumulated inside the cells during the static filling phase and converted to storage polymers (e.g., polyhydroxyalkanoates or glycogen). These storage polymers are utilized in the subsequent aeration phase. This kind of substrate utilization pattern can support slow-growth across granules and generate minimal stratification in the granules. HPr is more complex than HAc and not easily assimilated by microorganisms. At higher concentrations, HPr can be inhibitory to microorganisms. Toxicity is mainly caused by the un-dissociated form of propionic acid on bacterial membranes⁸⁵. Slower and distinct substrate utilization of HPr may be responsible for the observed delay in granulation and establishment of BNR using HPr as sole carbon source. The substrate utilization pattern was different as compared to HAc. HPr was mostly utilized during the aeration phase. The substrate utilization pattern and associated bacterial community may be the reasons for hairy outgrowth in the granules formed using HPr as sole carbon source (Fig. 3.12). However, the HPr-related effects on granulation were not observed with mixed substrate (HAc-HPr).

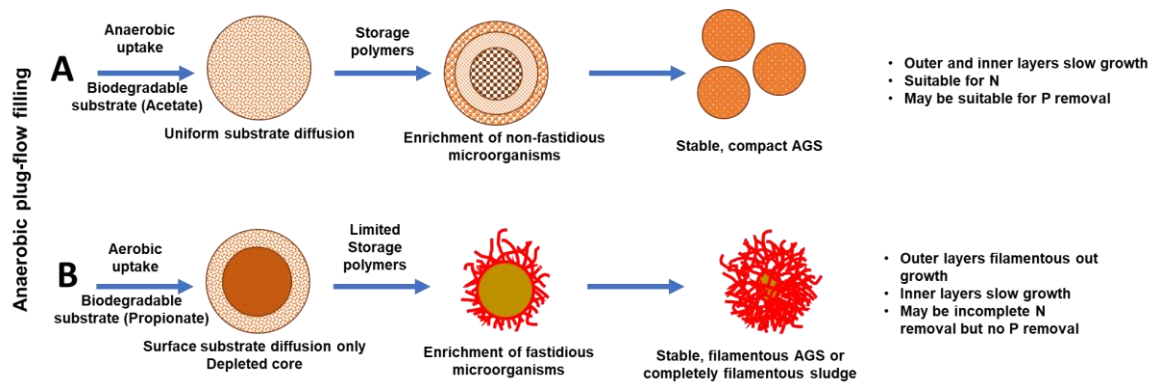


Fig. 3.12. Formation of aerobic granular sludge in SBRs fed with acetate or acetate-propionate (A) and propionate (B).

The role of CSC particles in activated sludge SBRs is multi-fold which includes (i) decreased sludge washout during initial days, (ii) formation of particulate biofilms, and (iii) increased inter-particle interactions leading to higher shear. Washout of activated sludge is a common phenomenon in granular SBRs during first few days, due to strong selection pressures like short setting time. The sludge washout was found to be much lower in SBRs augmented with CSC particles. Minimizing sludge washout from the bioreactor was possible by increasing its settling properties. The flocculation and re-flocculation abilities of activated sludge was increased by 2-fold in the presence of CSC particles, suggesting crucial role in improving the settling properties. Secondly, CSC particles act as micro-carriers for bacterial attachment and formation of particulate biofilms which again contributes to biomass retention in the SBR. Thirdly, the shear emanating from higher inter-particle interactions (among CSC particles, particulate biofilms and aggregates) contributes to compactness and shaping up of aggregates into granules in the system. Though sludge comprised of biofilms and granules in the first few weeks, it was dominated by granules after 30 days. This was likely as CSC particles (due to small amount) only contribute a fraction of overall biomass developed in the granular SBRs. The sludge is expected to harbour two sub-types of dominant microbial growth namely, biofilms and granules, along with co-existing flocs (Fig. 3.13). However, it is unclear regarding the contribution of biofilms versus granules to the observed superior nutrient

removals, particularly phosphorus removal via EBPR, in the SBRs augmented with CSC particles. Therefore, it is desirable to investigate the role of granule sub-types in nutrient removal and selective enrichment of microbial groups of interest to nutrient removal, if any.

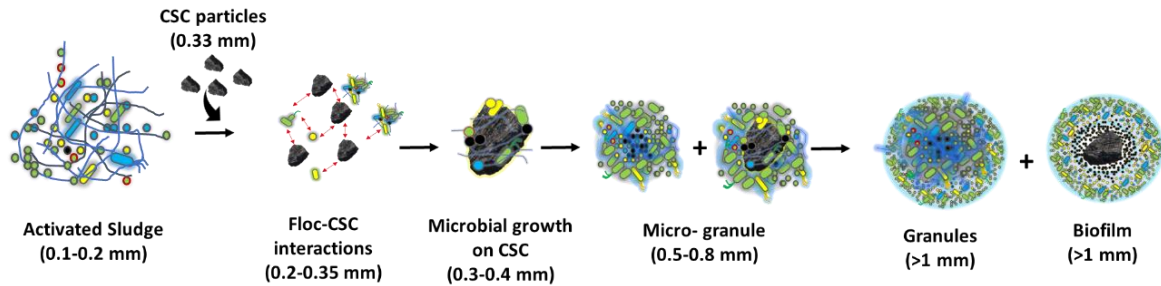


Fig. 3.13. Role of CSC particles in formation of aerobic granular sludge in SBRs inoculated with activated sludge.

3.4 Conclusions

Granulation and nutrient removals were higher using HAc or HAc-HPr as carbon sources than HPr as sole carbon source. Addition of CSC particles to SBRs was found to be beneficial to granulation and establishing nutrient removal pathways. First granules were observed within 5 days in the presence of CSC particles as against 17 days in the SBR operated without CSC particles. Improved granulation was associated with significant improvements in COD, nitrogen and phosphorus removal efficiencies. Phosphorus removal was achieved through EBPR pathway. Addition of CSC particles have improved flocculation, and re-flocculation properties of activated sludge, thereby minimizing its washout from the SBR during the initial days of operation. The findings described in this chapter would be useful for improving granulation and nutrient removal in granular SBRs.

Chapter 4

Understanding the effect of charcoal-augmentation on biological nitrogen and phosphorus removal in aerobic granular sludge reactors

Abstract

The objective of this study was to investigate the role of charcoal particles on enhancement of biological nutrient removal and response to environmental conditions. For this, the biomass was first separated based on size and then on type (granules and biofilms). High bio-P removal and EBPR was associated with the granules with larger size (>0.5 mm) biomass fraction, corroborating with abundance of PAOs. The smaller size (0.25 mm) biomass fraction was associated with lower bio-P removal. Further separation of larger size biomass fraction indicated higher abundance of PAOs in the biofilms as compared to coexisting granules. Differential enrichment of PAO clade I in acetate and both clade I and II in acetate-propionate combination was observed. Further experiments suggested that PAO clade I can shift from poly-P dependent to glycogen dependent metabolism. The biological nutrient removal was severely inhibited at salinities ranging from 2 to 10 ppt. Complete loss in nitrogen and phosphorus removal function was observed at 10 ppt salinity.

Keywords Aerobic granules; Carbon substrate, Charcoal particles EBPR, Nutrient removal, PAO, salinity.

4.1 Introduction

Aerobic granular sludge (AGS) process promises effective simultaneous COD, nitrogen and phosphorus removal from the wastewater²⁷. However, biological removal of nitrogen (N) and phosphorus (P) is related to granulation, wastewater characteristics (i.e., composition, and salinity) and the operating conditions (i.e., dissolved oxygen, anaerobic-aerobic conditions, and temperature)^{30,27}. A good understanding of the key factors which regulate N and P cycling across the AGS is required for implementing effective and energy-efficient N and P removal pathways. Understanding the abundance, spatial distribution and behavior of the microbial populations controlling N and P transformations is important for successful implementation^{95,96}. The different surface to volume ratio and aerobic zone volume fractions of individual granules contribute to differences in bacterial population and nutrient conversion rates³⁵. Henriot et al.⁹⁷ reported two types of granules, white and brown colored granules coexisting in the same bioreactor. Both the granule types had similar abundance of *Candidatus Accumulibacter*. But, the abundance of *Ca. Accumulibacter* was different at 30% and 67% in white and brown colored granules, respectively. Thus, it is imperative to find microscale (e.g., microstructure, bacterial composition), and macroscale (e.g., colour, size, settling velocities) differences in the heterogeneous population of granules.

External agents such as metal ions, magnetite, and granular activated carbon have been added to the bioreactors for promoting cultivation of AGS from activated sludge inoculum^{88,92}. Addition of charcoal particles to large scale wastewater treatment plants is a technologically and economically feasible approach. Hence, the effect of addition of coconut shell charcoal (CSC) particles was studied on granulation and nutrient removal (Chapter 3). Enhanced granulation of activated sludge coupled to rapid establishment of nutrient (N and P) removal pathways was achieved in the presence of CSC particles. P removal pattern and enrichment of PAOs was distinct in the bioreactor augmented with CSC particles. The

biomass cultivated in the presence of CSC particles was comprised of particulate biofilms (CSC-supported) and granules. Understanding the relative contribution of particulate biofilms *vis-a-vis* granules in the nutrient removal, particularly P, is of fundamental importance.

Studies on PAO have reported the enrichment of different clades of PAOs in the same biomass⁹⁸. Recently, it was demonstrated that distinct and enriched PAO clades have different characteristics in terms of morphology, metabolism, ability to denitrify and tolerance to salinity^{99,100}. The observed differences in these studies were directly linked to the influent phosphorus to carbon (P/C) ratios. The insights on the differential ability of the PAO clades to prevail in varying influent P levels or resist stress (e.g., salinity) is thought to be a controlling factor for enrichment strategies^{99,100}. There are limited studies on the impact of salinity on PAOs and EBPR. In many cases, there is no report on the functional microbial populations involved or P removal itself. Moreover, the differences in enrichment strategies or salinity effect on EBPR are studied at 20 ± 1 °C^{100,101}, but not at ≥ 30 °C. Therefore, it becomes important to study the response of PAOs under tropical SBR conditions for better understanding about the conditions favoring the specific clades.

The main objective of this study was to delineate the biomass cultivated in the bioreactors based on size and type for better understanding nitrogen and phosphorus removal mechanisms. The granule subtypes were divided into granules without CSC core and granules with CSC core (referred to as biofilms). Furthermore, phosphorus removal by granule subtypes was determined at varied (i) phosphorus to carbon (P/C) ratios and (ii) salinities. This study contributes to the fundamental understanding of the metabolism of granule subtypes formed in sequencing batch reactors (SBRs) augmented with CSC particles, and may help to improve strategies for enrichment of PAOs.

4.2 Materials and methods

4.2.1 Source of biomass

Cultivation of biomass in SBRs with and without CSC particles was mentioned in Chapter 3. The biomass was harvested on day 212 of start-up (towards the end of experiment) from two SBRs with CSC particles and fed with acetate (HAc) and acetate-propionate (HAc-HP_r) containing wastewater. The two biomass samples were sorted into different size fractions and types as detailed below.

4.2.2 Sorting of biomass based on size and type

A series of sieves, with mesh size of ≥ 0.5 , 0.25, 0.12, and ≤ 0.12 mm, were used for size fractionation of biomass. For this, biomass was percolated through the sieve with the largest mesh size. Each sieve was carefully removed for collecting size-separated biomass. The different size groups were used in batch tests and for extracting genomic DNA.

The 500 μm size biomass fraction was further segregated manually into granules and biofilms (granules with CSC core). The obtained granules and biofilms were used in the batch tests. A subsample of granules and biofilms was processed for extracting genomic DNA.

4.2.3 Nutrient removal by different size groups

Short-term experiments were performed using different size biomass fractions (0.5, 0.25, 0.12 and < 0.12 mm) for determining nutrient removal. The experiments were performed in a 3-litre SBR with 6 h cycle. Each SBR was inoculated separately with size fractioned biomass and fed with synthetic wastewater. The operating conditions of the SBR were detailed in Chapter 3. HAc or HAc-HP_r served as respective carbon source during the experiment. Orthophosphate and ammonium at 10 mg L⁻¹ P and 10 mg L⁻¹ N, respectively, used as sole phosphorus and nitrogen sources. The experiment was conducted for minimum of 5 days (equivalent to 20 batches). Liquid samples were collected for determining the nutrient

removal performance. The biomass samples were processed for estimating the abundance of functional bacteria.

4.2.4 Nutrient removal by granule subtypes

Short-term experiments were performed on the granule subtypes (granule and biofilms) obtained from 500 μm size fraction. The experiments were performed in a 3-liter SBR with 6 h cycle. Each SBR was inoculated separately with either granules or biofilm biomass and fed with synthetic wastewater. The operating conditions of the SBR were detailed in Chapter 3. HAc or HAc-HPr served as respective carbon source during the experiment. Orthophosphate and ammonium at 5 mg L^{-1} P and 5 mg L^{-1} N, respectively, served as phosphorus and nitrogen sources. The experiment was conducted for minimum of 10 days (equivalent to 40 batches). Liquid samples were collected for determining the nutrient removal performance. Biomass was processed for estimating the abundance of functional bacteria. For estimating the storage polymers (glycogen (gly), polyhydroxy butyrate (PHB), polyhydroxy valerate (PHV)), biomass samples were frozen immediately at $-80\text{ }^{\circ}\text{C}$ before lyophilization to arrest biochemical conversions.

4.2.5 P removal at different P/C ratios

To investigate the effect of the external P content on biological P removal, batch experiments were performed at different initial P concentrations (0 to 45 mg L^{-1} $\text{PO}_4^{3-}\text{-P}$). The biomass harvested from the SBR treating wastewater containing 10 mg L^{-1} $\text{PO}_4^{3-}\text{-P}$ was used in the fractionation and batch experiments. A 3-liter SBR was operated as detailed in Chapter 3 (3.2.4) for determining P removal at different influent P concentrations. Two independent tests were performed to vary the external P concentrations. In one of the tests, the influent P concentration was increased stepwise from 10 to 15, 30 and then to 45 mg L^{-1} . The corresponding influent P/C ratios (mol/mol) were determined to be 0.08, 0.15, and 0.23. In the second test, the influent P concentration was decreased stepwise from 10 to 7, 5, 2.5

and 0 with corresponding P/C ratio (mol/mol) of 0.04, 0.028, 0.01, and 0. The SBR was operated for a minimum of 10 days at each P/C ratio. The batch tests were performed either with HAc or HAc-HPr as the carbon source. At the end of each experimental phase, liquid were sampled at different time points during individual cycles. The PO_4^{3-} -release rates and COD-uptake rates were calculated from cycle data.

4.2.6 Effect of salinity on nutrient removal

To investigate the effect of salinity on nutrient removal performance and granular stability, enriched PAO I and PAO II biofilms from HAc and HAc-HPr, respectively, were collected and subjected to varying salinity. For this, 4 g AGS was subjected to 0, 2, 5, 8 and 10 ppt salinity. The desired salinity was achieved by diluting the seawater (34ppt) appropriately with demineralized water and amended with the nutrients (Appendix II). The experiments were performed in 1 liter volume SBR with 6 h cycle detailed in Chapter 3. Liquid samples were collected for monitoring ammonium, nitrite, nitrate, phosphate, and COD. At the end of experiment, biomass was collected for genomic DNA extraction and qPCR.

4.2.7 DNA extraction

The genomic DNA was extracted from biomass, different size fractions of biomass, and granules subtypes using QIAGEN DNA mini kit following the manufacturer's protocol. The DNA from each biomass sample was extracted immediately after the batch tests. Concentrations were determined using a NanoDrop® Spectrophotometer.

4.2.8 qPCR

qPCR was performed for estimating the abundance of different PAO clades for IA, IB, IC, ID of type I and IIE, IIG, IIH, and II-I of type II. The microorganisms involved in nitrogen removal pathways was determined using specific primers (*amoA*, *amx*, *nor*, *nar*, *nirS*, *norB/qnorB*, *nosZ*). Primer sequences and PCR conditions were detailed in Appendix I.

4.2.9 Polyphosphate staining using DAPI

Granule samples were collected at the end of aeration period by centrifugation (8000 g, 5 min), washed and macerated between two slides. The slides were then stained for 30 min with DAPI (10 $\mu\text{g mL}^{-1}$ final concentration). Images were captured using DAPI filter (ex: 340-380 nm; em: 450-650 nm) using epifluorescence microscope (Carl Zeiss, India). The images were photographed after exposing to the laser light for at least 1 min to detect yellow fluorescence emanating from poly-P¹⁰².

4.2.10 Analytical methods

Determination of TSS, VSS and PO_4^{3-} -P concentrations were performed according standard methods⁶⁴ HAc and HPr was determined using Agilent 7890A gas chromatography (GC), equipped a flame ionization detector¹⁰³. GC capillary column (15m \times 0.53mm \times 0.5 μm) using nitrogen gas as carrier gas at 2 mL min^{-1} for used for separation. Temperature of the injector, column and detector was 200 °C, 105 °C and 300 °C, respectively. The detector gases were dry air (400 mL min^{-1}) and hydrogen (40 mL min^{-1}), nitrogen was used as make-up gas (40 mL min^{-1}). Glycogen was determined using 0.9 M HCl (5 mL) and digestion (5 h).¹⁰¹ For PHB and PHV content¹⁰¹ 20 mg of dried biomass was combined with 2 mL methanol (in 3% H_2SO_4), and 2 mL chloroform with benzoic acid as internal standard. Samples were heated for 5 h at 100 °C and purified using 1.9 mL of chloroform. After vigorous shaking and centrifugation (1500 g; 3 min), the chloroform containing phase was transferred to GC vial for split injection (1 μL). Helium was used carrier gas (30 cm s^{-1}). Temperature of the injector, column and detector was 200 °C, 160 °C and 220 °C, respectively.

4.3 Results and Discussion

4.3.1 Prelude

Size and density are the two important parameters determining the settling properties of the biomass and biomass-liquid separation. Formation of AGS and establishment of nutrient

removal pathways were faster in the SBRs operated with CSC particles using HAc or HAc-HPr as substrate. The COD, ammonium and phosphorus removal were at 98%, 95%, and 65%, respectively, for HAc substrate fed SBR. COD, ammonium and phosphorus removals were at 96%, 99%, and 85%, respectively, for HAc-HPr substrate fed SBR. These results encouraged us to an extensive study aimed to understand the bio-P removal mechanisms in CSC-augmented SBRs.

4.3.2 Coexistence of granule subtypes

A total of four fractions (>0.5, 0.25-0.5, 0.12-0.25, <0.12 mm) were collected from each biomass sample. PAOs were abundant in biomass size fractions with size >0.25 mm and >0.5 mm. The abundance was least in smaller sized biomass fraction (<0.12 mm). PAO clade I (clade IA and IB, IC) was mostly abundant in size >500 μm (Fig. 4.1A) in HAc-fed SBR, whereas both PAO I and II (IIE) were enriched in HAc-HPr fed SBR (Fig. 4.1B). P removal profiles contained P release and P uptake phases under anaerobic and aerobic conditions, respectively (Fig. 4.1). In the anaerobic phase, P release was determined to be higher at 2 mg L⁻¹ PO₄³⁻-P (HAc) and 4 mg L⁻¹ PO₄³⁻-P (HAc-HPr) by >0.5 mm size biomass fraction as compared to just 0.5 mg L⁻¹ with >0.25 mm size fraction. In the aerobic phase, the uptake was found to be at 6 mg L⁻¹ PO₄³⁻-P (HAc) and 11 mg L⁻¹ PO₄³⁻-P (HAc-HPr) by >0.5 mm biomass fraction. P removal profiles exhibited by >0.5 mm biomass fraction was typical of EBPR pathway.

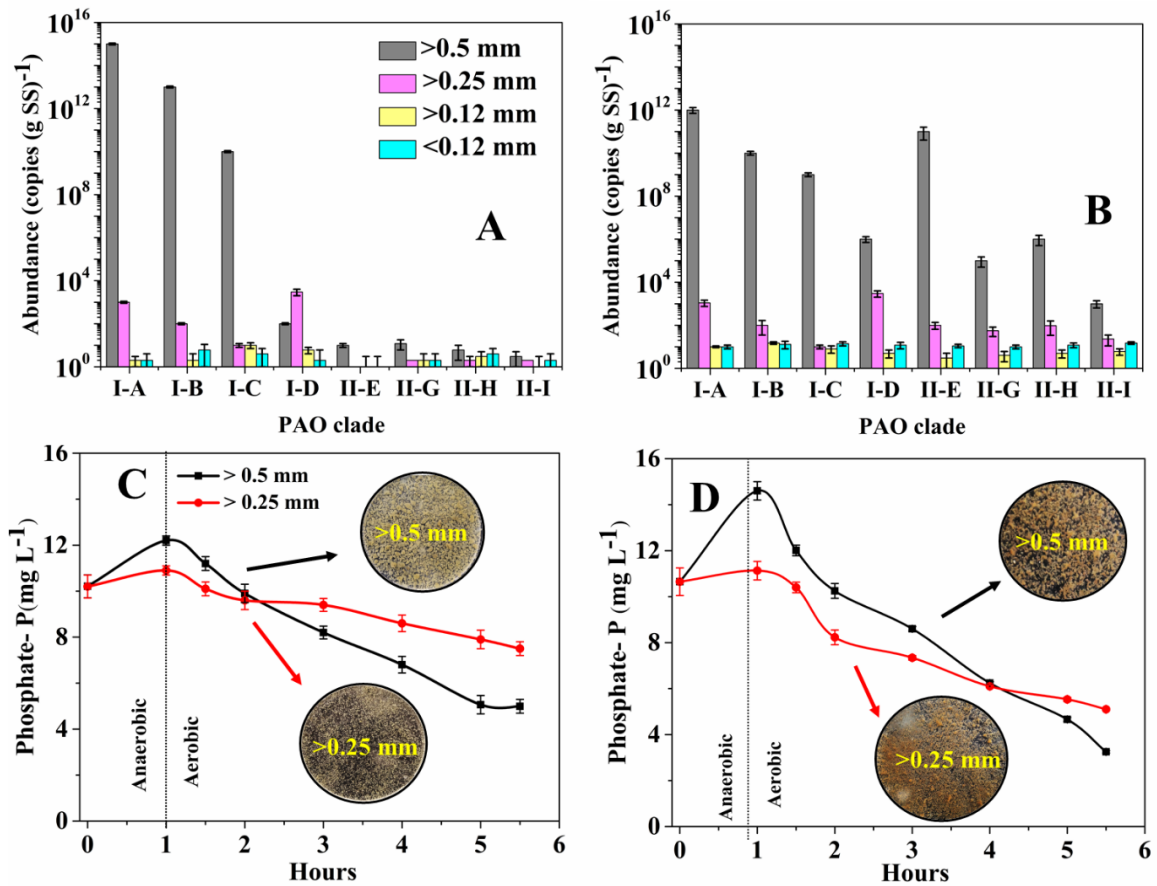


Fig. 4.1. Phosphorus removal profiles by biomass cultivated in HAC (A, C), and HAC-HPr (B, D) fed carbon substrates and with CSC particles.

Net phosphorus removals by >0.5 mm biomass was determined to be at 60% and 75% for HAC and HAC-HPr, respectively. In contrast, phosphorus removal by >0.25 mm biomass was in the range of 20 to 35%. Thus, confirming the characteristic EBPR profile for AGS with size >0.5mm, but not with 0.25mm and lower sized AGS (Fig. 4.1C and D). The large sized (>0.5 mm) biomass fraction performing effective P removal through EBPR was selected for further studies on nutrient removal.

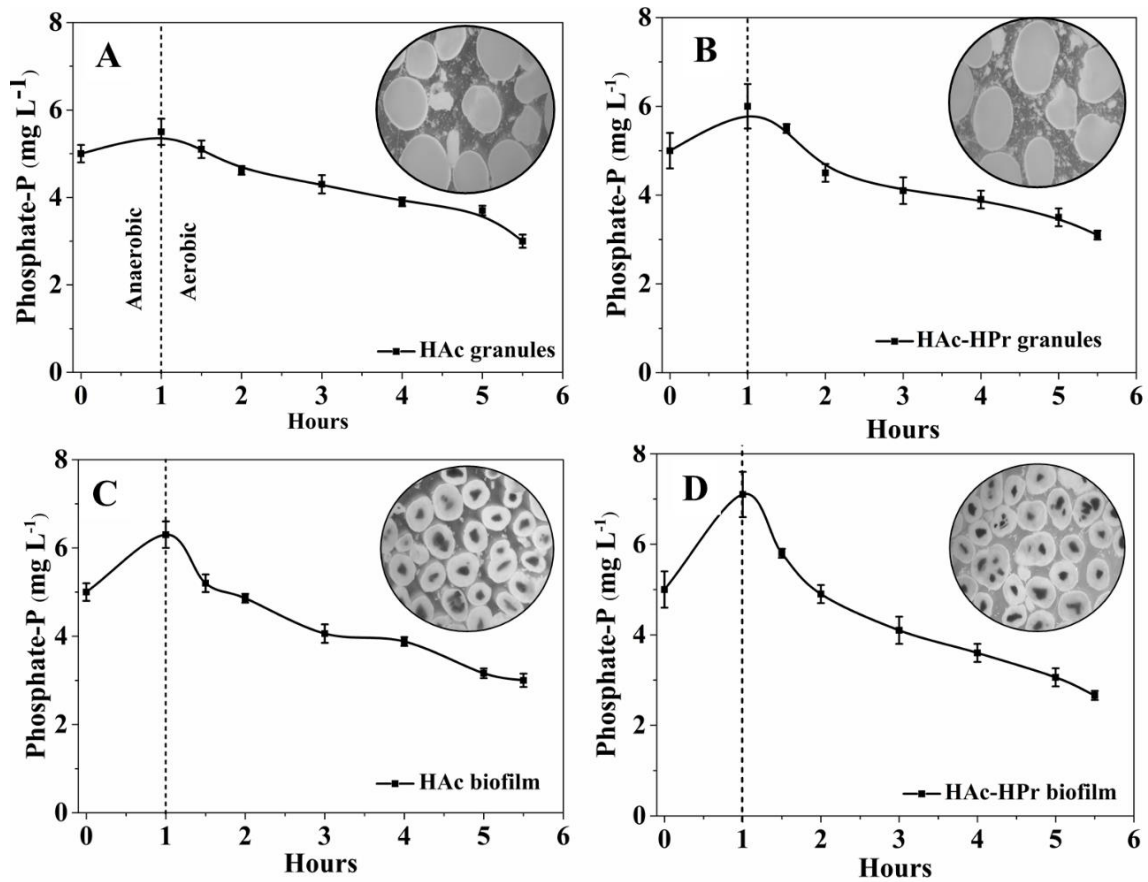


Fig. 4.2. Phosphorus removal profiles exhibited by granules and biofilms separated from HAc (A,C), and HAc-HPr (B,D) fed SBRs. Inset, microscopic view of manually segregated granules and biofilms.

In order to understand segregation of PAOs, if any, the biomass performing EBPR was segregated into biofilms and granules. Interestingly, the biofilms and granules exhibited distinct P removal profiles (Fig. 4.2). P release ($2.5\text{-}3.5\text{ mg L}^{-1}\text{ P}$) as well as P uptake ($5\text{-}7\text{ mg L}^{-1}\text{ P}$) was higher in the P removal profiles exhibited by the biofilms. However, P release and P uptake were lower with the granules. These differences in P removal profiles resulted in net P removal efficiencies of about $70\pm 5\%$ and $50\pm 6\%$, respectively, for biofilms and granules. Thus, biofilms are probably the major contributors for enhanced P removal observed in the SBRs operated with CSC particles. This was supported by the abundance of PAO clade I and II in biofilms. Although it is not understood, biofilms appear to be a preferred habitat for PAOs. Despite high abundance of PAO clades (Fig. 4.3A and B), qPCR showed no distinct pattern in the abundance of ammonium oxidizing bacteria. The abundance of anammox and

denitrifying bacteria were relatively higher in the biofilms formed using HAC-HPr (Fig. 4.3B) as compared to their counterparts developed using HAC (Fig. 4.3A).

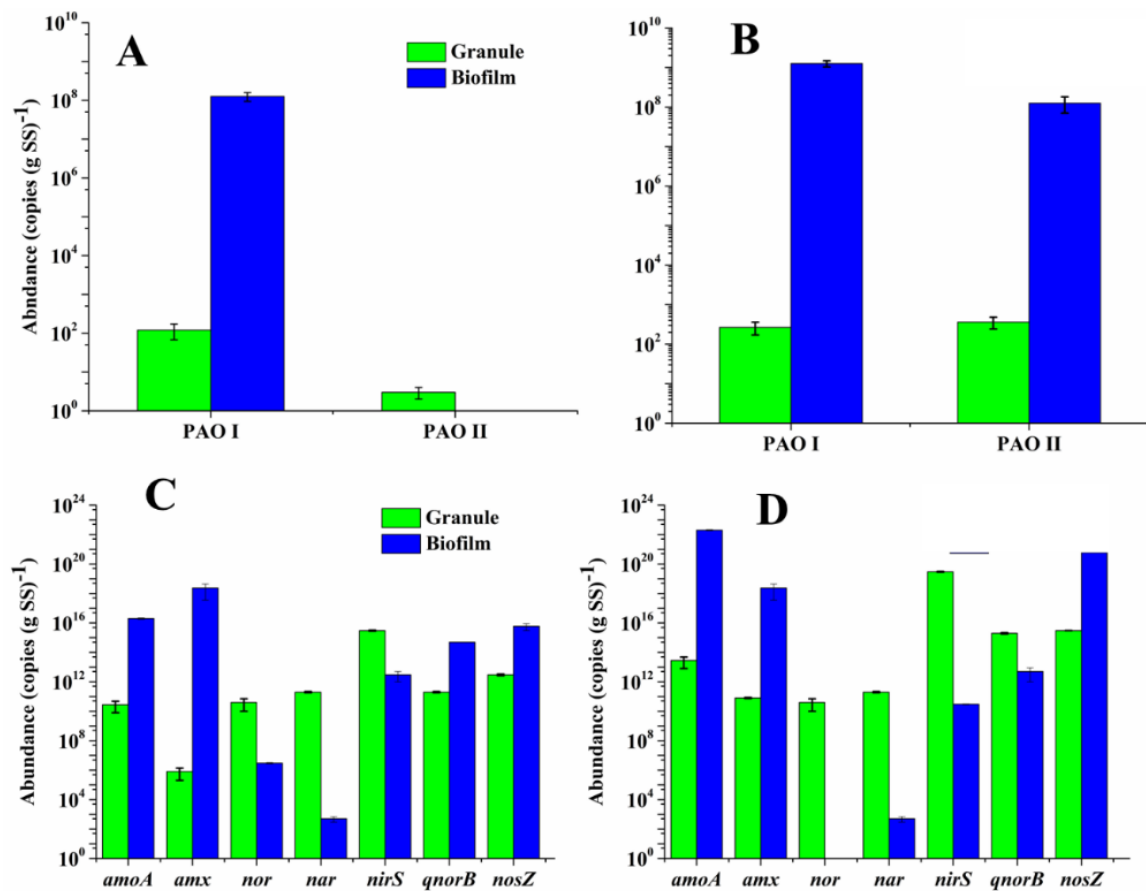


Fig. 4.3. Abundance of PAO clades (A,B) and microorganisms of nitrogen removal (C,D) in granules and biofilms separated from HAC (A,C) and HAC-HPr (B,D) fed SBRs. PAO I (clade IA) and PAO II (clade IIE).

Previous studies have reported biomass segregation and formation of different types of granules in the same bioreactor treating synthetic wastewater^{97,104,105}. Winkler et al.¹⁰⁵ reported segregation was due to microorganisms present in fast and slow settling particles while, Barr et al.¹⁰⁴ reported 97% enrichment of *Candidatus Accumulibacter phosphatis* (PAO) and 0.9% of *Candidatus Competibacter phosphatis* in white granules. However, *Candidatus Competibacter phosphatis* (γ -GAO) was abundant at 58% in the yellow granules. Barr et al.¹⁵³¹⁰⁴ suggested development of different granule types was partly caused by higher

EPSs production by PAOs. These authors also mentioned that segregation of microorganisms between granule types could not be attributed to specific operational conditions.

Unlike previous studies, the segregation of microbial groups observed in this study was related to addition of CSC particles and biofilm formation. CSC particles with attached growth were found to settle faster than the aggregates at least during initial days of SBR operation. Bacterial attachment and growth of biofilms is relatively faster than appearance of aggregates and granules. Thus, attachment and biofilm formation process would have facilitated retention and growth of PAOs present in the activated sludge. It may be noted that a significant portion of activated sludge inoculated into SBRs is lost during initial days. The results obtained in this study indicated that CSC particles minimizes biomass (activated sludge) washout from the SBR. Attachment and biofilm formation by PAOs on CSC particles is likely responsible for their retention, abundance and establishment of EBPR pathway.

4.3.3 EBPR biochemical conversions

In this study, enriched PAO I was cultivated, whereas no GAO (*Candidatus Competibacter phosphatis*) was detected in HAc. A PAO I and II enriched biomass was obtained with 2% GAO when HAc-HPr was used. Fig. 4.4 shows carbon (HAc or HAc-HPr) and phosphorus utilization patterns during individual SBR cycle. In both substrate conditions, the supplied volatile fatty acids (VFA) (i.e., HAc or HPr) were majorly consumed within first 60 min. The VFA uptake rates were at $196 \text{ mg L}^{-1} \cdot \text{h}$ and $100 \text{ mg L}^{-1} \cdot \text{h}$ for HAc (Fig. 4.4A) and HPr (Fig. 4.4B), respectively. From the kinetic data, P/VFA (P-mol/C-mol VFA) was calculated to explain PAO metabolism at the clad level¹⁰¹. The coexistence of GAO is always foreseen as a potential factor affecting phosphorus stoichiometric conversions⁹⁸. During the anaerobic VFA uptake, from the P/VFA ratios, metabolism typical to PAOs was observed. At the end of the anaerobic phase, the average P/VFA ratios were at 0.3 ± 0.05 (HAc), and 0.46 ± 0.01 (HAc-HPr), respectively. For VFA uptake by PAOs, the required energy is derived from the

hydrolysis of intracellular poly-phosphate pool resulting in depletion of the P-reserves in the biomass, concomitantly increases the P-content in bulk liquid.

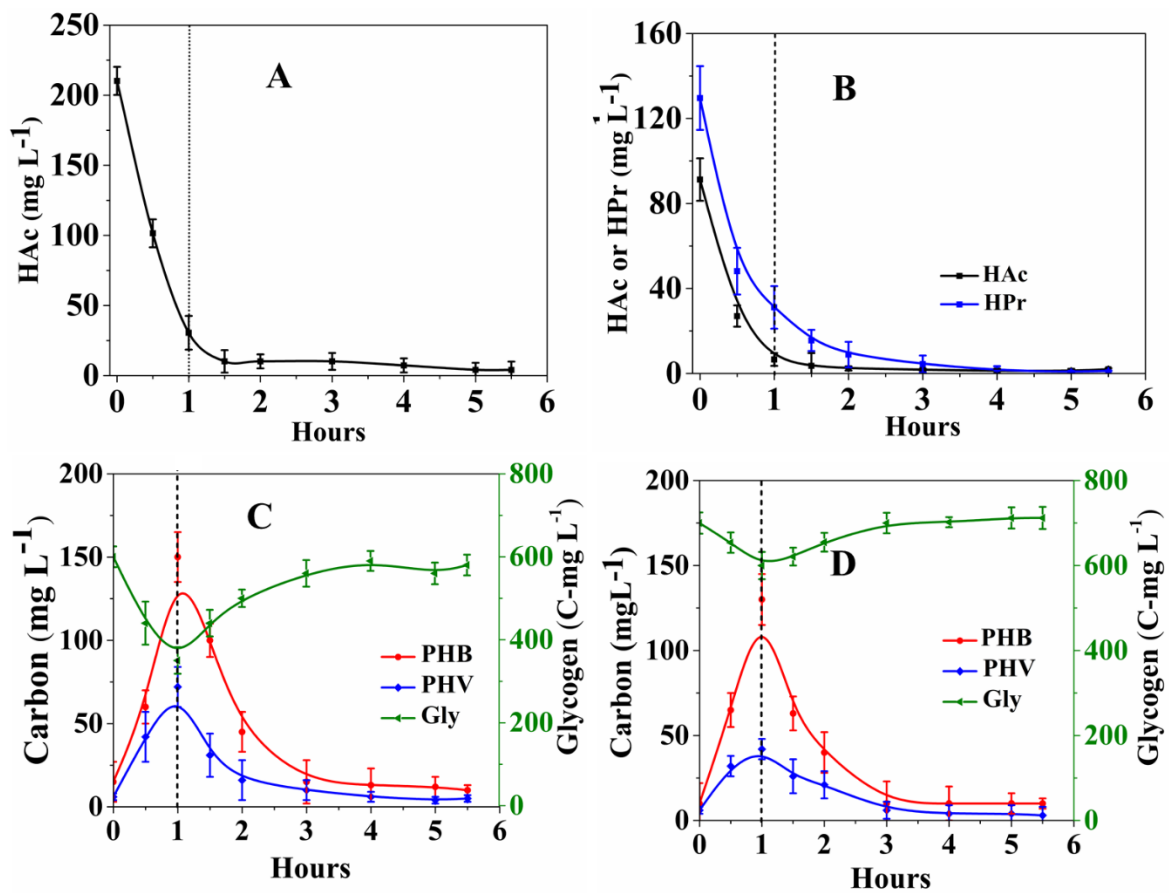


Fig. 4.4. Kinetics of carbon utilization and phosphorus metabolism in HAc biofilms (A) and HAc-HPr biofilms (B). glycogen and PHAs in typical SBR cycle for HAc (C) and HAc-HPr (D) biofilms.

A concomitant increase in PHA (PHB or PHV) storage in the biomass was observed in this phase (Fig. 4.4A and B). In subsequent aeration phase, the stored PHAs were partially consumed to replenish the biomass poly-P pool (Fig. 4.4A and B), the remaining being converted to glycogen (Fig. 4.4A and B)¹⁰⁶. The only major difference between PAO and GAO metabolism is that, the energy for VFA uptake under anaerobic conditions in GAO is derived from the intracellular glycogen. The VFA to polymer ratios were determined to be at 0.75 (gly/PHA), and 0.36 (PHV/VFA) using HAc as sole carbon substrate. The ratios were 0.83 (gly/HAc), and 0.3 (PHV/HAc) for biomass using HAc-HPr as carbon substrate. These ratios indicate involvement of PAO metabolism for VFA uptake in the anaerobic phase (Fig.

4.4). This was further supported by the decrease in PHV and PHB content in proportion to the increase in Glycogen during aeration as observed in previous studies^{107,108}. It is also observed that, there are not many changes in the ratios between PAO I and PAO I and II mixed biomass. This is mainly due to the similar abundances of PAO I and II (Fig. 4.3B).

Table 4.1. Comparison of EBPR conversions observed in the biofilms from HAc (PAO I) and HAc-HPr (PAO I and II) with the published reports.

	Condition	P/VFA	Gly/VFA	Gly/PHA	PHA/VFA
PAO I*		0.19	0.75	2.02	0.36
	P-limiting	0.07	1.25	-	0.31
PAO I and II*		0.46	0.83	3.48	0.3
	P-limiting	0.7	0.96	-	0.8
GAO*		0.03-0.04	1.1	-	0.35
PAO- TCA pathway ¹⁰¹		0.75	-	0.42	0.89
PAO I ^{107,108}		0.54-0.7	0.38-0.74	-	0.02-1.31
PAO I and II ¹⁰⁸		0.08	1.08	-	0.28
PAO II ¹⁰⁸		0.01-0.22	0.96-0.98	-	0.23-0.32
GAO ¹⁰⁹		0.01-0.08	1.2	-	0.52-0.69
PAO II and GAO ¹⁰⁰		0.03	1.28	-	0.54
PAO ¹¹⁰		0.21-0.27	0.96-1.02	2.18-3.15	0.23-0.65

* This study

The P/VFA ratio was at 0.03 P-mol/C-mol and 0.04 P-mol/C-mol using HAc and HAc-HPr, respectively, for granules formed in SBRs without CSC particles. Glycogen consumption and PHA production are generally higher for GAOs, resulting in lower P/VFA ratios⁹⁸. Similar lower P/VFA values of 0.01 and 0.08 were reported for GAO metabolism (Table 4.1. Comparison of EBPR conversions observed in the biofilms from HAc (PAO I) and HAc-HPr (PAO I and II) with the published reports.). The lower P/VFA ratio indicates involvement of GAO metabolism in anaerobic VFA uptake. Therefore, GAOs compete with PAO for VFA¹⁰⁶. GAOs have a similar VFA uptake metabolism to that of PAOs, but are not capable to accumulate P. Therefore, enrichment and abundance of GAOs is undesirable for establishing EBPR pathway. Apart from feast-famine feeding strategy of SBR, temperature (>25 °C) can markedly influence competition between PAOs and GAOs.

Additionally, the anaerobic Gly/VFA ratios provide details on PAO or GAO metabolism based on the operation of glycolysis or tricarboxylic acid (TCA) cycle¹⁰¹. GAOs

depend on glycogen to derive energy using the glycolysis pathway, whereas PAOs use poly-P. Hence, PAOs contain higher poly-P content (Fig. 4.5. Microscopic visualization of DAPI stained poly-P from HAc (A) and HAc-HPr (B) biofilms. For comparison activated sludge without poly-P is shown (C).).

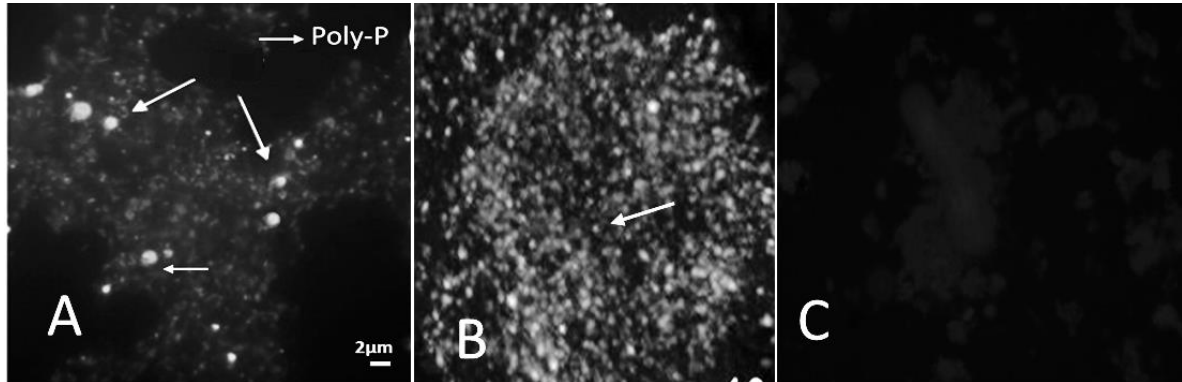


Fig. 4.5. Microscopic visualization of DAPI stained poly-P from HAc (A) and HAc-HPr (B) biofilms. For comparison activated sludge without poly-P is shown (C).

Consequently, the Gly/VFA ratio for known GAOs is higher (> 0.7) than for PAOs¹⁰¹. In this study, Gly/VFA ratio was 2.02 for HAc and 3.48 for HAc-HPr biofilms. This observation is in line with the high temperature EBPR (>25 °C) where the ratios are similar (2.1 and 3)^{110,111}. Additionally, PHA/VFA ratio of 0.3-0.65 indicates glycolysis involvement for producing PHA¹¹¹. The 16S rRNA sequencing and qPCR analysis showed no to limited (2%) known GAOs in the biomass sample (Chapter 3). Therefore, there were other possible carbon uptake metabolisms beyond the current understanding warranting further investigation. Based on the results discussed in this study, a schematic showing nitrogen and phosphorus metabolism by biofilms and granules is presented in Fig. 3.6.

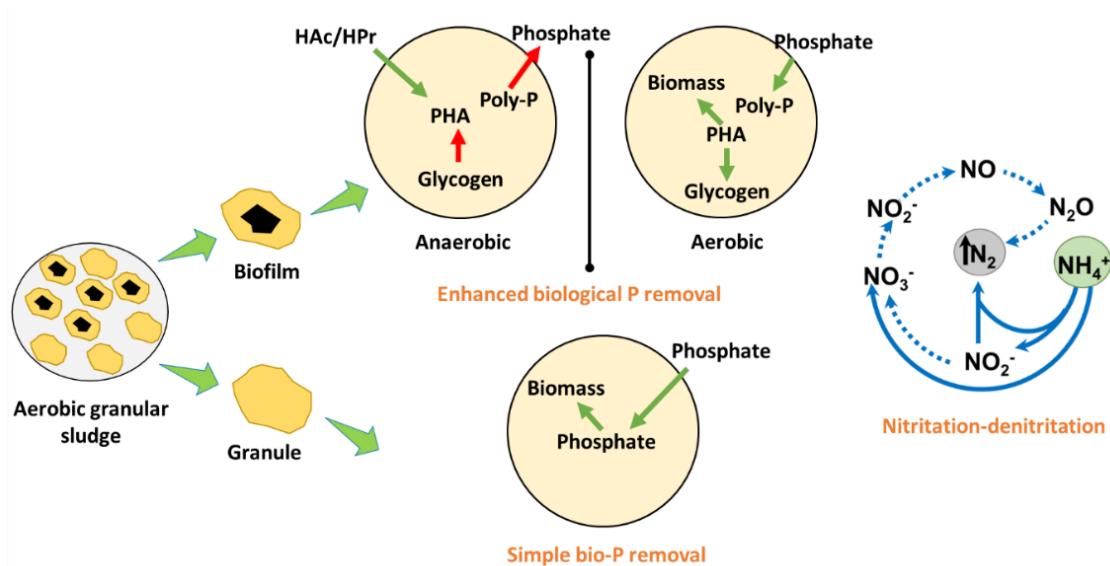


Fig. 4.6. Proposed nitrogen and phosphorus removal mechanisms in co-existing granules and biofilms.

4.3.4 Effect of influent P/C ratios

Besides the enrichment of PAOs, it was imperative to verify the abundance of PAO clades and their metabolism under phosphate limiting conditions. This may further help to develop an enrichment strategy for different PAO clades I or II for implementing EBPR process^{99,112,113}. The biomass abundant in PAO clades I and II were subjected to different influent ortho-phosphate concentrations. The increase in influent phosphate concentration (10 to 45 mg L^{-1} P) resulted in higher P-release (up to 18 mg L^{-1} P) and consequently higher ortho-phosphate concentration at the end of anaerobic phase and *vice versa*. The P/VFA ratio were between 0.1 and 0.7 P-mol/C-mol with the highest P-release at 0.025 P/C ratio (Fig. 4.7A). At the lowest influent P/C ratio, P/VFA of 0.07 P-mol/C-mol, indicating a mixed PAO-GAO metabolism (Table 4.1). Nevertheless, the population was dominated by PAO clade I. No known GAO was detected. This indicates that PAO clade I can perform mixed PAO-GAO metabolism under phosphorus limiting conditions, as reported previously¹¹⁴. The influent P/C ratio clearly affected the VFA uptake of biomass in the anaerobic phase. Since no significant changes in PAO clades abundance was observed at low P/C ratio (Fig. 4.7B), the observed

changes in the P removal pattern is related to the metabolic shift of PAO clade I similar to earlier reports¹¹⁴.

Furthermore, the biomass having PAO clades I and II developed using HAc-HPr did not shift to mixed PAO-GAO metabolism under P limiting conditions at P/C ratios 0.02 and 0.035 P-mol/C-mol. The influent P/C ratio did not seem to influence the anaerobic conversions of PAO clade I and II biofilms (Table 4.1). This observation was also supported by the increase in aerobic P-uptake by about 45% in presence of PAO clade II (Fig. 4.7A). Hence, low influent P/C ratios enable enrichment of PAO clade II and high P/C ratios support enrichment of PAO clade I. Substantial metabolic differences were between the PAO clades, suggesting potential niche differentiation between different subpopulations¹⁰⁷.

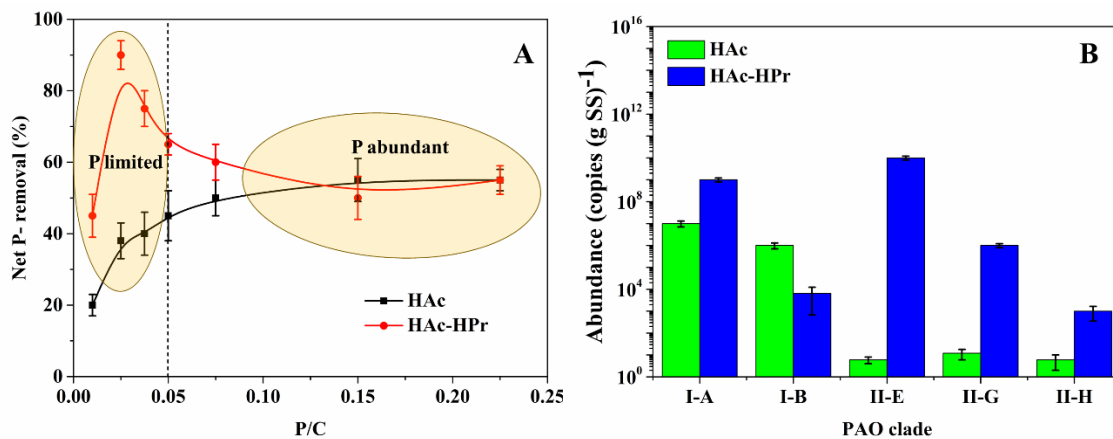


Fig. 4.7. Performance of biofilms at different influent P/C ratios (A) and abundance of PAO clades at low P/C ratios (0.01) (B).

4.3.5 Impact of salinity on PAO clades

The nutrient removal performance of biomass developed using HAc and HAc-HPr at different salinities are shown in Fig. 4.8. Nutrient removal was severely impacted by salinity. TOC removal was decreased by up to 30% at 10 ppt salinity. The impact of salinity was more severe on nitrogen and phosphorus removal. For instance, ammonium and total nitrogen removals of HAc biomass was decreased to 60% and 50%, respectively, at 2 ppt salinity. While ammonium and total nitrogen removals were decreased to about 70% and 60%,

respectively, at 2 ppt salinity for HAc-HPr grown biomass (Fig. 4.8B and C). Inhibition in P removal by HAc biomass was higher than HAc-HPr biomass at all the tested salinities (Fig. 4.8D).

AOBs and anammox were more sensitive to presence of seawater salt. In case of activity of PAOs, from the net P-removal profiles, at 2 ppt salinity, PAO I was more sensitive than combined PAO I and II¹⁰¹ (Fig. 4.9D). Complete activity of PAO I was lost at 5 ppt and PAO II at ≥ 10 ppt (Fig. 4.8D and Fig. 4.9). However, in presence of PAO II, PAO I seem to sustain even up to 5 ppt salinity (Fig. 4.9). Further probing the mechanism by which PAO activity was lost, it was observed that, the anaerobic P/VFA ratio was severely affected but more pronounced to PAO I. When the salinity was increased to 5 ppt, the anaerobic HAc uptake decreased by 60% and 31% respectively for PAO I and PAO II. It is Likely that below 3 ppt salinity inhibition of enzymes responsible for HAc uptake or, P-release enzymes (*ppk*). The P-release at 1% salinity was nearly zero, but HAc utilization continued, suggesting a switch in the metabolism from a poly-P dependent to glycogen dependent for energy source. This observation was also reported by Lopez et al.^{115,116}, when PAOs were subject to anaerobic starvation. Once the salinity concentration is above the maximum threshold concentration, salts are reported to accumulate, inhibiting the metabolic activities responsible for HAc uptake, utilization, and P- release¹¹⁴.

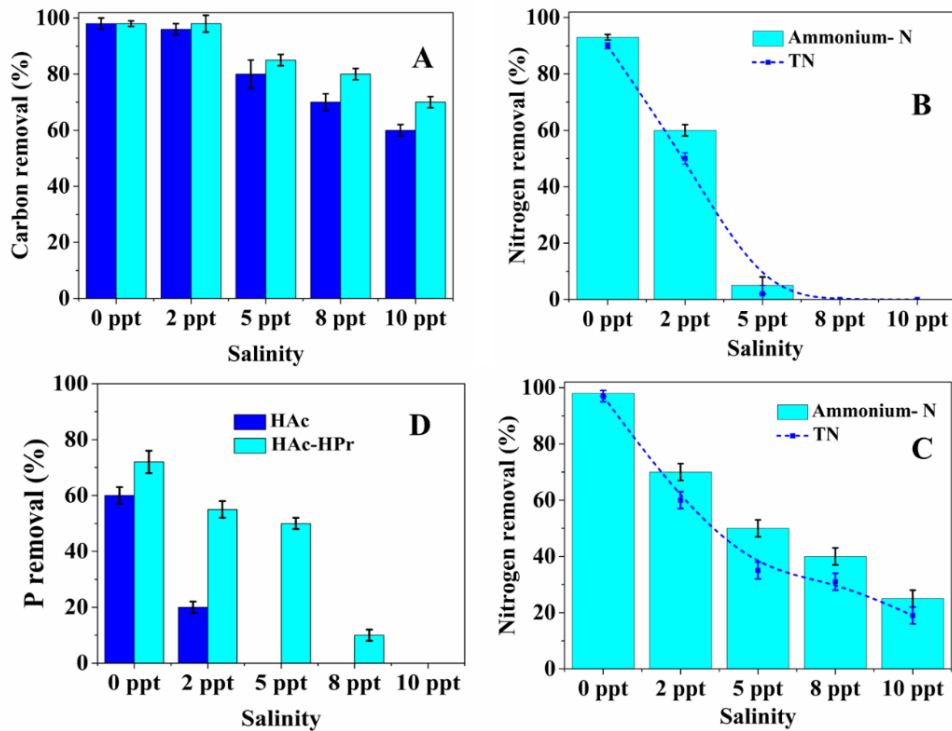


Fig. 4.8. Nutrient removal performance of biofilms developed using HAc and HAc-HPr at different salinities. TOC removal (A). Nitrogen removal by HAc biofilms (B). Nitrogen removal by HAc-HPr biofilms (C). Phosphorus removal by HAc and HAc-HPr biofilms (D).

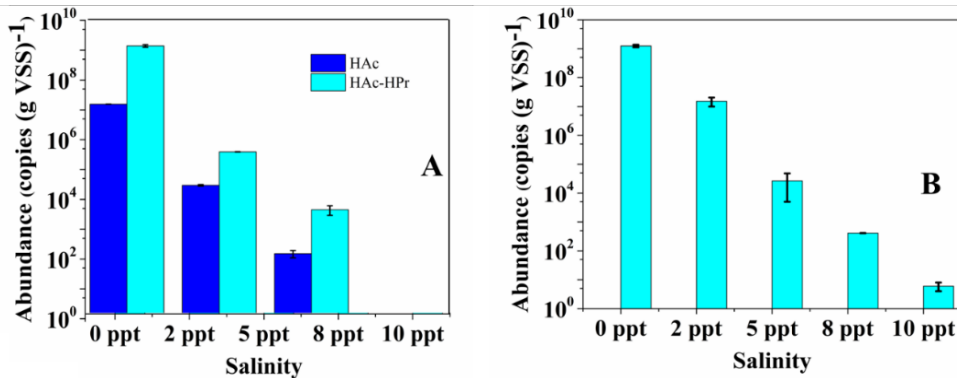


Fig. 4.9. Abundances of PAO clade IA (A). PAO clade IIE (B) after subjecting to different salinities.

4.3.6 Implications

This study evaluated the adaptability of pre-formed AGS performing N and P removal to salinity effects. The results suggested differential response of PAO clades to salinity. Previous studies have shown requirement of longer adaptation while granulation of activated sludge for establishing nutrient removal. More severe inhibition on NH_4^+ removal was reported under saline conditions. Strong inhibition ($\geq 50\%$) in nitrogen removal was observed at 5 ppt salinity. Previous studies also reported low ammonium removals of 20 to 40%⁴⁴. However,

much lower total nitrogen removals were observed due to NO_2^- accumulation. Most of the previous studies on aerobic granules and salinity have not reported P removal performance^{44,117,118}. Hence, assessment of the long-term effects of salinity on the overall microbial community and function may provide additional information on the potential selection or adaptation of salt-tolerant strains. Alternative strategies may be explored for minimizing longer adaptation periods, and avoiding indirect effects of ammonium removal on selection of PAOs under saline conditions.

4.4 Conclusions

This study deciphered the role of CSC particles in rapidly establishing nitrogen and phosphorus removal pathways in SBRs. Rapid bacterial attachment and biofilm formation during start-up phase has facilitated retention and growth of PAOs. Due to high abundance of PAOs, the segregated biofilms showed efficient P removal *via* EBPR than coexisting granules. The results showed that differential abundance of PAO clades I and II dependent on the carbon substrate (HAc or HAc-HPr). As the influent P/C ratio increased, the P uptake also increased. At lower P/C ratio ratios, PAO clade I shifted to GAO-metabolism. EBPR performing biomass was found to be sensitive to salinity changes. Both nitrogen and phosphorus removals were severely impacted at 2 to 10 ppt salinity, suggesting requirement of alternative approaches for biological treatment of saline wastewaters.

Chapter 5

De novo granulation of native seawater microorganisms for biological nitrogen and phosphorus removal under saline conditions

Abstract

Activated sludge has been used as the standard inoculum for cultivating aerobic granular sludge even for brackish and saline wastewater treatment. This approach was partly successful but faced severe difficulties to establish effective biological nutrient removal under saline conditions. To circumvent this problem, formation of aerobic granular sludge directly from halophilic bacteria of seawater was investigated for effective nutrient removal under saline conditions. For this, a sequencing batch reactor (SBR) was directly fed with nutrient-amended seawater without using seed biomass (activated sludge or granules) for developing halophilic aerobic granular sludge. Results demonstrated that it was indeed possible to cultivate aerobic granular sludge directly from the seawater-borne microorganisms without using seed biomass in the SBR. Formation of grain-shaped microbial growth was noticed within 7 days suggesting that granulation of halophilic bacteria of seawater is a rapid developmental process under saline conditions. Stable ammonium and total nitrogen removals were established very quickly within 10 days of SBR start-up. Ammonium and total nitrogen removals ranged from 92 - 100% and 81 - 90%, respectively, during 22 to 100 days of operation. Phosphorus removal improved progressively during SBR operation and stabilized at >76% by 2 months. Phosphorus removal profiles by halophilic aerobic granular sludge followed typical enhanced biological phosphorus removal process. The granules had less bacterial diversity than the seawater indicating selection and enrichment of certain bacterial groups during granulation and wastewater treatment. Granulation of autochthonous bacteria of seawater is a novel strategy for developing halophilic aerobic granular sludge and to achieve high nitrogen and phosphorous removals under saline conditions.

Keywords: Aerobic granular sludge; biological nutrient removal; nitrogen removal; enhanced biological phosphorus removal; saline wastewater treatment.

5.1 Introduction

Aerobic granular sludge (AGS) process has a growing interest for treating saline wastewaters because microbes of granules could tolerate higher salinities than activated sludge^{120,121}. Majority of the previous research was focused on cultivating granular sludge from activated sludge followed by acclimation of granules to higher salinities. In all these previous studies, freshwater microbial communities i.e. activated sludge or aerobic granules were used as the seed sludge for developing halotolerant aerobic granular sludge. However, several authors reported difficulties in establishing effective biological nitrogen and phosphorus removal under saline conditions by acclimation of freshwater microbial communities^{118,120, 43,44,46,50}. Poor total nitrogen removal efficiencies were often noticed under saline conditions mainly due to nitrite accumulation^{118,120,122}. Poor biological phosphorus removal was attributed to the effect of salinity and also nitrite on phosphate accumulating organisms^{43,123-125}.

Treatment of saline wastewaters basically requires the presence of halotolerant or halophilic microorganisms capable of removing simultaneously organic carbon, nitrogen and phosphorus. Comte et al.¹²⁶ showed that there is only a little overlap in the abundant bacterial taxa between freshwater and saline microbial communities¹²⁶. Therefore, gradual increase in salinity is required to select and enrich the less abundant salt-tolerant bacteria of freshwater microbial communities for treating saline wastewaters. Even gradual acclimation strategy did not successfully establish biological phosphorus removal when aerobic granular sludge was developed from activated sludge under saline conditions^{123,127}. An alternative approach for tackling this issue is to consider halophilic marine microorganisms which are already thriving in the presence of high salt for developing saline wastewater treatment.

There are no studies on previous cultivation of aerobic granular sludge directly from the autochthonous microorganisms of seawater and their nutrient removal performance under saline conditions. It is hypothesized that cultivation of aerobic granular sludge from

microorganisms indigenous to marine environment may avoid acclimation and may significantly reduce the start-up periods for establishing nutrient removal. Hence, the main objective was to evaluate cultivation of halophilic aerobic granular sludge from autochthonous bacteria of seawater for simultaneous removal of organic carbon, nitrogen and phosphorus. Experiments were carried out in a 3-litre volume SBR by directly feeding nutrient-amended seawater. SBR was not inoculated with seed biomass (i.e., activated sludge or granules) and seawater acted as the source for halophilic microorganisms. Granules formed from halophilic bacteria of seawater were characterized using scanning electron microscope (SEM), X-ray diffraction (XRD) and 16S rRNA gene sequencing. The nutrient removal capabilities of halophilic aerobic granular sludge were assessed under conditions (17 to 34 g L⁻¹ NaCl) typical to saline sewage.

5.2 Material and methods

5.2.1 Nutrient amended seawater

Seawater was collected from the coast of Bay of Bengal once in a week and used for preparing nutrient amended seawater. The seawater was amended with sodium acetate (517 mg L⁻¹), ammonium chloride (30 mg L⁻¹ NH₄⁺-N), and inorganic phosphorus (10 mg L⁻¹ PO₄³⁻-P) for preparing synthetic saline wastewater. The complete composition of nutrient-amended seawater was given in Appendix II. Nutrient-amended seawater was used as the source of nutrients and microorganisms. Henceforth, nutrient-amended seawater was referred to as synthetic saline wastewater.

5.2.2 Cultivation of halophilic aerobic granular sludge (hAGS)

Sequencing batch reactor setup and operation was detailed in Chapter 3. The SBR was ‘not inoculated’ with any kind of seed biomass (i.e., activated sludge or granules) at the beginning or any stage of operation. Seawater contained total viable bacterial counts of 4 x 10³ CFU mL⁻¹ and acted as the source of microorganisms for granulation. SBR was operated with 6 h

cycle and 4 cycles per day. The SBR was operated for 100 days to monitor granulation of seawater-borne microorganisms and nutrient removal under saline conditions. Liquid samples were collected regularly for determining nutrient removal performance. Biomass samples were collected regularly during SBR operation for monitoring formation of granules.

5.2.3 Nutrient removal capabilities at different salinities

Synthetic saline wastewater was prepared with different salinities of 17, 25 and 34 ppt by using different proportions of seawater. Batch experiments were carried out in 250 mL Erlenmeyer flasks with 100 mL of synthetic saline wastewater. The test flasks were inoculated with 1% (w/v) AGS collected from the SBR treating synthetic saline wastewater. Control flasks were setup with synthetic saline wastewater (34 ppt) without granular sludge to determine abiotic removal of nutrients, if any. These flasks were incubated in an orbital shaker set at 150 rpm and 30 °C. At the end of 24 h batch, liquid samples were collected and analysed for total organic carbon, reactive nitrogen compounds and phosphorus. The batch experiments were continued in fed-batch mode for 10 batches in order to examine the stability of granules and nutrient removal performance at different salinities.

5.2.4 Characterisation of halophilic aerobic granular sludge

Biomass samples collected from the SBR was monitored for progression of granulation using SMZ1000 stereomicroscope (Nikon, Japan) equipped with DP70 camera (Olympus, Japan) (Details given in chapter 2). Scanning electron microscope and energy dispersive spectroscopy (Philips XL30 FIBSEM) was performed on fixed and dehydrated granules (Details of fixation, dehydration was given chapter 2).

A fluorescence microscope was used for visualizing the cells present in the seawater and granules. Seawater (about 1 L) was centrifuged at 10000 rpm for 5 min to harvest the microbes. The cell pellet and granules were incubated in Syto 9 solution (10 µL of 5 µM) and

incubated under dark condition for 5 min. The cells were visualized through FITC filter using an epifluorescence microscope (Carl Zeiss, India) equipped with a digital camera (Jenoptik, Germany).

Physical characteristics such as water content, settling velocity, sludge volume index (SVI), mixed liquor suspended solids (MLSS) and mixed liquor volatile suspended solids (MLVSS) were determined according to standard methods⁶⁴.

The fractionation of P in the granular sludge was carried out according to the standards, measurements, and testing (SMT) programme of European Commission¹¹⁹. Briefly, halophilic AGS was obtained from SBR1 on day 25, 60, and 100, dried, and powdered. The powdered sample (400 mg) was fractionated into total P (TP), organic P (OP), inorganic P (IP), apatite P (AP; P bound to calcium), and non-apatite inorganic P (NAIP; P bound to aluminium, iron, and manganese oxyhydroxides) as per the SMT protocol. The P content of the fractions was measured using the molybdenum blue method⁶⁴.

Granular sludge collected from the SBR on day 100 was freeze dried overnight and powdered. XRD was performed using a Bruker diffractometer using Cu K α radiation ranging 2θ from 5 to 80°. The operational voltage and current were respectively, 40 kV and 30 mA. The peaks were compared against the standard JCPDF cards and reported. Granular sludge treating synthetic saline wastewater was acid-digested for determining metal ions (i.e., Na, K, Mg, Ca, Sr and Fe) using ICP-AES.

5.2.5 Genomic DNA extraction and bacterial community analysis

Genomic DNA of seawater and granular sludge treating synthetic saline wastewater were harvested on day 1 (seawater) and day 100 (hAGS) for determining bacterial community. Genomic DNA was isolated using QIAmp DNA Mini kit (Qiagen, Germany) as per the manufacturer's instructions. Sequencing of the 16S rRNA gene was performed on Illumina

MiSeq platform. Sequences were analyzed using standard protocols (Sequencing and analysis details given in chapter 2).

5.2.6 Nutrient analysis

Determination of total organic carbon, ammonium, nitrate, nitrite and phosphorus concentrations were performed according to standard methods⁶⁴.

5.3 Results and discussion

The main purpose of this study was to make use of autochthonous halophilic seawater bacteria in the form of granular sludge for effective removal of organic carbon, nitrogen and phosphorus from saline wastewater. Conventional approaches relied on developing halotolerant community through selection and enrichment of salt-tolerant microorganisms which often requires long start-up periods. Moreover, nitrogen and phosphate removal capabilities of aerobic granules were severely inhibited upon exposure to saline conditions^{43,118}. Recent studies indicated that halophilic biomass harbour superior nutrient removal capabilities compared to halotolerant biomass developed through enrichment in bioreactors^{128,129,130}. Though these strategies improved nitrogen removal considerably, biological phosphorus removal is still an issue to be addressed under saline conditions.

5.3.1 C, N and P removal from synthetic saline wastewater

Nutrient removal from synthetic saline wastewater during 100 days of SBR operation is shown in Fig. 5.1. Organic carbon removal was observed from the beginning (Fig. 5.1). Percentage carbon removal ranged from 94.5 to 100% with an average of $96.3\% \pm 1.4$ for entire SBR1 operation. Cycle measurements showed that most of the organic carbon (acetate) was removed within the first 1.5 to 2 h (Fig. 5.1B). The cycle period could be distinguished into anaerobic and aerobic phases based on the prevailing dissolved oxygen profile. Ammonium ion removal was also noticed from cycle 1 onwards (Fig. 5.1C). At the beginning,

ammonium ion removal was associated with accumulation of nitrate up to 40 mg L⁻¹ NO₃⁻-N (on day 3). In subsequent cycles, lower effluent nitrate concentrations were noticed indicating good denitrification by day 9. Ammonium-nitrogen and total nitrogen (TN) removals were at 57 and 45%, respectively, on day 9 of start-up (Fig. 5.1C). Thereafter, ammonium removal was further improved. After 10 days of SBR1 start-up, effluent concentrations of reactive nitrogen compounds (NH₄⁺-N, NO₃⁻-N and NO₂⁻-N) were below 5 mg L⁻¹. Ammoniacal nitrogen removal improved quickly and stabilized over >95% within 15 days of start-up. At steady-state (after 15 days), complete removal of 30 mg L⁻¹ NH₄⁺-N was observed by 5th h of cycle, corroborated with formation of smaller quantities of nitrite and nitrate (Fig. 5.1D). Interestingly, concentrations of nitrate and nitrite were subtle at ≤5 and 2 mg L⁻¹, respectively (Table 5.1). TN removal also improved to over 80% within day 15 of start-up and maintained thereafter.

Table 5.1. Nutrient removal performance and properties of granular sludge treating synthetic saline wastewater at 34 ppt.

Parameter	Time (d)				
	7	22	60	82	100
Ammonium-N removal (%)	53.5	92.3	95.4	100	100
Total N removal (%)	44.8	89.9	87.0	90.3	81.7
Phosphorus removal (%)	32.5	12.8	76.5	79.9	78.4
TOC removal (%)	98.0	99.0	99.0	99.0	99.0
MLSS (g L ⁻¹)	-	30.2 ± 1.7	31.2 ± 1.6	31.5 ± 1.4	34.4 ± 1.1
SVI ₅ (mL g ⁻¹)	-	1.9 ± 0.1	0.8 ± 0.1	2.4 ± 0.1	1.8 ± 0.2
Settling velocity (m h ⁻¹)	-	18.4 ± 1.4	26.6 ± 1.3	30 ± 0.8	32 ± 1.6

Fed-batch experiments showed that the nutrient removal under saline conditions was sustained only in the presence of AGS (Fig. 5.2). The removal of organic carbon, nitrogen, and phosphorus was found to be <5% when autoclaved AGS used as source of microorganisms (Fig. 5.2D), indicating biological nutrient removal.

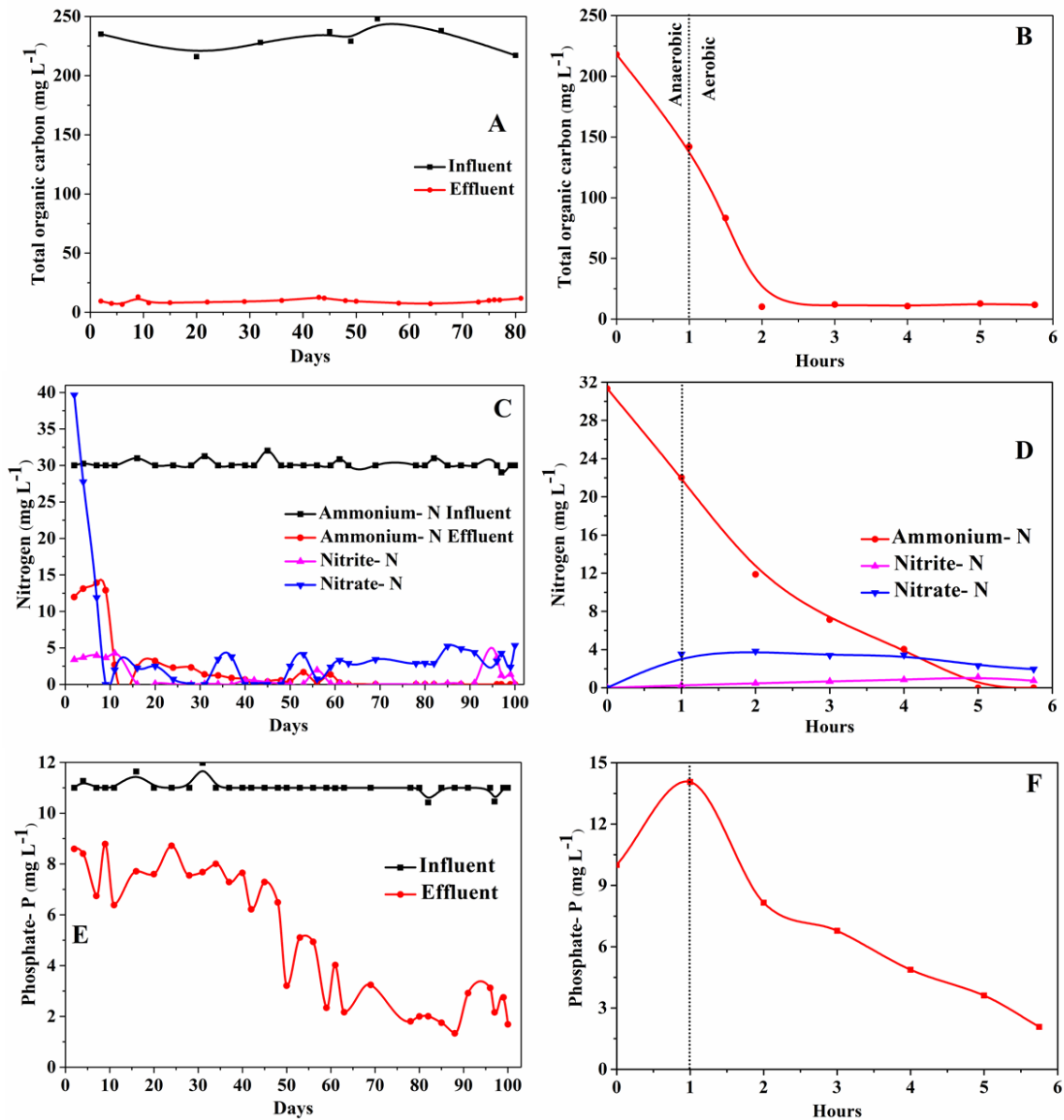


Fig. 5.1. Organic carbon, nitrogen, and phosphorus removal in a lab-scale (3 L volume) sequencing batch reactor fed with saline synthetic wastewater. Cycle profiles were collected from cycle 364 on day 91. TOC removal performance (A), TOC removal profile during 6 h cycle (B), ammonium removal performance (C), profile of nitrogen compounds during cycle (D), phosphorus removal performance (E), and phosphorus removal profile during cycle (F).

No significant accumulation of nitrite or nitrate during cycle indicates occurrence of simultaneous nitrification and denitrification or nitrification-denitrification pathways. The ammonium and total nitrogen removals were very stable throughout 100 days of experiment. Accumulation of nitrite is a primary bottleneck in biological treatment of saline

wastewaters^{43,46,117, 118,124,127}. Recent studies indicated that use of halophilic bacteria of fish-canning wastewater^{128,129} or estuarine sediment¹³⁰ as inoculum for improving nitrogen removal under saline conditions. The present study demonstrated the use of seawater-borne microorganisms for developing halophilic microbial community for achieving efficient nitrogen removal under saline conditions. The results confirmed that the halophilic bacteria of seawater are an effective solution for performing biological nitrogen removal under saline conditions by avoiding nitrite accumulation.

Phosphorus removal was also noticed from the beginning of SBR1 operation. However, phosphorus removal was lower at <50% during the first 60 days. Net phosphorus removal was still high because about 5 mg L⁻¹ of PO₄³⁻-P was removed during 6 h cycle period. Subsequently, phosphorus removal was further improved to about 76% by 60 days of start-up (Fig. 5.1E, Table 5.1. Nutrient removal performance and properties of granular sludge treating synthetic saline wastewater at 34 ppt.). Thereafter, phosphorus removal was stable until the end of experiment (Fig. 5.1E). Phosphorus removal could be distinguished into two phases such as increased P concentrations in anaerobic period (P release phase) and steady P decline phase in aerobic period (P uptake phase) during 6 h cycle (Fig. 5.1F). An increase of up to 4 mg L⁻¹ PO₄³⁻-P was observed during 1 h anaerobic fill period. In the subsequent aeration phase, much more phosphate (up to 12 mg L PO₄³⁻-P) was removed giving rise to an overall net removal of phosphate from the saline wastewater. After 60 days of operation, the PO₄³⁻-P was ≤ 3 mg L⁻¹ in the treated saline wastewater. P fractionation of biomass would give an indication on the P release ability and/or P removal mechanism. AP was found to be the most dominant P fraction contributing to >50% of IP in the halophilic AGS. NAIP and OP increased to 76 mg gVSS⁻¹ PO₄³⁻ - P and 96 mg gVSS⁻¹ PO₄³⁻ - P, respectively, in the granular sludge during SBR1 operation. The typical ortho-P removal profiles measured during the cycle showed the occurrence of enhanced biological phosphorus removal under

saline conditions. Unlike nitrogen removal, establishment of phosphorus removal required long term (60 days) reactor operation. Many of the previous studies have reported setback to phosphorus removal when activated sludge or aerobic granules were adapted to higher salinities^{43,46,118,131}. The salt ions have been reported to impact biological phosphorus removal by causing nitrite accumulation⁴³. Such an effect is unlikely due to non-accumulation of nitrite in the current study. Wang et al.¹²³ also reported inhibition of biological phosphorus removal in AGS without nitrite accumulation. Inhibition of biological phosphorus removal was not evident but it took long time to establish about >70% removal. The results described in this chapter confirmed that efficient EBPR is possible under saline conditions by developing halophilic community from seawater-microorganisms.

Nitrogen and phosphorus removals were found to be negligible when synthetic saline wastewater was incubated without granular sludge at 30 °C and with/without aeration. Removal of ammonium ion through deprotonation to NH₃, partitioning of NH₃ to gaseous headspace and finally its presence in the exhaust from the SBR was determined using acid trap. The ammonium removal through this abiotic process was found to be negligible at 1.6 mg NH₄⁺-N L⁻¹. These results and batch tests using autoclaved granular sludge suggested that ammonium was principally removed through a biological nitrogen removal process. Furthermore, ammonium removal through biological oxidation was supported by (i) a gradual decrease in ammonium ion concentration during aeration phase and (ii) formation of nitrite and nitrate though at smaller quantities. Establishment of complete ammonium oxidation and total nitrogen removals within 10 days of SBR start-up without using a seed inoculum under saline conditions was noteworthy finding.

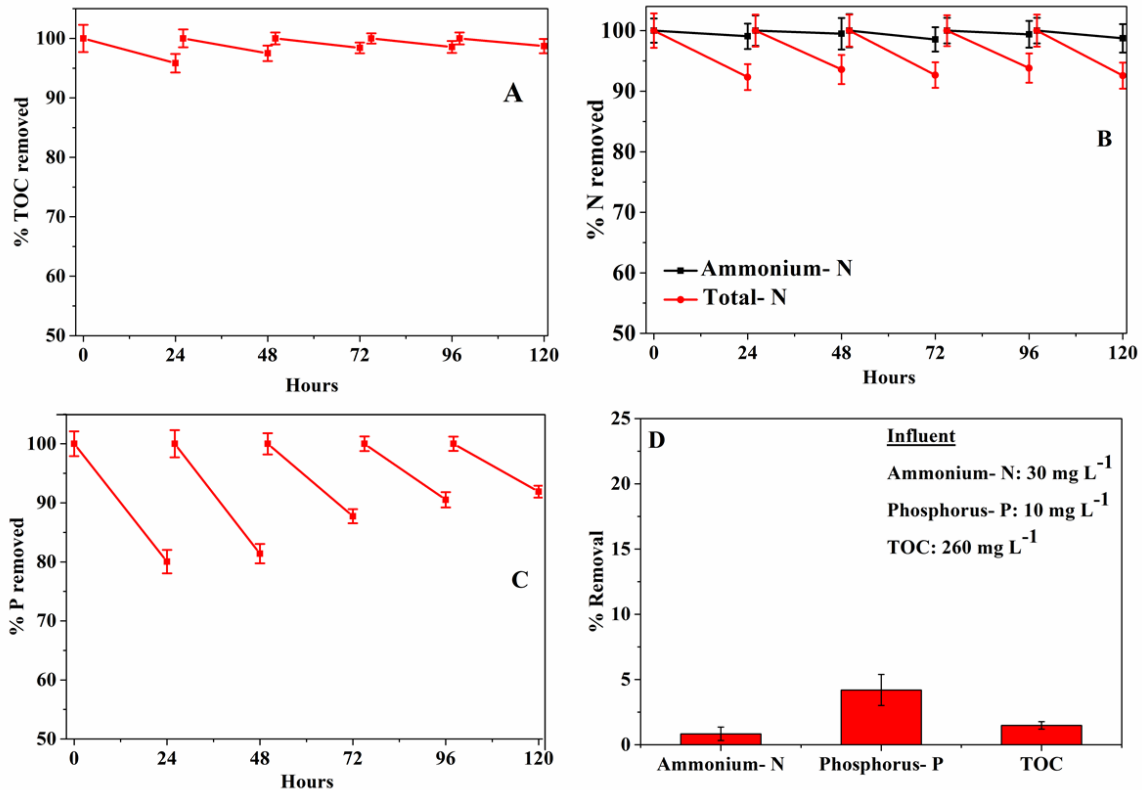


Fig. 5.2 Carbon, nitrogen and phosphorus removal by halophilic aerobic granular sludge in fed-batch experiments at 34 ppt. Carbon, nitrogen and phosphorus removal by halophilic aerobic granular sludge (A-C). Carbon, nitrogen and phosphorus removal in the presence of heat-killed aerobic granules (D). Fed-batch experiment was carried out for 5 batches to determine the contribution of biotic/abiotic mechanisms in nutrient removal under saline conditions.

5.3.2 C, N and P removal at different salinities

After establishing stable C, N and P removal at 34 ppt, the stability of nitrogen and phosphorus removal was evaluated at lower salinities (17 and 25 ppt) typical to saline sewage. Ammonium ion removals were lower during the first few cycles, mainly attributed to changes in mixing (from aeration to orbital shaking) and hydraulic retention time. But, ammonium removal was quickly re-established by 8th cycle leading to complete and stable nitrogen removal. Thus, nitrogen removal was considered to be not greatly impacted at lower salinities of 17 and 25 ppt. But, lower phosphorus removal was noticed at 17 and 25 ppt than at 34 ppt. It appears that the P removing organisms are more sensitive to sudden changes in salinity than those involved in nitrogen removal. Batch experiments were performed using the granules formed at 34 ppt. Thus, granules formed at higher salinity (34 ppt) were directly

used for treating lower salinity *viz.*, 17 or 25 ppt salinity wastewater. A gradual acclimation of biomass developed at 34 ppt to lower salinities may minimize detrimental effects on N and P removal.

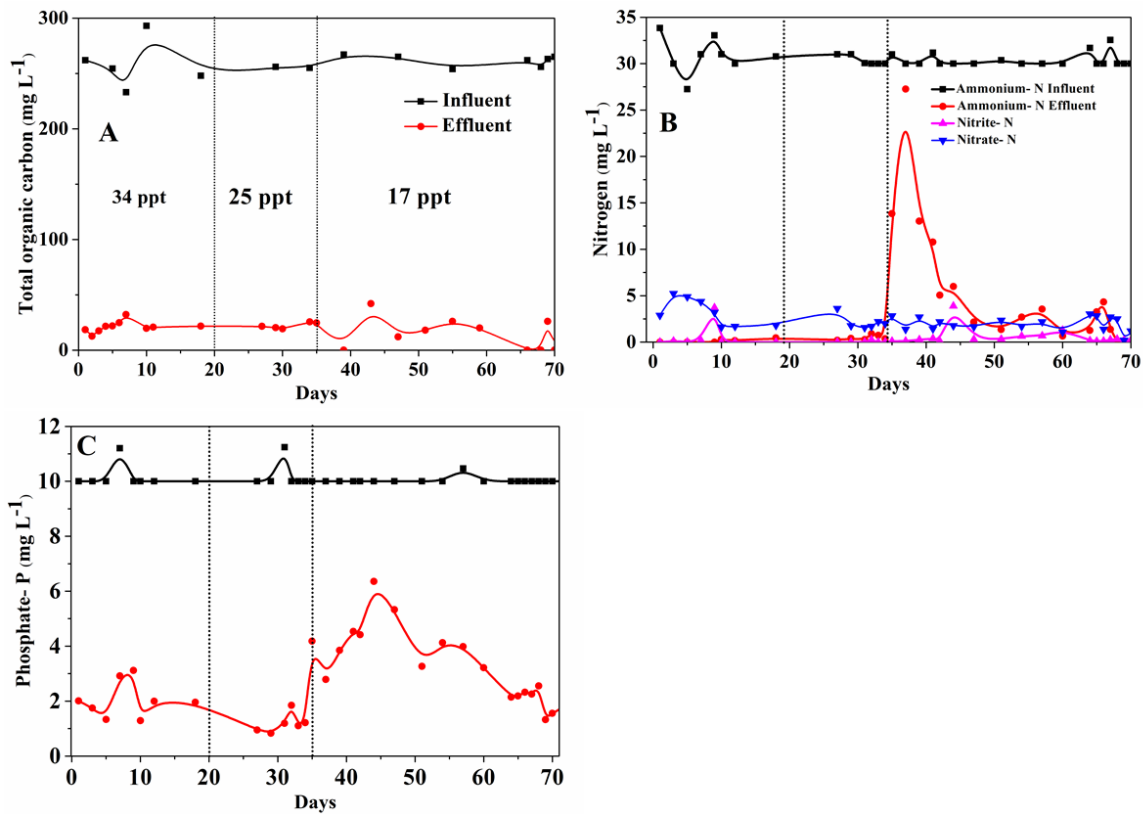


Fig. 5.3. Carbon (A), nitrogen (B) and phosphorus (B) removal by halophilic aerobic granular sludge in a lab-scale sequencing batch reactor (SBR2) operated at different salinities of 34, 25 and 17 ppt.

Stability of halophilic AGS structure and nutrient removal was evaluated in the SBR as well (Fig. 5.3). TOC removal (>98%) was unaffected when salinity decreased from 34 to 25 ppt and then to 17 ppt (Fig. 5.3A). N and P removals were also not impacted when salinity decreased from 34 ppt to 25 ppt (Fig. 5.3B and C). However, ammonium and P removals were decreased by 45% and 20%, respectively, immediately (1st cycle) after decreasing the salinity from 25 to 17 ppt. But, ammonium and TN removals were restored to normal levels within 10 days of SBR2 operation with no accumulation of either nitrite or nitrate.

5.3.3 Bacterial community analysis

Seawater and granular sludge samples were analyzed for bacterial community structure using 16S rRNA gene sequencing. The bacterial diversity of granules and seawater could be assigned, respectively, to 2978 and 649 OTUs. The alpha diversity index showed highest species richness (Shannon H-index) in seawater (7.4) than in the granular sludge (5.2) treating synthetic saline wastewater at 34 ppt. Simpson index also showed decreased species richness in granules as compared to the bacterial diversity observed in the seawater.

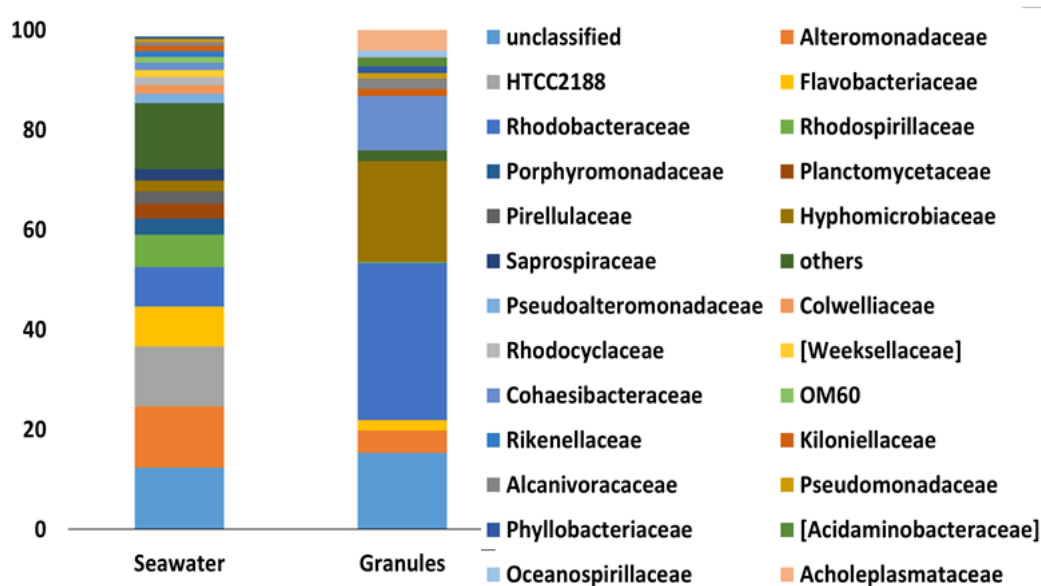


Fig. 5.4. Bacterial community of seawater and halophilic aerobic granular sludge determined by 16S rRNA gene sequencing. Bacterial community analysis at family level.

Bacterial community structure of seawater and granular sludge was presented at phylum, order and family level (Fig. 5.4). Bacterial community of seawater was dominated by Alphaproteobacteria (27%), Gammaproteobacteria (36%), Bacteroidetes (18%) and Flavobacteria (9.5%). In contrast, granular sludge formed from seawater microbes at 34 ppt was dominated by Alphaproteobacteria (76.4%) and Gammaproteobacteria (9.6%). Flavobacteria (2.7%), Phycispharea (3.6%), Planctomycetes (3.6%) and Bacteroidetes (2.9%) together accounted for about 11% of community of granules. High relative abundance of Alphaproteobacteria (76.4%) and Gammaproteobacteria (9.6%) in the halophilic aerobic

granular sludge is in agreement with previous studies on salt-tolerant microbial communities^{129,132}. Selective enrichment of bacterial groups in the granules and their retention in the bioreactor led to a reduction in species richness in granules as compared to seawater.

Huang et al.¹³⁰ also observed a reduction in species richness in the granules than estuarine sediment inoculum. Despite selection and enrichment, the halophilic aerobic granular sludge had fairly high species richness offering stability and diverse metabolic diversity. Several bacteria with a role in nutrient removal were detected in the granules performing simultaneous organic carbon, nitrogen and phosphorus removal from saline wastewater (*Table 5.2*). A shift in bacterial diversity is prominently observed between the bacterial community of seawater and granular sludge. The genus level classification of metagenomic sequences revealed very high proportion of unclassified fraction of 72.3% and 52.4% in seawater and granules, respectively. Therefore, other community analysis tools like high-throughput sequencing needs to be employed for identifying the microbes of important to nutrient removal under saline conditions. Future studies should focus on determining the salinity tolerance of halophilic aerobic granular sludge, characterization of the EPSs matrix of granules formed from seawater microbes and detailed understanding of granulation mechanisms under saline conditions. The settling and functional properties of halophilic aerobic granular sludge to higher salinities ($>34 \text{ L}^{-1} \text{ gNaCl}$) should be evaluated in future studies. The halophilic granules may show promising nutrient removal capabilities and biological treatment under hypersalinites.

Table 5.2 Functional bacteria detected in the granular sludge formed from seawater microbes.

Microorganisms	Prominent metabolic function
<i>Acinetobacter</i>	Phosphorus, PAO metabolism
<i>Alcanivorax dieselolei</i>	Nitrogen, denitrifier with high salt tolerance (15%)
<i>Aquamicrobium aerolatum</i>	Facultative aerobe
<i>Azospira</i>	Nitrogen, nitrogen fixer
<i>Bacillus cereus</i>	Sulphur, sulphate reducer
<i>Bifidobacterium adolescentis</i>	Nitrogen, ammonium oxidiser
<i>Candidatus Accumulibacter</i>	Phosphorus, PAO metabolism
<i>Clostridium</i>	Stickland reaction
<i>Collinsella aerofacium</i>	Obligate anaerobe
<i>Erythrobacter nanhaisediminis</i>	Nitrogen, aerobic denitrifier
<i>Labzenria aggregata</i>	Nitrogen, phototropic NO ₂ reducer
<i>Marinobacter bryozorum</i>	Nitrogen, denitrifier
<i>Marinobacter hydrocarbonoclasticus</i>	Nitrogen, denitrifier
<i>Methylobacterium adhaesium</i>	Nitrogen, nitrate as energy source
<i>Neptuniibacter caesarienesis</i>	Nitrogen, Strict aerobe with dissimilatory nitrate reduction
<i>Nitratireductor pacificus</i>	Nitrogen, denitrification (NO ₃ to NO ₂ only)
<i>Nitroreductor</i>	Nitrogen, NO _x reducer
<i>Nitrosomonas marina</i>	Nitrogen, ammonium oxidiser
<i>Nitrospira</i>	Nitrogen, ammonium oxidation via nitrite pathway
<i>Nonlabens tegetincola</i>	Phosphorus, hydrolyse phosphate, P- metabolism
<i>Oceanicola granulosus</i>	Nitrogen, denitrifier with PHA storage
<i>Paracoccus aminovorans</i>	Nitrogen, ammonium oxidizer
<i>Phaeobacter gallaeciensis</i>	Biotic/ abiotic surface colonizers, Fe- siderophores producers
<i>Planctomycete MS30D1</i>	Nitrogen, anammox
<i>Planctomycetes</i>	Nitrogen, Annamox
<i>Polymorphum gilvum</i>	Hydrocarbon degrading saline bacteria
<i>Pseudomonas balearica</i>	Nitrogen, denitrification
<i>Pseudomonas citronellosis</i>	Nitrogen, denitrifier
<i>Pseudoxanthomonas mexicana</i>	Nitrogen, denitrification (from NO ₂ to N ₂ only)
<i>Rhodocycales related organisms</i>	Phosphorus, PAO metabolism
<i>Roseibium denhamense</i>	Nitrogen, denitrifier Phototropic bacteriochlorophyll producer with phosphatase activity
<i>Roseibium hamelinense</i>	Nitrogen/ phosphorus, denitrifier with phosphatase activity
<i>Spirochaeta halophile</i>	Nitrogen, ammonium utiliser with high salt tolerance (12%)
<i>Stappia meyerae</i>	Carbon, CO oxidation/ CO ₂ fixation, denitrifier
<i>Stenotrophomanas acidaminiphila</i>	Nitrogen, NO _x reducer

5.3.4 Granulation of autochthonous planktonic microbial community

Macro-scale halophilic aerobic granular sludge was successfully developed from the planktonic microorganisms of seawater under saline conditions. It is first report on formation of functional granular sludge from marine planktonic microorganisms without using seed inoculum. An increase in the turbidity was noticed during the first few cycles in SBR1 indicating the growth of microbes present in the synthetic saline wastewater as well as retention of microbes in the SBR1 (Fig. 5.5). During initial days, turbidity increased quickly in the SBR1 indicating growth. However, the turbidity of the treated water leaving the SBR1 was much lower implying retention of microbial growth in the SBR (Fig. 5.5).

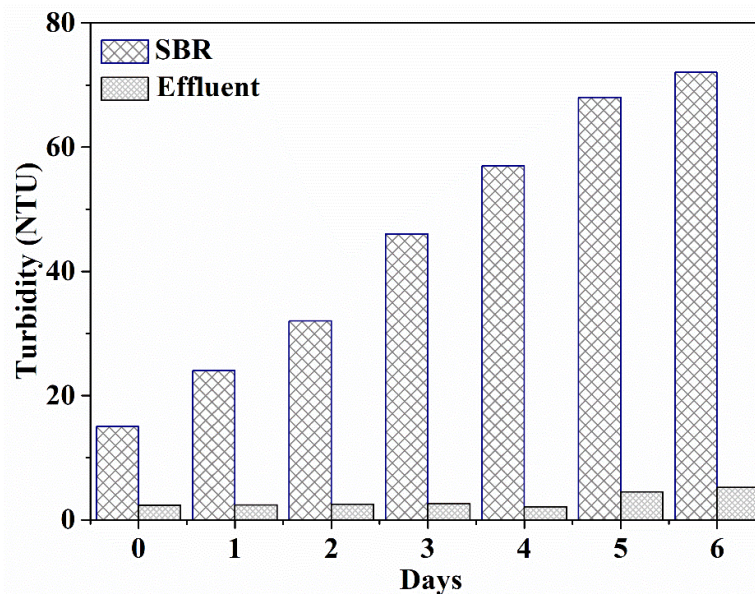


Fig. 5.5. Microbial growth and retention monitored as turbidity during the initial days of SBR operation. Turbidity was seen only during initial days. After a week, growth was mostly in the form of aggregates.

Microbial growth was clearly visible with the naked eye by 4th day (Fig. 5.6). The growth was mainly seen in the form of macro-scale patches suspended in the water column during aeration phase. These observations were corroborated with a steady increase in the MLSS and MLVSS values (Table 5.3). Biomass concentrations increased very quickly in the SBR1 due to growth and retention of well-settling microbial aggregates. The macro-scale patches

of microbial growth became denser and appeared like dense biomass particles within days (Fig. 5.6).

The microbial growth seemed like the typical granular growth observed in AGS reactors after a week (Fig. 5.6; Fig. 5.7). These biomass particles grew in size and became millimetre sized particles by day 15 to 22 of SBR operation. The size of these particles increased further up to 42 d of SBR1 operation. Some of these biomass particles were elongated and had irregular edges. Thereafter, the biomass particles with regular surface were evolved and size increased. An overall increase in MLSS and MLVSS was noticed during SBR1 operation (Table 5.3).

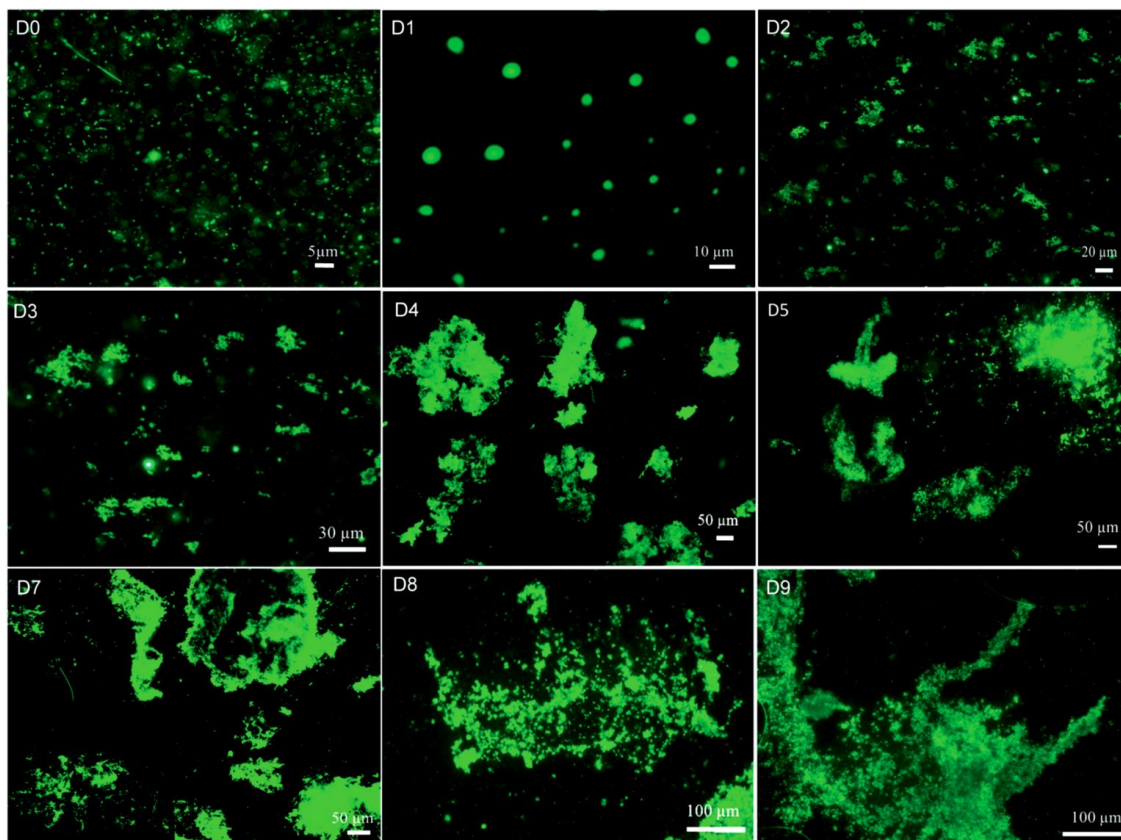


Fig. 5.6. Aggregate formation by the halophilic microbes of seawater during the initial days of granular sequencing batch reactor (SBR) operation. The 3-liter SBR (SBR1) was not inoculated and autochthonous planktonic bacteria present in the nutrient-amended sea

The lower SVI values were maintained through SBR1 operation. Lower SVI values were a clear indication that microbial growth predominantly in the form of dense aggregates but not

as flocs Table 5.3). High MLSS values can be partly attributed to the presence of high inorganic content which increased the density resulting in enhanced settling properties. It is to be noted that metal precipitates can influence the MLSS and in turn SVI values. Biomass evolved from planktonic autochthonous bacteria was dense, compact, and exhibited high hydrophobicity (Table 5.3). The biomass density of granules reached to $1.5 \pm 0.1 \text{ g ml}^{-1}$ by day 25 and increased even further to $1.7 \pm 0.05 \text{ g ml}^{-1}$ by day 100. The hydrophobicity of biomass was found to be high at 86% on day 25 and increased up to 96% by day 100 (Table 5.3).

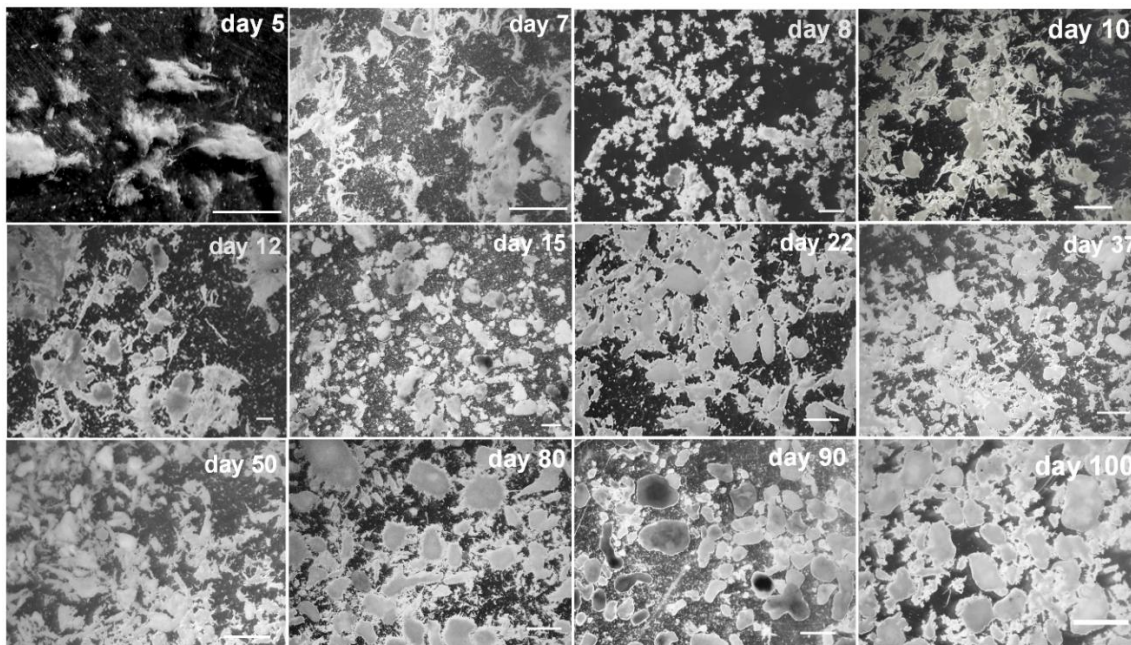


Fig. 5.7. Formation of aerobic granular sludge from microorganisms indigenous to seawater in a lab-scale (3 litre volume) sequencing batch reactor fed with nutrient-amended seawater. The reactor was not inoculated with either activated sludge or granular sludge. The autochthonous planktonic bacteria present in the influent synthetic saline wastewater was granulated to develop halophilic granular sludge. Scale bar = 1 mm.

Seawater fed into the SBR contained bacteria mainly in the dispersed form as individual cells (Fig. 5.8A). On the other hand, fluorescence microscopic images showed extensive bacterial colonization in the extra cellular polymeric substances (EPSs) matrix of granule (Fig. 5.8B).

SEM revealed the presence of rod and coccoid shaped bacteria and EPSs matrix on the granule surface (Fig. 5.8C and D).

Table 5.3 Properties of halophilic aerobic granular sludge formed from autochthonous planktonic bacterial community of seawater under saline conditions (34 ppt).

Parameters	SBR operation (day)		
	25	60	100
Density (g mL ⁻¹)	1.5 ± 0.1	1.6 ± 0.9	1.7 ± 0.5
Settling velocity (m h ⁻¹)	21.2 ± 1.2	26.6 ± 1.3	37.2 ± 1.6
Hydrophobicity (%)	86.5 ± 1.3	89 ± 1	96 ± 0.8
SVI ₅ (mL g ⁻¹)	6.0	7.1	8.3
MLSS (g L ⁻¹)	15.2 ± 1.1	21 ± 1.1	18.9 ± 1.6
Inorganic content (%)	7.9 ± 1.3	11.4 ± 0.9	17.6 ± 1.1

Table 5.4 Concentration of metal ions in the influent, effluent and granular sludge.

	Mg	Ca	Na	K	Sr	Fe
Influent* (mg L ⁻¹)	1189 ± 21	359 ± 31	7455 ± 34	353 ± 14	6 ± 0.5	2 ± 0.4
Effluent* (mg L ⁻¹)	857 ± 46	256 ± 54	5420 ± 349	277 ± 188	3.9 ± 0.15	BDL
Biomass# (mg (g dry wt.) ⁻¹)	153 ± 8	153 ± 4	113 ± 5	110 ± 4	113 ± 7	65 ± 6

*Values represent average ±SD of minimum of 10 cycles; BDL- <2µg L⁻¹, # average ±SD on day 98.

Precipitates were also observed on the surface of granules formed under saline conditions (Fig. 5.8E). EDX showed the presence of calcium and oxygen in these precipitates (Fig. 5.8F). XRD indicated the presence of calcium, magnesium and ammonium phosphate precipitates (Fig. 5.8G). The precipitates were found to be crystalline and amorphous in nature. The peaks of the XRD could be assigned to minerals such as apatite, whitlockite and struvite (PDF cards: 029-1193, 015-0762, 047-1744 and 041-0483) (Fig. 5.8G). ICP-AES analysis revealed a decrease in the concentration of metal ions i.e., magnesium, calcium, sodium, potassium, strontium, and iron in the biologically treated water (Table 5.5). Acid digestion and quantitative analysis showed retention of metal ions in the granules (Table 5.5).

Since the bioreactor was not inoculated with the active biomass (i.e., activated sludge), the granular sludge was formed by the growth of planktonic microorganisms present in the synthetic saline wastewater. Based on the microscopic observations, formation of AGS from microorganisms of seawater is proposed to involve the following steps: (i) growth of planktonic microorganisms present in the seawater, (ii) formation of bacterial aggregates by auto- and co-aggregation, (iii) growth of smaller aggregates into biomass particles and (iv) disassembly and re-growth of granules (Fig. 5.9). The metal cations abundant in the seawater can aid in the aggregation of microorganisms, formation of micro-aggregates, production of EPSs and shaping-up of macro-scale granules²⁷.

Table 5.5 Concentration of metal ions in the influent, effluent and granular sludge.

	Mg	Ca	Na	K	Sr	Fe
Influent* (mg L ⁻¹)	1189 ± 21	359 ± 31	7455 ± 34	353 ± 14	6 ± 0.5	2 ± 0.4
Effluent* (mg L ⁻¹)	857 ± 46	256 ± 54	5420 ± 349	277 ± 188	3.10 ± 0.15	BDL
Biomass# (mg (g dry wt.) ⁻¹)	153 ± 8	153 ± 4	113 ± 5	110 ± 4	113 ± 7	65 ± 6

*Values represent average ±SD of minimum of 10 cycles: BDL- <2µg L⁻¹, # average ±SD on day 98.

In addition, inorganic precipitates if formed can act as nuclei for the attachment of microorganisms and aid in increasing the settling properties of microbial aggregates^{27,29}. Indeed, XRD measurements of granules showed chemical signatures of Ca²⁺ and Mg²⁺ phosphate precipitates. This was in agreement with Li et al.¹²² on formation of Ca²⁺ and Mg²⁺ phosphate in the aerobic granular sludge developed from activated sludge while treating seawater-based wastewater. Thus, metal ions and their precipitates may play a role in bacterial aggregation and granulation.

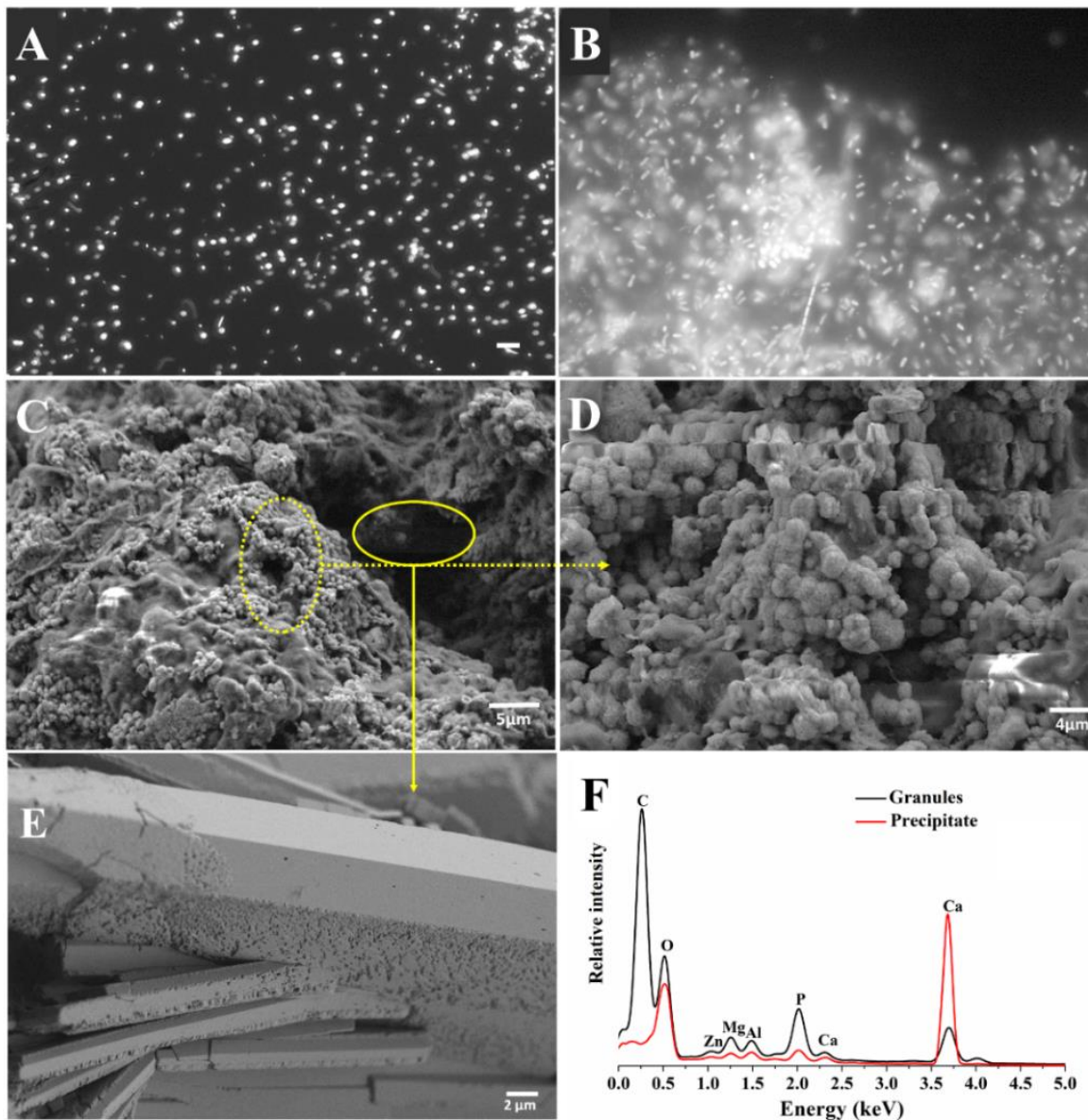


Fig. 5.8. Fluorescence microscope images of bacteria in (A) seawater and (B) in an individual granule. Scale bar = 2 μm. (C and D) Scanning electron microscope images of the granules, (E) precipitates observed within the granule, (F) EDX spectra of the precipitates, and (G) X-ray diffractogram of halophilic aerobic granular sludge.

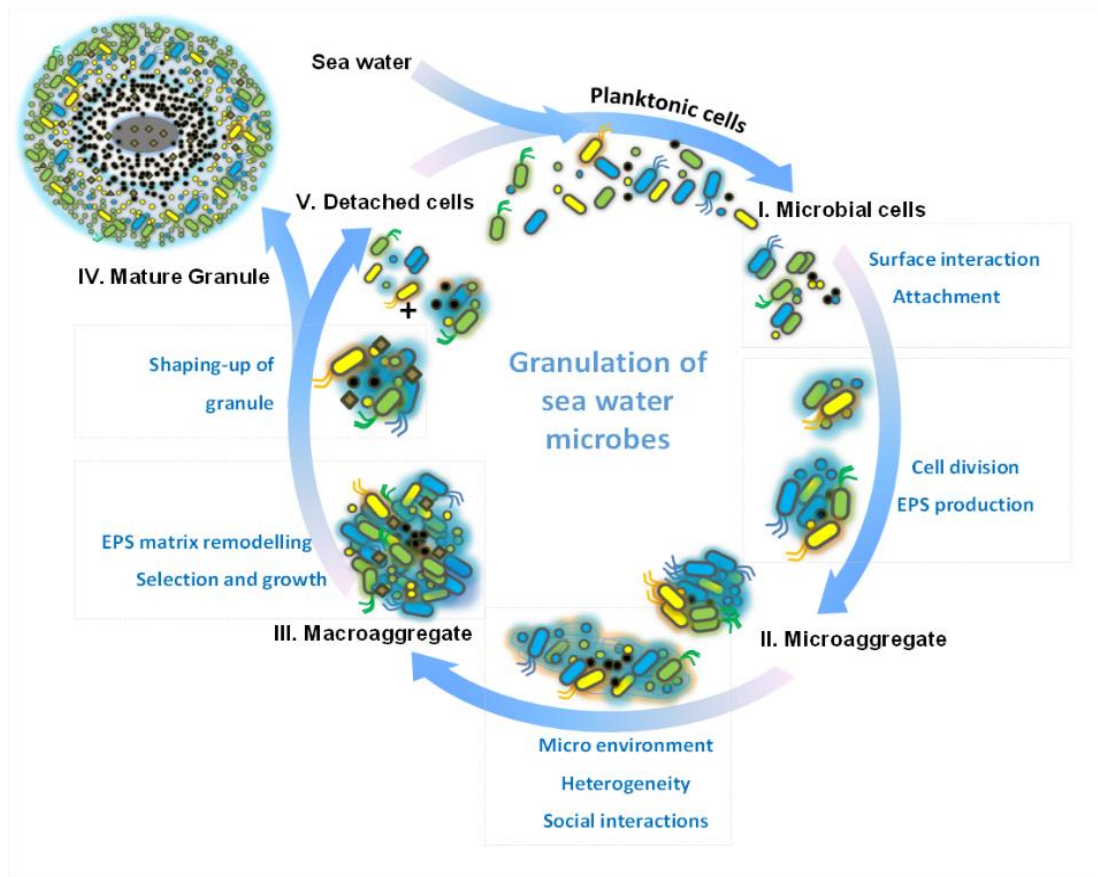


Fig. 5.9. Proposed mechanism of granulation of autochthonous planktonic bacterial community of seawater for saline wastewater treatment.

5.4 Conclusions

This study demonstrated cultivation of halophilic AGS (hAGS) from autochthonous planktonic bacteria of seawater without using inoculum (i.e., activated sludge or AGS) in the SBR. hAGS was formed directly from the autochthonous planktonic microorganisms present in the seawater. AGS formed from autochthonous bacteria of seawater exhibited efficient nitrogen and phosphorus removal efficiencies under varied salinities. Unlike halotolerant biomass (developed either from activated sludge or AGS by enrichment), the nutrient removal capability of hAGS developed from autochthonous planktonic bacteria of seawater was resilient to changes in the salinity. The approach described here on the use of autochthonous planktonic bacterial community of seawater is promising for developing AGS process for saline sewage and industrial effluents.

Chapter 6

Evaluating biological nitrogen and phosphorus removal at hypersalinities

Abstract

Biological nutrient removal and physical properties of halophilic aerobic granular sludge (hAGS) cultivated from autochthonous seawater-born microorganisms were investigated under hypersaline seawater conditions. hAGS achieved stable total nitrogen (TN) and total phosphorus (TP) removals of $96\pm 3\%$ and $95\pm 4\%$, respectively, from seawater-based wastewater at 34 ppt. At 40 to 120 ppt salt, stable TN and TP removals of 82–99% and 95–96%, respectively, were maintained over 4 months under seawater conditions. Ammonium and phosphorus were mainly removed by nitrification-denitrification and enhanced biological phosphorus removal pathways, respectively. Stappiaceae (45%) and Rhodobacteraceae (21%) were the dominant genera in hAGS performing nutrient removal at 120 ppt salt. hAGS contained acid-soluble extracellular polymeric substance as the major structural polymer which increased from 0.43 ± 0.02 g (g TS)⁻¹ at 34 ppt to 0.93 ± 0.03 g (g TS)⁻¹ at 120 ppt salt. Cultivation of hAGS from autochthonous wastewater-microorganisms can be a promising approach for achieving biological nitrogen and phosphorus removals from hypersaline seawater-based wastewaters.

Keywords: Ammonium removal, Phosphorus removal, Nitrification-denitrification, Nutrient removal, Saline wastewater

6.1 Introduction

Wastewaters with high salt concentrations ($> 1 \text{ g L}^{-1} \text{ NaCl}$) are generated by one or multiple routes such as (i) use of seawater or brackish water in non-potable applications for washing and toilet flushing¹³³, (ii) use of seawater and excessive salts in different industrial activities like seafood processing, vegetable pickling, fish canning, oil production, tanning, paper making, pharmaceutical and chemical production⁴⁴, and (iii) introduction of seawater into groundwater and sewer networks in coastal areas. Based on the salt content, wastewaters are classified into saline and hypersaline containing at least 10 and 30 $\text{g L}^{-1} \text{ NaCl}$, respectively¹³².

Apart from high salt content, these wastewaters contain high levels of chemical oxygen demand (COD), biochemical oxygen demand, total nitrogen (TN), and phosphorus as major contaminants¹²⁰. Aquaculture industry, a lifeline in coastal areas generates wastewater which typically contains salt ($\sim 30 \text{ g L}^{-1}$), nitrogen ($\sim 60 \text{ mg L}^{-1}$), and phosphorus ($\sim 5 \text{ mg L}^{-1}$)¹³⁵. Whereas, fish canning wastewaters typically composed of up to 90 $\text{g L}^{-1} \text{ COD}$, 3 $\text{g L}^{-1} \text{ TN}$ and $>30 \text{ g L}^{-1} \text{ salt}$ ¹³⁴. Phosphorus concentrations can be up to 12 mg L^{-1} ¹³⁶ in hypersaline domestic wastewaters. Severe inhibition of biological phosphorus removal was observed during adaptation of allochthonous community (i.e., activated sludge or aerobic granular sludge) to saline conditions^{43,118,137,138,114}. Thus, investigation of phosphorus removal under hypersaline conditions is of importance for developing sustainable wastewater treatment.

Gradual adaptation of freshwater microbial communities (i.e., activated sludge, aerobic granular sludge) to salinity has been shown to improve nutrient removals under saline conditions^{139,140}. The development of halotolerant microbial communities from freshwater-biomass has been successful to some extent for achieving nutrient removal under saline conditions^{141,123}. However, it has limitations such as long adaptation periods, lower nitrogen and phosphorus removals, limited salt tolerance, and poor sludge settling characteristics in

hypersaline conditions. These challenges are due to a little overlap in the abundant bacterial taxa between the freshwater- and marine-microbial communities¹²⁶. In a completely different inoculum-independent approach, halophilic aerobic granular sludge (hAGS) was cultivated directly from the autochthonous planktonic microbial community of seawater for efficient biological nutrient removal (Chapter 5).

This study was aimed at investigating the physical and nutrient removal properties of hAGS developed through granulation of autochthonous seawater-born microorganisms. It was hypothesized that hAGS cultivated from the autochthonous seawater-borne microorganisms can (i) achieve high nitrogen and phosphorus removals, (ii) significantly minimize adaptation periods, and (iii) thrive under hypersaline seawater conditions. Nutrient removal performance and structural stability of hAGS were evaluated under seawater conditions at 34 to 120 ppt salt concentrations.

6.2 Material and methods

6.2.1 Nutrient amended seawater

Seawater was used to prepare synthetic saline wastewater as described in chapter 5. The composition of synthetic saline wastewater was detailed in Appendix II.

6.2.2 Cultivation of halophilic aerobic granular sludge (hAGS)

A 3-litre volume sequencing batch reactor (SBR) was operated for cultivation of hAGS. SBR operation was mentioned in Chapter 3. hAGS cultivated from the autochthonous seawater-borne microorganisms was harvested on day 110 and used for determining nutrient removal under hypersaline seawater conditions. The SBR was operated at room temperature ($31\pm 5^{\circ}\text{C}$).

6.2.3 Nutrient removal from hypersaline seawater-based wastewater

SBR1 was inoculated with 7 g L^{-1} hAGS and fed with seawater-based wastewater. Removal of 30 to 90 mg L^{-1} $\text{NH}_4^+\text{-N}$, 50 to 150 mg L^{-1} of $\text{NO}_3^-\text{-N}$ and 11 mg L^{-1} $\text{PO}_4^{3-}\text{-P}$ was

studied over 3-month period. SBR1 was operated at 34 ppt salt under similar conditions as mentioned in Chapter 5. Liquid samples were collected regularly at the end of 6 h cycle and also hourly intervals for determining nutrient removal performance.

SBR2, similar to SBR1 in configuration was inoculated with 4 g L⁻¹ hAGS for studying nutrient removal at hypersaline seawater conditions. In this experiment, salinity of the seawater-based wastewater was increased in a stepwise manner up to 120 ppt salt by dosing with sodium chloride. All other experimental conditions were kept constant. The physical properties of hAGS and removal of 517 mg L⁻¹ COD, 30 mg L⁻¹ NH₄⁺-N, and 11 mg L⁻¹ PO₄³⁻P were studied under seawater conditions at salinities of 34 to 120 ppt. Liquid samples were collected regularly towards the end of 6 h cycle for monitoring nutrient removal performance. Sludge samples were collected once a week for determining stability and characteristics.

6.2.4 Microscopy

Stereomicroscope and scanning electron microscope (SEM) were used to determining the morphological changes in AGS as detailed in chapter2.

6.2.5 Genomic DNA extraction and bacterial community

hAGS was harvested from SBR2 on day 90 (70 ppt salt), day 140 (100 ppt salt), and day 170 (120 ppt salt) for determining bacterial community. Genomic DNA was isolated using QIAmp DNA Mini kit (Qiagen, Germany) as per the manufacturer's instructions.

Sequencing of the 16S rRNA gene on Illumina HiSeq 2500 platform and analysis of sequences were performed as detailed in Chapter 3.

6.2.6 Extracellular polymeric substances (EPSs) matrix of hAGS

The halophilic granules were collected from SBR2 on day 1 (34 ppt salt), day 90 (70 ppt salt), and day 170 (120 ppt salt) for determining the EPS content. Alginate-like exopolymer

(ALE) was extracted using the sodium carbonate method⁸⁴. Briefly, 1 g (dry weight) hAGS was added to 250 mL flask containing 100 mL 0.5% (w/v) Na₂CO₃, stirred at 400 rpm in a water bath at 80 ± 1 °C for 3 h. After centrifugation (4000 g, 4 °C, 20 min), pH of the supernatant was adjusted to 2.2 with 1 M HCl under stirring. It was subjected to another round of centrifugation (4000 g, at 4 °C, 20 min) for recovering ALE in the pellet.

Pellet obtained in the first centrifugation step was processed for recovering acid-soluble EPSs¹⁴². Pellet was washed thrice with ultrapure water and added to 100 mL 0.4 M acetic acid in a 250 mL Erlenmeyer flask which was placed in a water bath at 95 ± 1 °C under stirring for 20 h. Supernatant was collected by centrifugation (4000 g, 4 °C, 20 min) and filtered through 0.22 µm cellulose acetate filter (Millipore). The filtrate was added to an equal volume of 98% ethanol. Acid soluble EPSs was recovered by centrifugation (4000 g, 4 °C, 20 min) and lyophilized to obtain in powder. The amount of granules used for extraction was quantified in terms of total solids (TS) and volatile solids (VS) according to standard methods⁶⁴.

6.2.7 Analytical methods

Liquid samples were processed and analyzed for total organic carbon (TOC), ammonium, nitrate, nitrite, and phosphorus. Sample processing and analytical procedures were detailed in Chapter 2.

Physical characteristics such as water content, settling velocity, SVI, MLSS and MLVSS were determined according to standard methods⁶⁴.

6.3 Results and discussion

Two important aspects of saline wastewater treatment such as nutrient removal capabilities and physical properties of biomass were addressed. Stability and nutrient removal capabilities of granular sludge were successfully maintained under varied hypersaline seawater conditions using hAGS cultivated from autochthonous seawater microorganisms.

hAGS possessed plasticity and retained biological nitrogen and phosphorus removal capabilities at hypersaline conditions ranging from 34 to 120 ppt.

Table 6.1 Nitrogen removal performance of hAGS in a 3-litre sequencing batch reactor (SBR1) treating seawater-based wastewater.

Influent (mg L ⁻¹)		Effluent (mg L ⁻¹)		Total-N removal (%)	SBR operation (d)
Ammonium-N	Nitrate-N	Ammonium-N	Nitrate-N		
30	0	0.1 ± 0.1	2.8 ± 1.3	87 ± 5	1-20
30	60	1.2 ± 0.9	2.6 ± 2.2	93 ± 3	21-28
60	60	3.0 ± 0.6	0.8 ± 0.2	94 ± 1	29-33
60	100	0.8 ± 0.9	1.6 ± 0.3	98 ± 1	34-53
90	100	0.5 ± 0.1	1.4 ± 0.7	99 ± 1	54-75
90	150	0.2 ± 0.1	2.3 ± 3	97 ± 2	76-92

6.3.1 Nutrient removal from hypersaline seawater-based wastewater

6.3.1.1 TOC removal

TOC removal was observed from the beginning indicating quick start-up at 34 ppt. Effluent TOC was below 10 mg L⁻¹ during the whole SBR1 operation at 34 ppt (Fig. 6.1A). Carbon removal was evident by dissolved oxygen (DO) consumption and TOC removal during the cycle. A rapid decrease in the DO of seawater-based wastewater to below 1 mg L⁻¹ was noticed within the first 15 min of the filling phase. This decrease in DO continued and became anaerobic (DO < 0.08 mg L⁻¹) due to TOC consumption by intense microbial respiration. In the plug-flow filling phase, about 120 to 200 mg L⁻¹ TOC was removed. Remaining TOC was removed in the aeration phase (Fig. 6.1B). In summary, TOC removal was stable at 95 ± 2 % during 92 days of SBR1 operation at 34 ppt. TOC removal continued to occur even at higher salinities up to 120 ppt as well (Fig. 6.2A). TOC was <35 mg L⁻¹ in the treated seawater-based wastewater with salinities up to 50 ppt (Fig. 6.2). However, TOC values in the treated wastewater increased up to about 50 mg L⁻¹ at 60 to 120 ppt (Fig. 6.2A and 2B). Despite that, the average TOC removal was always maintained >93% (Table 6.2). The DO profile was substantiated by the TOC removal profiles. The TOC removal profiles followed similar trends at different salinities. However, there were differences in the amount

of TOC removed during the anaerobic filling phase, time taken for 90% TOC removal, and TOC residuals. Time taken for removing 90% TOC increased from 3 h to 5 h when salinity increased from 60 to 120 ppt. About 55% TOC was removed during the filling phase at 34 to 50 ppt but decreased to 45% at 60 to 120 ppt.

Table 6.2 Nutrient removal performance of hAGS in a 3-litre sequencing batch reactor (SBR2) treating hypersaline seawater-based wastewater.

Salt (ppt)	Effluent concentration (mg L ⁻¹)*				Days
	TOC	Ammonium-N	TIN-N	Phosphate-P	
34	12±3	0.2±0.1	2.4±0.8	1.9±0.7	0-21
40	14±3	1.0±0.7	3.2±1.7	0.3±0.7	22-42
50	22±7	0.2±0.2	1.2±0.6	1.3±1.1	43-61
60	42±12	0.2	0.2±0.4	0.4±0.3	62-80
70	36±11	0.2	0.4±0.5	0.5±0.4	81-100
80	38±3	0.2	0.2±0.1	0.2±0.2	101- 111
90	40±5	0.4±0.4	1.8±1	0.1±0.1	112-132
100	40±5	0.2	0.4±0.3	0.4±0.3	133-140
120	40±4	BDL	0.5±0.5	0.3±0.2	141-165

*Values represent average ± SD from a minimum of 10 cycles. BDL: below detection limit. TIN: total inorganic nitrogen

The above data clearly shows that acetate removal was not negatively impacted at higher seawater salinities. This was in agreement with previous research that the removal of organic carbon has not been a problem under seawater conditions^{122,129,130}. However, poor settling characteristics and severe loss of biomass from the bioreactor can result in poor organic carbon removal. Nitrogen and phosphorus removals were often compromised particularly with allochthonous microbial community requiring long periods for the gradual development of the halotolerant community^{43,118,121,133,143}.

6.3.1.2 Nitrogen removal

Ammonium removal was at >99 % during the first 20 days of SBR1 at 34 ppt (Fig. 6.1c). TN removal was at 87±5 % indicating removal of ammonium and nitrogen oxides (NO₂⁻ and NO₃⁻) formed via nitrification (Table 6.2). In subsequent cycles, nitrogen removal was evaluated by increasing ammonium concentration as well as introducing nitrate in seawater-based wastewater (Fig. 6.1C). hAGS were able to successfully remove 60 to 90 mg

$\text{L}^{-1} \text{NH}_4^+\text{-N}$ and 60 to 150 $\text{mg L}^{-1} \text{NO}_3^-\text{-N}$ from seawater-based wastewater. Ammonium, nitrate, and TN removals were found to be at 88-100 %, 86-99 %, and 87-99 %, respectively, from day 20 to 80 of SBR1 operation. TN removal was slightly decreased to 94 % when nitrate concentration increased to 150 $\text{mg L}^{-1} \text{NO}_3^-\text{-N}$ (Fig. 6.1C). Within the next few cycles, the TN removals improved to 98 % by day 92. Increasing the concentration of ammonium and nitrate by keeping acetate concentration constant led to lower the carbon to nitrogen (C/N) ratio from an initial 4.2 to 0.5 in the seawater-based wastewater. Such a decrease in C/N ratio had no marked influence on nutrient removal under seawater conditions. Cycle profiles revealed the formation of subtle amounts of nitrite and nitrate during 30 $\text{mg L}^{-1} \text{NH}_4^+\text{-N}$ removal. Nitrate removal was noticed from cycle 1. In the beginning, about 40 $\text{mg L}^{-1} \text{NO}_3^-\text{-N}$ and 6 $\text{mg L}^{-1} \text{NH}_4^+\text{-N}$ were removed within 1 h of the cycle. During later stages of SBR1 operation, almost 50 % of reactive nitrogen (ammonium and nitrate) was removed during the anaerobic phase (Fig. 6.1D). During this period, the pH also increased from 8.4 to 9.1 ± 0.1 due to heterotrophic denitrification. Towards the end of SBR1 operation, ammonium, nitrate, and total nitrogen removals were maintained at 100, 98, and 98%, respectively.

Ammonium removal was relatively stable and ranged from 96 to 100% at varied salt concentrations of 40 to 120 ppt (Fig. 6.2C). This was in agreement that ammonium can be successfully removed from saline conditions by adapting freshwater-microbial communities such as activated sludge or granular sludge^{144,137}. However, removal of ammonium by the halotolerant community was mostly associated with the accumulation of nitrite leading to incomplete nitrogen removal^{44,118,124}. Ammonium, nitrate and nitrite concentrations were 0.2-2.2 $\text{mg L}^{-1} \text{NH}_4^+\text{-N}$, <2.9 $\text{mg L}^{-1} \text{NO}_3^-\text{-N}$ and 0.5-4 $\text{mg L}^{-1} \text{NO}_2^-\text{-N}$, respectively, in the treated wastewater. TN removal was in the range of 87 to 99% at 40 to 120 ppt. In fact, ammonium removal profiles appeared similar irrespective of the salinity of seawater-based wastewater. The build-up of nitrate concentrations up to 4-5 $\text{mg L}^{-1} \text{NO}_3^-\text{-N}$ was observed during 6 h cycle

at 34 to 40 ppt. But, a substantially lower concentration of $<1 \text{ mg L}^{-1} \text{ NO}_3^- \text{-N}$ was observed at 50 to 120 ppt. Nitrite concentrations of $2\text{-}3 \text{ mg L}^{-1} \text{ NO}_2^- \text{-N}$ were detected during the cycle at all the salinities (Fig. 6.2D). Kinetics of ammonium, nitrate, and nitrite during the SBR cycles suggests the occurrence of partial nitrification of ammonium to nitrite (nitritation) and nitrite denitrification to nitrogen (denitrification).

Table 6.3 Characteristics of hAGS treating hypersaline seawater-based wastewater in a 3-litre sequencing batch reactor (SBR2).

Parameters	Salinity (ppt)			
	34	70	100	120
Density (g mL^{-1})	1.6±0.09	1.5±0.04	1.7±0.01	1.91±0.02
Settling velocity (m h^{-1})	37±1.6	51±1	59±1.2	69.5±1.4
Particle size (mm)	1.7±0.5	1.8±0.6	1.75±0.5	1.9±0.7
Hydrophobicity (%)	96±0.8	95±1.2	96±1.6	98±2
MLSS (g L^{-1})	3.3±1.2	4.2±0.3	4.8±0.4	5.0±0.1
MLSS/MLVSS	1.21	1.25	1.2	1.3
Inorganic content (%)	17.6±1.1	20.4±2	21.1±3.1	23.4±2.5
SVI ₅ (mL g^{-1})	8.3	21.3	18.2	19.6
SVI ₅ /SVI ₃₀ ratio	1.01	1.01	1.04	1.06
TIN removal (mg N (gVSS)^{-1})	10±0.3	9.5±0.2	8.4±0.8	8.0±0.1
Phosphate removal (mg P (gVSS)^{-1})	3±0.3	3.1±0.1	2.8±0.7	2.7±0.5

At mesophilic temperatures ($>25 \text{ }^\circ\text{C}$), the specific growth rate for AOBs are higher than NOBs. Due to a lower oxygen half-saturation coefficient, AOB has more tolerance to lower dissolved oxygen conditions than NOB. Periodic anoxic-aerobic operation condition is known to inhibit NOB⁶³. The bioreactor conditions such as periodic anoxic-aeration strategy, low dissolved oxygen ($<0.08 \text{ mg L}^{-1}$) in the anoxic phase, and mesophilic temperature ($31\pm 5 \text{ }^\circ\text{C}$) have strongly supported the establishment of nitritation.

Heterotrophic denitrification of nitrite was supported by acetate (electron donor). Sequencing data confirmed the prevalence of AOB and denitrifying bacteria in the hAGS. Thus, ammonium removal at hypersalinities was majorly mediated by the biological nitritation-denitrification pathway. Specific TIN removal decreased from $10\pm 0.3 \text{ mg N (g VSS)}^{-1}$ at 34 ppt to $8.0\pm 0.1 \text{ mg N (g VSS)}^{-1}$ at 120 ppt due to increase in inorganic content (Table

6.3). However, biological nitrogen capabilities of hAGS were not impacted largely under hypersaline seawater conditions.

6.3.1.3 Phosphorus removal

Phosphorous removal was at $80 \pm 8\%$ from cycle 1 of SBR1 at 34 ppt. It was improved to 97% and higher by day 35 (Fig. 6.1E). However, a slight decrease in phosphorous removal to about 88% was noticed at the highest nitrogen loading ($2.8 \text{ gN L}^{-1} \text{ d}^{-1}$). Phosphorous removal profiles contained release and removal phases, in the anaerobic (first 60 min) and aeration (60 min to 240 min) phases, respectively (Fig. 6.1F). The concentration of phosphorous released during the anaerobic phase increased from 4 to $11 \text{ mg L}^{-1} \text{ PO}_4^{3-}\text{-P}$ when nitrogen loading was increased (Fig. 6.1F).

Phosphorous removal by hAGS in SBR2 operated at varied hypersalinties was shown in Fig. 2E. Phosphorus removal was at 81% in the beginning and improved to 96% on day 20 at 34 ppt (Table 6.3). When salinity increased to 50 ppt, phosphorous removal was slightly impacted and decreased to 85%. However, phosphorous removal was improved during subsequent cycles and stabilized at 96% at 60 ppt. Again, a small perturbation in phosphorous removal was noticed when salinity increased to 70 ppt. Improvement and stability in phosphorous removal were noticed during subsequent cycles up to 120 ppt. Phosphorous levels were $<1 \text{ mg L}^{-1} \text{ PO}_4^{3-}\text{-P}$ in the treated wastewater at 80 to 120 ppt (Table 6.3). Phosphorous removal profiles typically consisted of two distinct phases that were corroborated with plug-flow filling (anaerobic) and aeration phases (Fig. 6.2F). Each profile had an initial phosphorous release during the plug-flow filling phase followed by phosphorous uptake during the aeration phase. Moreover, the phosphorus profiles recorded at different salinities were alike.

There are limited studies on successful biological phosphorus removal from seawater-based wastewaters. de Graff et al.¹⁴¹ reported successful biological phosphorus removal under seawater conditions at 35 ppt by adapting aerobic granular sludge from Nereda® plant to seawater-based wastewater. However, phosphorus concentrations of $6\pm 3 \text{ mg L}^{-1} \text{ PO}_4^{3-}\text{-P}$ were noticed in the treated wastewater over 12 months of bioreactor operation. But, hAGS cultivated from the autochthonous seawater microbiome showed very efficient phosphorus removal under seawater condition at 34 ppt. Stable removal of $4.9\pm 0.2 \text{ mg L}^{-1} \text{ PO}_4^{3-}\text{-P}$ was observed over 3 months with effluent phosphate concentrations of $0.12\pm 0.01 \text{ mg L}^{-1}$ in the treated wastewater. However, it is not known whether biological phosphorus removal of hAGS can be sustained at higher salinities ($> 34 \text{ ppt}$).

On the whole, biological phosphorus removal by hAGS was largely unaffected at salinities of 34 to 120 ppt. The amount of phosphorus release increased substantially from $4\pm 1 \text{ mg L}^{-1} \text{ PO}_4^{3-}\text{-P}$ at 34 ppt to $13\pm 2 \text{ mg L}^{-1} \text{ PO}_4^{3-}\text{-P}$ at 120 ppt (Fig. 6.2F). The observed phosphorus removal profiles were similar to those achieved by aerobic granular sludge while treating freshwater-based wastewater¹⁴⁵. In the anaerobic phase, the release of up to $2.9\pm 0.3 \text{ mgP (gVSS)}^{-1}$ was noticed at hypersalinity. It was corroborated with rapid P uptake of $3.98 \text{ mgP (gVSS)}^{-1}$ in the subsequent aeration phase. This was slightly higher than the P uptake of $3.1\pm 0.2 \text{ mgP (gVSS)}$ by seawater-adapted aerobic granular sludge reported by de Graff et al.¹⁴¹. The release and uptake of significant quantities of phosphorus under anaerobic and aerobic phases, respectively, is attributable to the unique metabolism of polyphosphate accumulating organisms. Granules provide an ideal environment for the enrichment of PAOs¹⁰⁵.

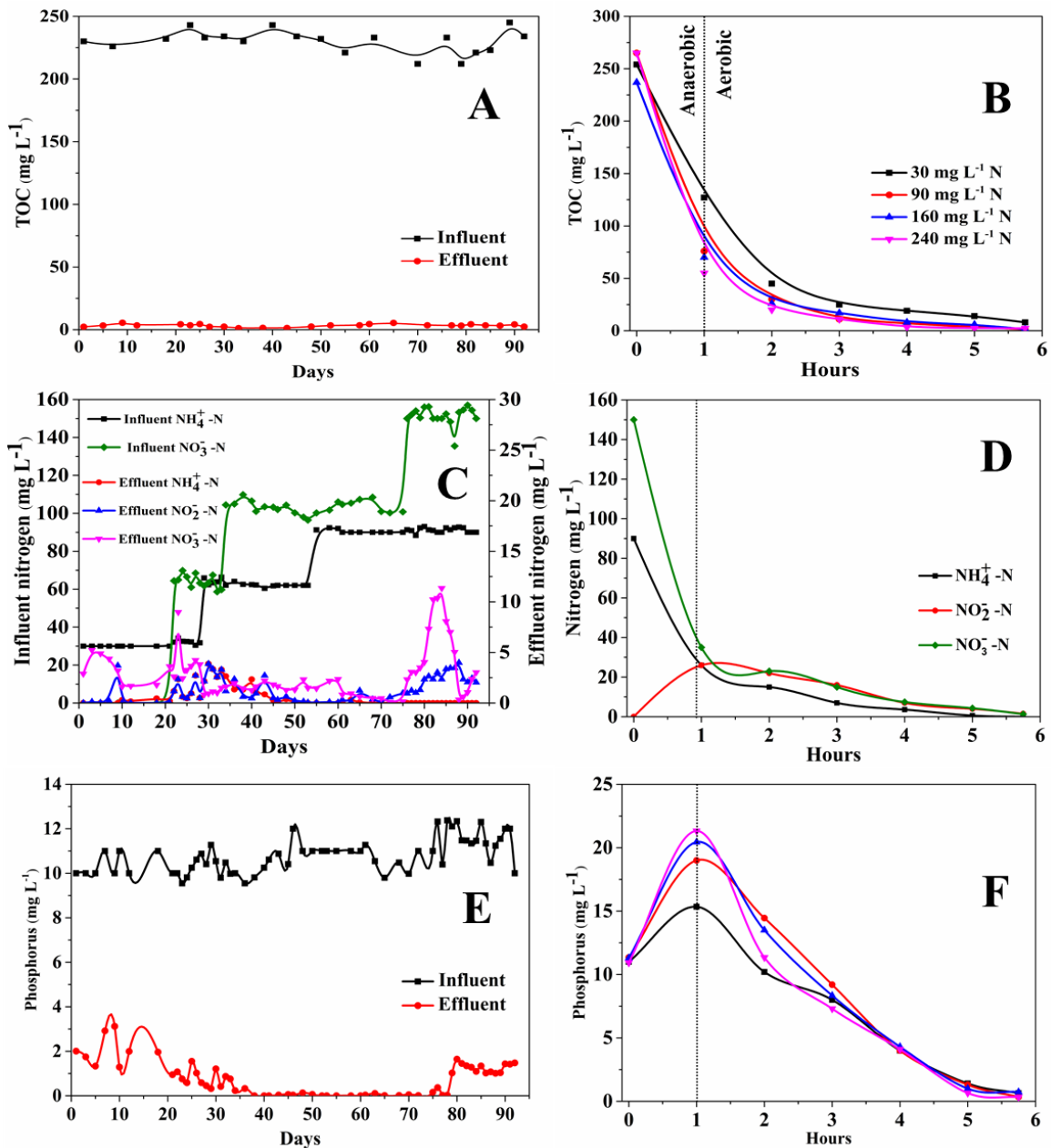


Fig. 6.1. Carbon (A), nitrogen (B) and phosphorus (C) removal performance of 3 litre sequencing batch reactor (SBR1) treating seawater-based wastewater (34 ppt) at different ammonium and nitrate concentrations. Removal profiles of carbon (D), nitrogen (E), and phosphorus (F) in 6 h cycles at different ammonium and nitrate concentrations. SBR1 was inoculated with halophilic aerobic granular sludge cultivated from autochthonous seawater microbes.

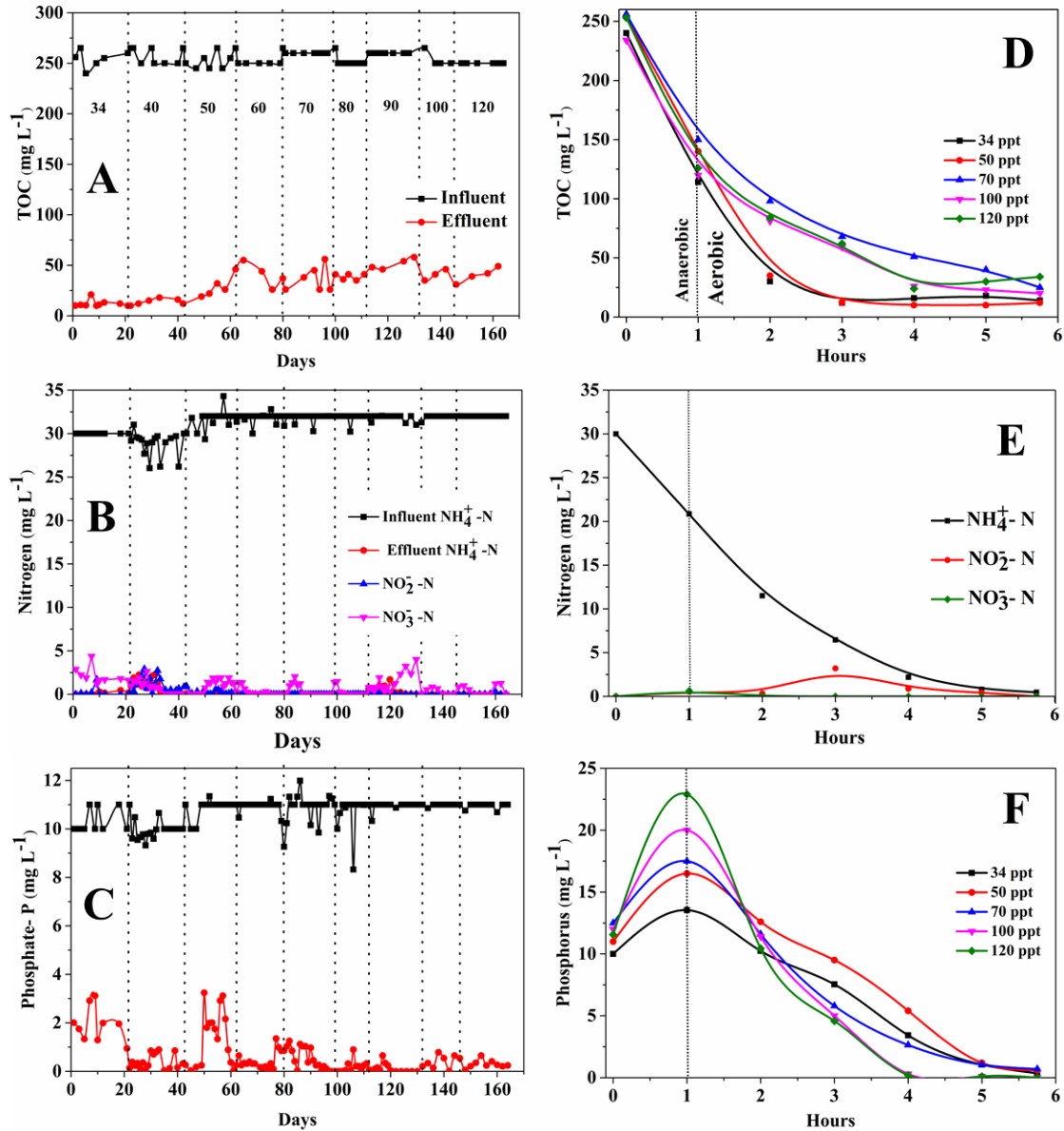


Fig. 6.2 TOC (A), reactive nitrogen (B) and phosphorus (C) removal performance of 3 litre sequencing batch reactor (SBR2) treating seawater-based wastewater at different salinities from 34 to 120 ppt. Profiles showing removal of TOC (D), nitrogen removal at 120 ppt (E) and phosphorus (F). SBR2 was inoculated with halophilic aerobic granular sludge cultivated from autochthonous seawater microbes at 34 ppt.

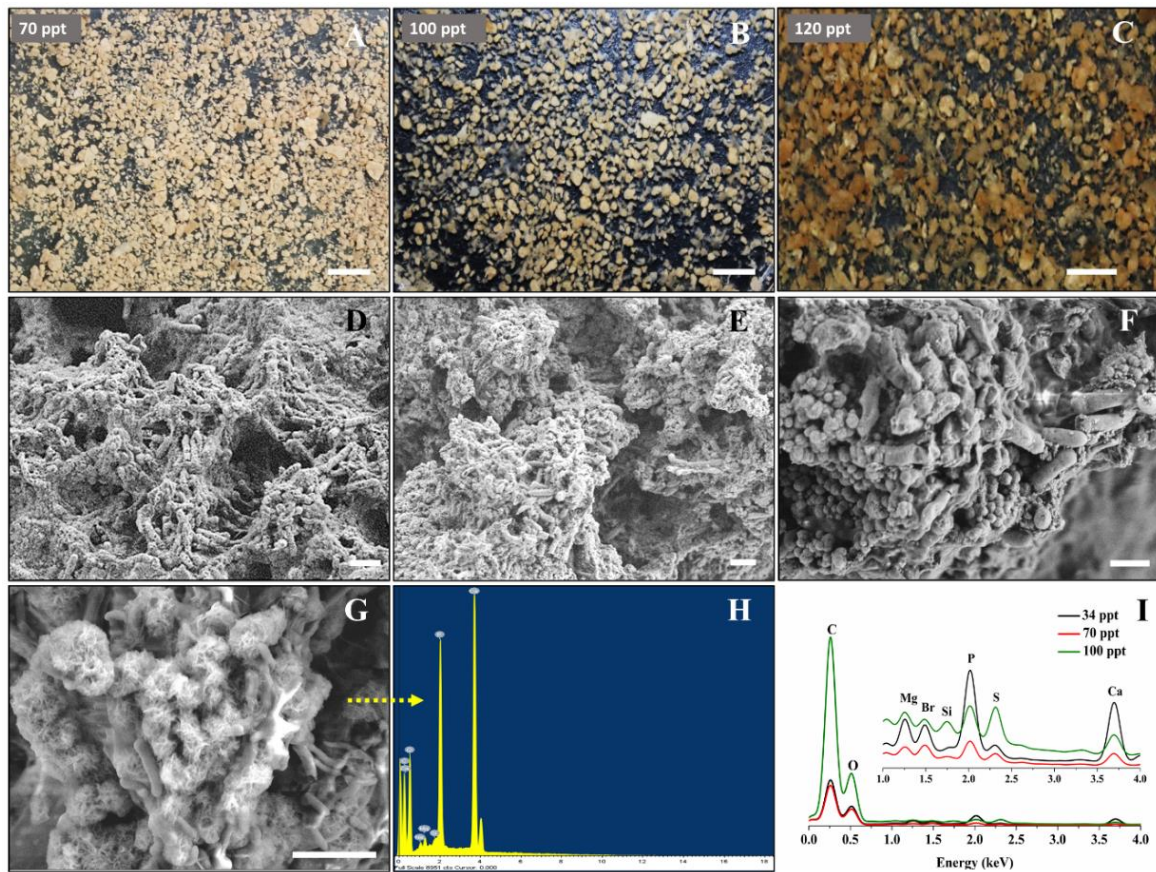


Fig. 6.3 Change in morphological features of hAGS treating seawater-based wastewater at different salinities. Stereomicroscope images (A-C); Scale bar= 1cm., and SEM micrographs (D-F), precipitates within hAGS at 120 ppt and EDX spectra of hAGS (E). EDX spectrum of precipitate at 120 ppt (F). Scale bar = 2μm.. Salinities at of 70 ppt (A,D), 100 ppt (B, E), 120 ppt (C,F) are shown.

6.3.2 Properties of halophilic aerobic granular sludge

It is necessary for the biomass to maintain structural stability and good settling properties to avoid washout from the biological treatment system. It has been widely reported that biomass (i.e., activated sludge, aerobic granular sludge) developed for treating freshwater-based wastewater exhibits poor settling properties or even gets disassembled when used for treating saline wastewaters¹⁴⁶. This can be a serious issue because it can lead to eventual washout of biomass from the treatment plants. This is the very reason that stability of aerobic granular sludge is considered an important criterion for its successful and widespread implementation in wastewater treatment plants²⁹. hAGS were resilient to changes

in the granular structure and settling properties. hAGS maintained typical granular morphology at different salinities from 34 to 120 ppt. The pigmentation of granules changed from creamy brown at 34 ppt to deep brown at 120 ppt (Fig. 6.3A-C). But, the formation of flocculent growth was not evident at any stage of reactor operation. The size of granules was in the range of 1.9 to 2.2 mm. Compact microbial structure with rod shaped cells in an extracellular matrix was evident in the hAGS (Fig. 6.3D-G). This was also evident in the higher settling velocities, biomass density and SVI₅ values (Table 6.3). A marginal increase in SVI₅ values from 8.3 mL g⁻¹ at 34 ppt to 18 to 20 mL g⁻¹ was noticed at hypersalinities. Maintenance of good granulation at hypersalinities was indicated by SVI₅/SVI₃₀ values of 1.01 to 1.06. Notably, the inorganic content of hAGS increased markedly from 17.6% at 34 ppt to 23.4% at 120 ppt to the formation of inorganic precipitates (Table 6.3). This was indicated by a higher granular density of 1.91±0.02 g mL⁻¹ at 120 ppt. Biomass density and SVI₅ values were very much different from freshwater-based aerobic granular sludge and typical to hAGS. The hAGS have continued to show the compact microbial structure and excellent settling properties despite thriving under hypersalinities. SEM and EDX provided evidence for the presence of inorganic precipitates and chemical signatures, respectively. EDX spectra revealed signature peaks for calcium and phosphate in the precipitates of hAGS. An increase in inorganic content and formation of calcium phosphate precipitates was noticed at higher salinities (Fig. 6.3H and I). It is still unclear whether these inorganic precipitates can act as nuclei for accelerating granulation and improving granular stability under seawater conditions.

6.3.3 EPSs matrix of hAGS

Considerable changes in the EPSs content were noticed when hAGS were subjected to hypersalinities. The sodium carbonate extraction method often applied for extracting the ALE yielded only 0.1±0.2 g (g TS)⁻¹ from hAGS treating seawater-based wastewater at 34

ppt. ALE yield decreased to $0.06\pm 0.01 \text{ g (g TS)}^{-1}$ and $0.04\pm 0.01 \text{ g (g TS)}^{-1}$ at 70 and 120 ppt, respectively. ALE has been the major EPS recovered from AGS treating freshwater-based wastewater systems⁸⁴. In fact, ALE continues to be the dominant structural EPS when aerobic granules were adapted to saline conditions^{122,147,130}. Contrastingly, acetic acid extraction revealed a substantial increase in the EPSs content at higher salinities. The acid-soluble EPSs content increased from $0.43\pm 0.02 \text{ g (g TS)}^{-1}$ at 34 ppt to $0.93\pm 0.03 \text{ g (g TS)}^{-1}$ at 120 ppt. The matrix of hAGS cultivated from the seawater microbe was dominated by acid-soluble EPSs. This increase was mainly contributed by the polysaccharide which increased from $32\pm 4\%$ at 34 ppt to $53\pm 6\%$ at 120 ppt. Non-reducing sugars accounted for $>48\%$ of polysaccharide content of hAGS. A marginal increment was observed in the protein fraction from $26\pm 5\%$ at 34 ppt to $41\pm 4\%$ at 70 ppt and to $48\pm 2\%$ at 120 ppt. Disruption of hAGS was superior with acetic acid suggesting the structural role of acid-soluble EPSs. Substantial increase in acid-soluble EPSs also suggests the selection of bacteria and implications in structural stability at hypersalinity.

6.3.4 Bacterial community

A total of 886362 sequence reads were obtained from hAGS treating seawater-based wastewater using the Illumina HiSeq platform. After downstream analyses, sequences were assigned to a total of 23127 operational taxonomic units (OTUs) of which 2836 OTUs were selected (>5 reads) for further analysis. The rarefaction curve employed to observe richness among the samples indicated a reasonable sample volume to represent the microbial community. The alpha diversity index showed highest species richness (Shannon H-index) in granules at 70 ppt (6.4) followed by 100 ppt (6.1), and 120 ppt (5.7) (Fig. 6.4A). The observed species decreased by ~ 1.9 times when salinity increased from 70 to 120 ppt which was reflected in the equitability (E) or evenness of individual distribution among the families (Fig. 6.4A).

The taxonomic analysis at the genus level was presented in Fig. 6.3B. Proteobacteria predominated during the entire SBR2 operation at different salinities. Tenericutes were the second dominant phylum at 70 ppt covering almost 31% of the total genome which decreased to <4% at 100 ppt. Planctomycetes dominance increased by 12% at 100 ppt and decreased to <3% at 120 ppt. Moreover, the relative abundance of these two phyla was over 60% in the granules at all the salinities. Proteobacteria maintained over 50% abundance in all samples and increased to about 90% at 120 ppt. Within the proteobacteria, α -proteobacteria and γ -proteobacteria were dominant at 37.4% and 10.2%, respectively, at 70 ppt. The members of γ -proteobacteria further enriched to 36% at 100 ppt but decreased to 6.2% at 120 ppt. Granules treating seawater-based wastewater at 120 ppt contained α -proteobacteria, γ -proteobacteria and δ -proteobacteria at 82%, 6% and 2%, respectively.

Rhodocyclaceae (18%), Lentimicrobiaceae (12%), were Moraxellaceae (12%) were identified as the major bacterial families in the granules thriving at 70 ppt. However, Stappiaceae (45%), Rhodobacteraceae (21%) were the dominant bacterial families in the granules at 120 ppt. *Stappia* was the dominant genus at 43% and other prominent members including *Tropicibacter*, *Nitratireductor*, and *Marinobacter* were detected. Less abundant (<1%) genera detected in the granules that could be assigned with important nutrient removal activities were identified. Prominent changes were observed in the abundance of *Thaurea* (16%), *Lentimicrobium* (11%), *Psychrobacillus* (10%), *Terrimonas* (6%) at 70 ppt to <1% at 120 ppt granules, and *vice-versa* with *Stappia* at the genus level (Fig. 6.4). The microbiome of granules became more dissimilar with respect to prevailing salinities, indicating that salinity shapes up bacterial communities to maintain the system functioning. These differences might be in part to the change in physicochemical conditions as well. Unclassified sequences at genus level were fairly high and represents 15% (70 ppt), 13% (100 ppt), and

43% (120 ppt) of the total sequences may serve important roles in granulation and nutrient removal under hypersaline environment warranting further comprehensive investigation

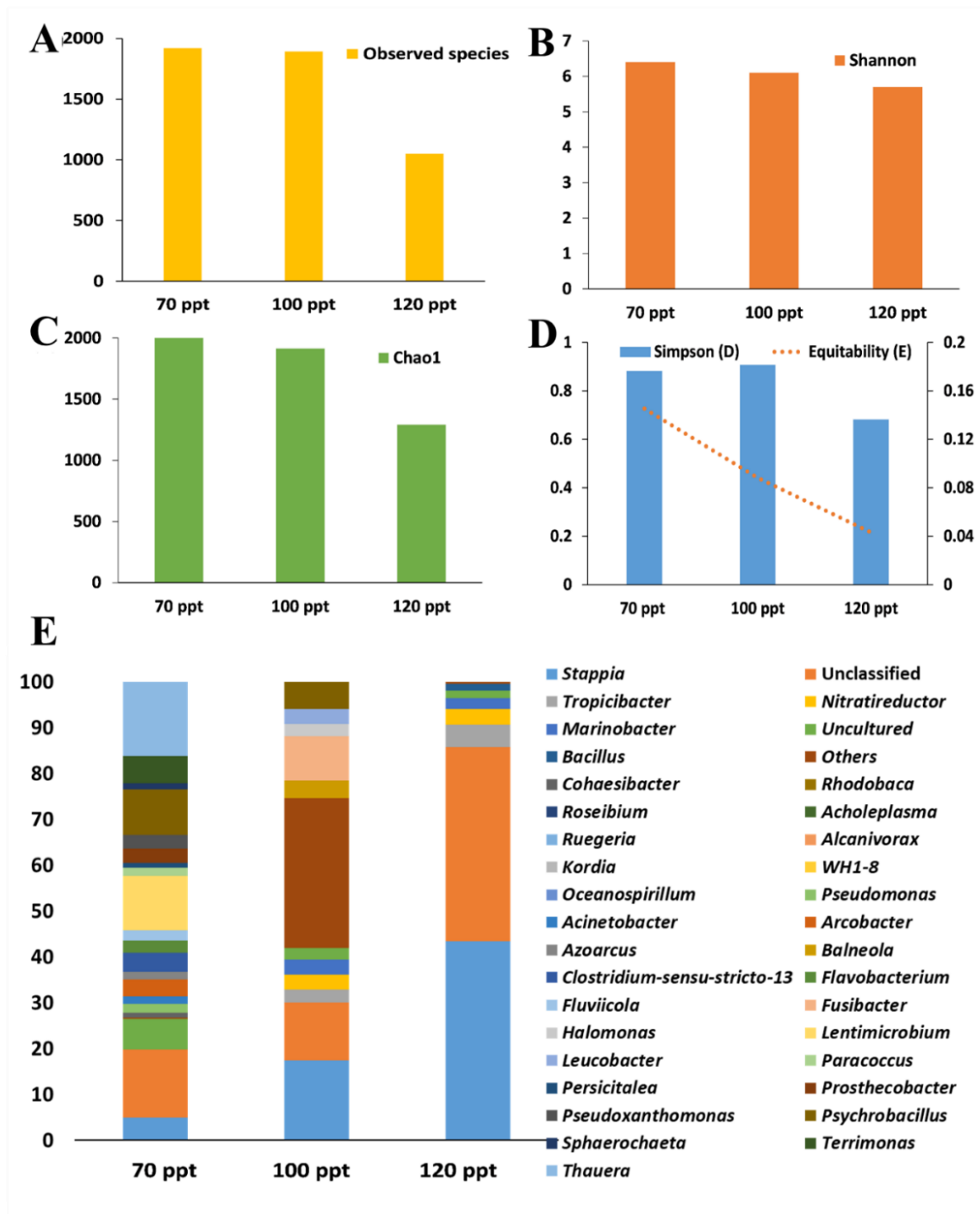


Fig. 6.4 Bacterial community of halophilic aerobic granular sludge treating hypersaline seawater-based wastewater based on 16S rRNA sequencing using HiSeq platform. (A): Observed species, (B): Shannon diversity index, (C): Chao1, (D): Simpson, (E): Genus level classification.

6.3.5 Halotolerant versus halophilic granular sludge

Effect of salinity on biological treatment has been evaluated by gradually adapting activated sludge or aerobic granular sludge (freshwater-microbial communities) to increasing NaCl concentrations^{43,118,138,108,114}. The structural and functional properties of these freshwater-microbial communities are vulnerable to salinity because most of the freshwater microbes fail to function under saline conditions¹³². A decrease in the settling properties due to breakdown of aerobic granular sludge was observed¹¹⁸. Several studies reported decreased TN and phosphorus removals at elevated NaCl concentrations^{137,143}. Bassin et al.¹¹⁸ reported complete ammonium removal but poor TN removals due to high nitrite accumulation at 33 g L⁻¹ NaCl. Phosphorus removal by aerobic granular sludge was completely inhibited at 33 g L⁻¹¹¹⁸. Recently, de Graff et al.¹⁴¹ reported improved nitrogen and phosphorus removals under seawater conditions (35 ppt) using seawater-adapted aerobic granular sludge¹⁴¹. It was reasoned that NaCl salinity may not be a correct indicator for assessing seawater salinity on biological nutrient removal. Good phosphorus removals of salt-adapted aerobic granular sludge under seawater conditions were attributed to high Na⁺/K⁺ ratios and the role of K⁺ in the metabolisms of polyphosphate accumulating organisms.

The gradual adaptation process is aimed at selecting and enriching the salt-tolerant microorganisms, a minority in the freshwater-microbial communities, for developing a salt-tolerant microbial community for biological treatment under saline conditions. In contrast, selection and enrichment of halophilic autochthonous microorganisms avoid the osmotic effects of salt ions as these microbes naturally thrive under seawater conditions. This study showed that hAGS developed from autochthonous seawater microorganisms exhibit good nitrogen and phosphorus removals under hypersaline seawater conditions. The Na⁺/K⁺ ratios were in the range of 32.7 to 123.3, at 40 to 120 ppt, respectively, and higher than 25.9 of seawater-based wastewater. Both NaCl and seawater salinities are included in the case of

hypersaline seawater-based wastewater. Nevertheless, the high K^+ and other cations present in the seawater may contribute to the structural and functional stability of hAGS.

6.4 Conclusions

This study demonstrated efficient biological removal of 30 to 90 mg L⁻¹ NH₄⁺-N, 50 to 150 mg L⁻¹ NO₃⁻-N and 11 mg L⁻¹ PO₄³⁻-P under hypersaline seawater conditions at 34 to 120 ppt. The stability and nutrient removal properties of halophilic aerobic granular sludge were not impacted over a wide range of hypersalinities under seawater conditions. Acid soluble EPSs but not alginate like-exopolymer was responsible for maintaining the structural stability of halophilic aerobic granular sludge. Halophilic aerobic granular sludge cultivated from the autochthonous community is promising for achieving biological nitrogen and phosphorus removals during the biological treatment of hypersaline wastewaters

Chapter 7

Major findings and future research directions

Aerobic granular SBRs show promise for the treatment of industrial and domestic wastewater. Microbial granulation was successfully achieved in laboratory scale sequencing batch reactors for nitrogen and phosphorus removal under freshwater and seawater conditions. Based on the research findings, the key outcomes are presented and an elaborate recommendation for the future investigations on fundamental aspect and technological fronts are discussed at the end of this chapter.

7.1 Major findings

Aerobic granular sludge has attracted tremendous research interest and has a potential for developing compact and high-rate process for wastewater treatment and resource recovery. Understanding the mechanism of granulation is important to fully exploit the benefit of this emerging technology. The investigations described in this thesis were carried out to assess the bacterial metabolic processes in relation nitrogen and phosphorus removal and to granulation process in sequencing batch reactors. The main goal of the study was to establish effective and simultaneous nitrogen and phosphorus removal under freshwater and saline conditions while deciphering mechanisms. The results demonstrate the viability of AGS process for effective N and P removal in fresh water (Chapters 2 to 4) and saline to hypersaline seawater conditions (Chapter 5 and 6) under tropical climate conditions.

Aerobic granular sludge (AGS) technology is increasingly considered for wastewater treatment. However, there are concerns on the long-term stability and function of AGS. The COD/N ratio is one of key parameter that can influence stability and ammonium removal. Low COD/N ratios are found in high strength wastewaters like anaerobic digestion liquor, municipal solid waste leachates and industrial effluents. This study evaluated both granular stability as well as ammonium removal at varied COD/N ratios (0.1 to 18) during 440 days of experiment. Granules were stable and exhibited efficient ammonium and total nitrogen removals at 0.03 to 4 kg NH₄⁺-N m⁻³ d⁻¹ and varied COD/N ratios. Interestingly, major

proportion of ammonium was removed under anaerobic conditions without accumulation of either nitrite or nitrate. Enrichment of ammonium oxidising bacteria, anammox and denitrifiers was evident at high ammonium concentrations. Nitrite oxidising bacteria were completely eliminated from the granules. Bacterial community coupled with chemical data revealed operation of nitrification-anammox pathway, particularly when COD/N was below 1. However, removal of high-strength ammonium could be partly explained by the existing nitrogen pathways suggesting novel mechanisms. This work shows that AGS is suitable for treating high-strength ammonium wastewaters.

Reliable cultivation of AGS is important for its successful implementation in wastewater treatment plants. Understanding of granulation and development of newer strategies are desirable for reliable and rapid cultivation of AGS capable of biological nutrient removal. Here, addition of coconut charcoal particles was investigated for improving granulation in SBRs. Formation of granules was observed much faster in the presence of charcoal particles using acetate or acetate-propionate based synthetic wastewater indicating enhancement of granulation rate. Addition of charcoal particles decreased the sludge washout during initial days by increasing the flocculation properties. Importantly, bacterial attachment and growth on charcoal particles resulted in development of particulate biofilms contributing to biomass retention. Enhanced granulation was possible by minimizing biomass washout, forming particulate biofilms and increased inter-particle interactions among charcoal, particle biofilms and aggregates. Interestingly, efficient nitrogen and phosphorus removals were observed in charcoal-augmented SBRs. Ammonium removal was mainly driven by nitrification-denitrification with formation of subtle amounts of nitrate/nitrite. The P removal in the presence of charcoal was about 2-fold higher and mediated by EBPR. It was supported by higher abundance of PAOs in the biomass formed in the presence of charcoal particles. Differential enrichment of PAO clades was

observed in the SBRs fed with either acetate (PAO clade I) or acetate-propionate (PAO clades I and II). Development of granules and its bacterial community for performing efficient N and P removal was shaped up by charcoal particles and carbon substrate.

In order to understand the role of charcoal particles on enhancement of phosphorus removal, the biomass was separated into biofilms and granules. The biofilms showed higher P removal via EBPR pathway than the co-existing granules. This was related to higher abundance of PAOs in the biofilms. The biofilms were either enriched with PAO clade I or PAO clade I and II depending on the feed substrate, acetate or acetate-propionate, respectively. The attachment and biofilm formation by PAOs (present in the activated sludge inoculum) on charcoal particles is likely responsible for their retention, abundance and establishment of EBPR. However, the nutrient (N and P) removals by the developed EBPR biomass was severely impacted at moderate salinities (2 to 10 ppt salt), suggesting requirement of alternative approach for saline wastewaters.

Based on salt content, wastewaters are classified into saline and hypersaline containing at least 10 and 30 g/L NaCl, respectively. Wastewaters with high salt concentrations (>1 g/L NaCl) are generated by use of seawater or brackish water for washing and toilet flushing (Cui et al. 2009), use of seawater and excessive salts in different industrial activities (seafood processing, vegetable pickling, fish canning, oil production, tanning, paper making, pharmaceutical and chemical production), and seawater ingress into groundwater and sewer networks in coastal areas. To achieve biological treatment under saline to hypersaline conditions, formation of aerobic granular sludge directly from halophilic bacteria of seawater was investigated. This is completely a new approach and relies on making use of the microorganisms already thriving in the wastewater without using seed biomass (activated sludge or granules). Proof-of-concept was demonstrated on cultivating aerobic granular sludge directly from the seawater-borne microorganisms

without using seed biomass for achieving nutrient removal under saline conditions. This approach allowed rapid formation of granules from the halophilic bacteria of seawater under saline conditions. Interestingly, N and P removals were rapidly established indicating that the required functional microorganisms are present in the seawater. The granules had less bacterial diversity than the seawater indicating selection and enrichment of certain bacterial groups during granulation and wastewater treatment. Granulation of autochthonous bacteria of seawater is a novel strategy for developing halophilic aerobic granular sludge and to achieve high nitrogen and phosphorous removals under saline conditions. These halophilic granules were found to be suitable for achieving biological nutrient removal under varied salinities (17 to 34 ppt) typical to saline sewage.

Aerobic granules cultivated from halophilic bacteria performed simultaneous COD, nitrogen and phosphorus removal at hypersalinity ranging from 34 ppt to 120 ppt. Ammonium and phosphorus were majorly removed by nitrification-denitrification and EBPR pathways, respectively. The granules had compact microstructure and stable during long-term experiments. The extracellular matrix of halophilic granules was found to be different and dominated by acid soluble exopolymer. Rapid cultivation, stability and efficient nutrient removal capabilities suggest that autochthonous wastewater-microbes can be considered for achieving biological treatment under saline conditions.

7.2 Recommendations for future investigations

This thesis provides fresh new perspectives on cultivation of granules, microbial community assembly, and functional drivers of diversity in complex communities. There are many natural progressions to this work. The recommended investigations on fundamental aspects and technological fronts are summarised below.

- Efficient removal high-strength ammonium by AGS suggests the suitability of AGS to treatment of industrial wastewater. Therefore, future investigations must be performed using real industrial effluents.
- The experimental results on high ammonium removal under low COD/N ratios could partially accommodate on the mechanisms of existing nitrogen pathways. However, stable isotopes of nitrogen can give an insight into operating nitrogen removal pathways and may provide information on novel pathways (if any).
- Addition of charcoal particles proved to be successful in shortening the bioreactor start-up time for granulation and establishment of nitrogen and phosphorus removal in laboratory scale SBRs. The AGS developed in this study are suitable for treating domestic wastewater. Hence, the benefits of charcoal particles addition can be explored in pilot/full-scale wastewater treatment plants.
- This study showed enhanced granulation and enrichment of PAOs in the presence of charcoal particles. Further analysis by 16r RNA gene sequencing and qPCR suggested that abundance of PAOs was higher in the biofilms than co-existing granules. Other techniques including high-throughput sequencing and fluorescence in situ hybridization (FISH) may be used to provide further evidence on differential enrichment of PAOs in co-existing granule subtypes.
- It appears that a novel method granulation without inoculum described in this work is more feasible for rapid granulation and nutrient removal under seawater-based wastewater or saline conditions. The current study successfully proved granulation in laboratory scale reactors. Expanding and up-scaling to pilot/full- scale treatment systems is interesting on the technological aspects. Granulation process was detailed based on the microscopic, chemical analysis and 16S rRNA gene sequencing. Use of omic-tools (genomic, proteomic and transcriptomic) coupled with biochemical analysis may provide

further insight into interactions among different bacteria involved in aggregation, and granulation.

- The results described here showed production of enormous amount of EPS during granulation. The EPS from AGS formed under freshwater conditions was rich in alginate-like exopolymer. Whereas granules cultivated from seawater bacteria under saline conditions was rich in acid-soluble exopolymer. The composition of these biopolymers is not explored. Molecular tools may be applied to characterize the dominant structural polymers in granules formed under saline conditions.

The granular sludge generated during treatment process is currently considered a waste. Also, large part of operational cost of treatment plants is used in sludge handling. Recovery of value-added products from the sludge not only reduces waste volume but partly recovers the operational cost. The potential resources specific to AGS are phosphorus and biopolymer. Recovery techniques may be applied to generate phosphorus rich products for use in agriculture. The biopolymer constitutes nearly 50% of the AGS by dry weight basis. Therefore, biopolymer extraction alone can decrease the content of biosolids significantly. Future research may focus on extraction of valuable resources from waste AGS as part of sludge management.

References

1. Ledezma, P., et al., **2015**. Source-separated urine opens golden opportunities for microbial electrochemical technologies. *Trends in Biotechnology*, 33(4), 214-220.
2. Fowler, A. L., et al., **2015**. Phosphorus digestibility and phytate degradation by yearlings and mature horses. *Journal of Animal Science*, 93(12), 5735-5742.
3. Steffen, W., et al., **2015**. Planetary boundaries: Guiding human development on a changing planet. *Science*, 347(6223).
4. Gruber, N., and Galloway, J. N., **2008**. An Earth-system perspective of the global nitrogen cycle. *Nature*, 451(7176), 293-296.
5. Goldschmidt, V. M., **1937**. The principles of distribution of chemical elements in minerals and rocks. The seventh Hugo Müller Lecture, delivered before the Chemical Society on March 17th, **1937**. *Journal of the Chemical Society (Resumed)*, 655-673.
6. Nancharaiah, Y. V., et al., **2016**. Recent advances in nutrient removal and recovery in biological and bioelectrochemical systems. *Bioresource Technology*, 215, 173-185.
7. Rittmann, B. E., et al., **2011**. Capturing the lost phosphorus. *Chemosphere*, 84(6), 846-853.
8. Fields, S., **2004**. Global nitrogen: Cycling out of control. *Environmental Health Perspective*, 112, A557-A563.
9. Smil, V., **2002**. Nitrogen and food production: proteins for human diets. *AMBIO: A Journal of the Human Environment*, 31(2), 126-131.
10. Pinder, R. W., et al., **2013**. Impacts of human alteration of the nitrogen cycle in the US on radiative forcing. *Biogeochemistry*, 114(1), 25-40.
11. Muller, A., et al., **2017**. Strategies for feeding the world more sustainably with organic agriculture. *Nature Communications*, 8(1), 1-13.
12. Jasinski, S. M., **2021**. USGS phosphate rock statistics and information. (703) 648–7711. <https://www.usgs.gov/centers/nmic/phosphate-rock-statistics-and-information>.
13. Cordell, D., et al., **2009**. The story of phosphorus: Global food security and food for thought. *Global environmental change*, 19(2), 292-305.
14. Coleman, D., **2004**. World population in 2300: A century too far? *World Population to 2300*. UN report, 127-136.
15. Cordell, D., et al., **2011**. Towards global phosphorus security: A systems framework for phosphorus recovery and reuse options. *Chemosphere*, 84(6), 747-758.
16. Vaccari, D. A., **2015**. How do you spot a trend? An examination of recent phosphate rock production. In the special issue on sustainable phosphorus. *Global Environmental Research*, 19, 3-8.
17. Ashley, K., et al., **2011**. A brief history of phosphorus: from the philosopher's stone to nutrient recovery and reuse. *Chemosphere*, 84(6), 737-746.
18. Nedelciu, C. E., et al., **2020**. Global phosphorus supply chain dynamics: Assessing regional impact to 2050. *Global Food Security*, 26, 100426.

19. Cornel, P., and Schaum, C. J. W. S., **2009**. Phosphorus recovery from wastewater: needs, technologies and costs. *Water Science and Technology*, 59(6), 1069-1076.
20. Parsons, S. A., and Smith, J. A., **2008**. Phosphorus removal and recovery from municipal wastewaters. *Elements*, 4(2), 109-112.
21. Kallis, G., and Butler, D., **2001**. The EU water framework directive: measures and implications. *Water policy*, 3(2), 125-142.
22. Scholz, R. W., and Wellmer, F. W., **2015**. Losses and use efficiencies along the phosphorus cycle. Part 1: Dilemmata and losses in the mines and other nodes of the supply chain. *Resources, Conservation and Recycling*, 105, 216-234.
23. Carrera, J., et al., **2003**. Biological nitrogen removal of high strength ammonium industrial wastewater with two-sludge system. *Water Research*, 37, 4211–4221.
24. De Kreuk, M. K., and van Loosdrecht, M. C., **2006**. Formation of aerobic granules with domestic sewage. *Journal of Environmental Engineering*, 132(6), 694-697.
25. Wilfert, P., et al., **2015**. The relevance of phosphorus and iron chemistry to the recovery of phosphorus from wastewater: a review. *Environmental Science and Technology*, 49(16), 9400-9414.
26. Iskander, S. M., et al., **2016**. Resource recovery from landfill leachate using bioelectrochemical systems: opportunities, challenges, and perspectives. *Bioresource Technology*, 201, 347-354.
27. Nancharaiah, Y. V., and Reddy, G. K. K., **2018**. Aerobic granular sludge technology: mechanisms of granulation and biotechnological applications. *Bioresource Technology*, 247, 1128-1143.
28. Henze, M., et al., (Eds.). **2008**. *Biological wastewater treatment*. IWA publishing.
29. Nancharaiah, Y. V., and Sarvajith, M., **2019**. Aerobic granular sludge process: A fast growing biological treatment for sustainable wastewater treatment. *Current Opinion in Environmental Science and Health*, 12, 57-65.
30. Morgenroth, E., et al., **1997**. Aerobic granular sludge in a sequencing batch reactor. *Water Research*, 31(12), 3191-3194.
31. Nancharaiah, Y.V., et al., **2006**. Biodegradation of nitrilotriacetic acid (NTA) and ferric–NTA complex by aerobic microbial granules. *Water Research*, 40, 1539–1546.
32. Nancharaiah, Y. V., et al., **2019**. Aerobic granular sludge: The future of wastewater treatment. *Current Science (India)*, 117(3), 395-404.
33. Bengtsson, S., et al., **2018**. Treatment of municipal wastewater with aerobic granular sludge. *Critical Reviews in Environmental Science and Technology*, 48(2), 119-166.
34. Winkler, M.-K.H et al., **2015**. Influence of partial denitrification and mixotrophic growth of NOB on microbial distribution in aerobic granular sludge. *Environmental Science Technology*. 49, 11003–11010.
35. Winkler, M.-K.H., et al., **2012**. Integration of anammox into the aerobic granular sludge process for main stream wastewater treatment at ambient temperatures. *Water Research*, 46, 136–144.
36. Ren, Y., et al., **2017**. Treatment of old landfill leachate with high ammonium content using aerobic granular sludge. *Journal of Biological Engineering*, 11, 42.
37. Tsuneda, S., et al., **2006**. High-rate nitrification using aerobic granular sludge. *Water Science and Technology*, 53, 147–154.

38. Liu, W., et al., **2019**. Functional and compositional characteristics of nitrifiers reveal the failure of achieving mainstream nitrification under limited oxygen or ammonia conditions. *Bioresource Technology*, 275, 272–279.
39. Wei, D., et al., **2012**. Aerobic granulation and nitrogen removal with the effluent of internal circulation reactor in start-up of a pilot-scale sequencing batch reactor. *Bioprocesses Biosystems Engineering*, 35, 1489–1496.
40. Yu, X., et al., **2014**. Use of aerobic granules for treating synthetic high-strength ammonium wastewaters. *Environmental Technology*. 35, 1785–1790.
41. Wilén, B. M., et al., **2018**. The mechanisms of granulation of activated sludge in wastewater treatment, its optimization, and impact on effluent quality. *Applied Microbiology and Biotechnology*, 102(12), 5005-5020.
42. Lin, H., et al., **2020**. Reviewing bottlenecks in aerobic granular sludge technology: Slow granulation and low granular stability. *Environmental Pollution*, 263, 114638.
43. Pronk, M., et al., **2014**. Evaluating the main and side effects of high salinity on aerobic granular sludge. *Applied Microbiology and Biotechnology*, 98(3), 1339-1348.
44. Figueroa, M., et al., **2008**. Treatment of saline wastewaters in SBR aerobic granular reactors. *Water Science and Technology*, 58(2), 479-485.
45. Taheri, E., et al., **2012**. Treatment of saline wastewater by a sequencing batch reactor with emphasis on aerobic granule formation. *Bioresource Technology*, 111, 21-26.
46. van der Akker, et al., **2015**. Evaluation of granular sludge for secondary treatment of saline municipal sewage. *Journal of Environmental Management*, 157, 139-145.
47. Rockström, J., et al., **2009**. A safe operating space for humanity. *Nature* 461, 472–475.
48. Zhang, F., et al., **2020**. Simultaneous ammonium oxidation denitrifying (SAD) in an innovative three-stage process for energy-efficient mature landfill leachate treatment with external sludge reduction. *Water Research*, 169, 115156.
49. Renou, S., et al., **2008**. Landfill leachate treatment: review and opportunity. *Journal of Hazardous Materials*, 150, 468–493.
50. Wang, Y., et al., **2017**. Time-resolved analysis of a denitrifying bacterial community revealed a core microbiome responsible for the anaerobic degradation of quinoline. *Scientific Reports*, 7 (1), 1–11
51. Xu, J., et al., **2017**. Enhanced bacterial quorum aggregation on a zeolite capping layer for sustainable inhibition of ammonium release from contaminated sediment. *Water Science and Technology*, 76, 3428–3440.
52. Mery-Araya, C., et al., **2019**. Using carbon substrate as a selection pressure to enhance the potential of aerobic granular sludge microbial community for removing contaminants of emerging concern. *Bioresource Technology*, 290, 121705.
53. Zeng, W., et al., **2014**. Population dynamics of nitrifying bacteria for nitrification achieved in Johannesburg (JHB) process treating municipal wastewater. *Bioresource Technology*, 162, 30–37.
54. Corsino, S.F., et al., **2018**. Aerobic granular sludge treating high strength citrus wastewater: analysis of pH and organic loading rate effect on kinetics, performance and stability. *Journal of Environmental Management*, 214, 23–35.
55. Li, A., et al., **2010**. Fate of aerobic bacterial granules with fungal contamination under different organic loading conditions. *Chemosphere*, 78, 500–509.

56. Yuan, Q., et al., **2019**. Strategies to improve aerobic granular sludge stability and nitrogen removal based on feeding mode and substrate. *Journal of Environmental Science*, 84, 144–154.
57. Hellinga, C., et al., **1998**. The SHARON process: An innovative method for nitrogen removal from ammonium-rich wastewater. *Water Science and Technology*, 37, 135–142.
58. Yu, X., et al., **2014**. Use of aerobic granules for treating synthetic high-strength ammonium wastewaters. *Environmental Technology*, 35, 1785–1790.
59. Lochmatter, S., et al., **2014**. Nitrogen removal over nitrite by aeration control in aerobic granular sludge sequencing batch reactors. *International Journal of Environmental Research and Public Health*, 11, 6955–6978.
60. Wang, K., et al., **2017**. Efficient utilization of waste carbon source for advanced nitrogen removal of landfill leachate. *BioMed Research International*. 2017, 2057035.
61. Luo, J., et al., **2014**. Impact of influent COD/ N ratio on disintegration of aerobic granular sludge. *Water Research*, 62, 127–135.
62. Nancharaiyah, Y.V., and Venugopalan, V.P., **2011**. Denitrification of synthetic concentrated nitrate wastes by aerobic granular sludge under anoxic conditions. *Chemosphere*, 85, 683–688.
63. Sarvajith, M., et al., **2018**. Textile dye biodecolourization and ammonium removal over nitrite in aerobic granular sludge sequencing batch reactors. *Journal of Hazardous Materials*, 342, 536-543.
64. APHA, **2005**. *Standard Methods for the Examination of Water and Wastewater*, 20th edition, American Public Health Association, Washington, DC, USA.
65. Sarma, S. J., et al., **2017**. Finding knowledge gaps in aerobic granulation technology. *Trends in Biotechnology*, 35(1), 66-78.
66. McIlroy, S.J., et al., **2014**. ‘*Candidatus* Competibacter’-lineage genomes retrieved from metagenomes reveal functional metabolic diversity. *The ISME Journal*, 8 (3), 613–624.
67. Rubio Rincon, F.J., et al., **2019**. Effect of lactate on the microbial community and process performance of an EBPR system. *Frontiers in Microbiology*, 10, 125.
68. Wang, D., et al., **2017**. Free nitrous acid-based nitrifying sludge treatment in a two-sludge system enhances nutrient removal from low-carbon wastewater. *Bioresource Technology*, 244, 920–928.
69. Bai, Y., et al., **2012**. Abundance of ammonia-oxidizing bacteria and archaea in industrial and domestic wastewater treatment systems. *FEMS Microbiology Ecology*, 80, 323–330.
70. Wagner, J., et al., **2015**. Aerobic granular sludge technology and nitrogen removal for domestic wastewater treatment. *Water Science and Technology*, 71 (7), 1040–1046.
71. Lin, Y.M., et al., **2012**. The contribution of exopolysaccharides induced struvites accumulation to ammonium adsorption in aerobic granular sludge. *Water Research*, 46 (4), 986–992.
72. Anthonisen, A.C., et al., **1976**. Inhibition of nitrification by ammonia and nitrous acid. *Journal of Water Pollution Control Federation*. 835–852.
73. Vadivelu, V.M., et al., **2007**. Free ammonia and free nitrous acid inhibition on the anabolic and catabolic processes of *Nitrosomonas* and *Nitrobacter*. *Water Science and Technology*, 56, 89–97.

74. Gao, S.H., et al., **2015**. The concentration-determined and population-specific antimicrobial effects of free nitrous acid on *Pseudomonas aeruginosa* PAO1. *Applied Microbiology and Biotechnology*, 99, 2305–2312.
75. de Kreuk, M.K., et al., **2005**. Simultaneous COD, nitrogen, and phosphate removal by aerobic granular sludge. *Biotechnology and Bioengineering*. 90(6), 761-769.
76. Lochmatter, S., and Holliger, C., **2014**. Optimization of operation conditions for the start-up of aerobic granular sludge reactors biologically removing carbon, nitrogen, and phosphorous. *Water Research*, 59, 58-70.
77. Zhang, E., et al., **2008**. Ammonia–nitrogen and orthophosphate removal by immobilized *Scenedesmus* sp. isolated from municipal wastewater for potential use in tertiary treatment. *Bioresource Technology*, 99(9), 3787-3793.
78. Giesen, L.M.M., et al., **2013**. Advancements in the application of aerobic granular biomass technology for sustainable treatment of wastewater. *Water Practice & Technology*, 8(1), 47-54.
79. Li, A. J., et al., **2011**. Granular activated carbon for aerobic sludge granulation in a bioreactor with a low-strength wastewater influent. *Separation and Purification Technology*, 80(2), 276-283.
80. Liang, X. Y., et al., **2017**. Effects of magnetic nanoparticles on aerobic granulation process. *Bioresource Technology*, 227, 44-49.
81. Rosenberg, M., et al., **1980**. Adherence of bacteria to hydrocarbons: a simple method for measuring cell-surface hydrophobicity. *FEMS Microbiology Letters*, 9 (1), 29-33.
82. Wilén, B. M., et al., **2003**. The influence of key chemical constituents in activated sludge on surface and flocculating properties. *Water Research*, 37(9), 2127-2139.
83. Beun, J. J., et al., **1999**. Aerobic granulation in a sequencing batch reactor. *Water Research*, 33(10), 2283-2290.
84. Felz, S., et al., **2016**. Extraction of structural extracellular polymeric substances from aerobic granular sludge. *Journal of Visualised Experiments*, (115), e54534.
85. Garrity, J., et al., **2007**. N-lysine propionylation controls the activity of propionyl-CoA synthetase. *Journal of Biological Chemistry*, 282(41), 30239-30245.
86. Horswill, A. R., and Escalante-Semerena, J. C., **2002**. Characterization of the propionyl-CoA synthetase (*PrpE*) enzyme of *Salmonella enterica*: residue Lys592 is required for propionyl-AMP synthesis. *Biochemistry*, 41(7), 2379-2387.
87. Liu, Z., et al., **2014**. Study on the process of aerobic granule sludge rapid formation by using the poly aluminium chloride (PAC). *Chemical Engineering Journal*, 250, 319-325.
88. Zhou, J. H., et al., **2015**. Granular activated carbon as nucleating agent for aerobic sludge granulation: Effect of GAC size on velocity field differences (GAC *versus* flocs) and aggregation behavior. *Bioresource Technology*, 198, 358-363.
89. Wang, X. H., et al., **2012**. Enhanced aerobic nitrifying granulation by static magnetic field. *Bioresource Technology*, 110, 105-110.
90. Brodowski, S., et al., **2006**. Aggregate-occluded black carbon in soil. *European Journal of Soil Science*, 57, 539–546.
91. Fan, X. Y., et al., **2018**. Shifts in bacterial community composition and abundance of nitrifiers during aerobic granulation in two nitrifying sequencing batch reactors. *Bioresource Technology*, 251, 99-107.

92. Tao, J., et al., **2017**. Effect of granular activated carbon on the aerobic granulation of sludge and its mechanism. *Bioresource Technology*, 236, 60-67.
93. Wan, C., **2015**. Formation of bacterial aerobic granules: role of propionate. *Bioresource Technology*, 197, 489-494.
94. Lin, Y. M., et al., **2013**. The chemical and mechanical differences between alginate-like exopolysaccharides isolated from aerobic flocculent sludge and aerobic granular sludge. *Water Research*, 47(1), 57-65.
95. Herbert, R. A., **1999**. Nitrogen cycling in coastal marine ecosystems. *FEMS Microbiology Reviews*, 23(5), 563-590.
96. Chon, K., et al., **2011**. Abundance of denitrifying genes coding for nitrate (*narG*), nitrite (*nirS*), and nitrous oxide (*nosZ*) reductases in estuarine versus wastewater effluent-fed constructed wetlands. *Ecological Engineering*, 37(1), 64-69.
97. Henriot, O., **2016**. Improving phosphorus removal in aerobic granular sludge processes through selective microbial management. *Bioresource Technology*, 211, 298-306.
98. Schuler, A. J., and Jenkins, D., **2003**. Enhanced biological phosphorus removal from wastewater by biomass with different phosphorus contents, part I: experimental results and comparison with metabolic models. *Water Environment Research*, 75(6), 485-498.
99. Flowers, J. J., et al., **2009**. Denitrification capabilities of two biological phosphorus removal sludge dominated by different '*Candidatus Accumulibacter*' clades. *Environmental Microbiology Reports*, 1(6), 583-588.
100. Welles, L., et al., **2016**. Prevalence of '*Candidatus Accumulibacter phosphatis*' type II under phosphate limiting conditions. *AMB Express*, 6(1), 1-12.
101. Smolders, G. J. F., et al., **1994**. Stoichiometric model of the aerobic metabolism of the biological phosphorus removal process. *Biotechnology and Bioengineering*, 44(7), 837-848.
102. Seviour, R. J., et al., **2008**. Ecophysiology of the Actinobacteria in activated sludge systems. *Antonie Van Leeuwenhoek*, 94(1), 21-33.
103. Kim, H., et al., **2019**. Method development for the quantitative determination of short chain fatty acids in microbial samples by solid phase extraction and gas chromatography with flame ionization detection. *Journal of Analytical Science and Technology*, 10(1), 1-6.
104. Barr, J. J., **2010**. Granule formation mechanisms within an aerobic wastewater system for phosphorus removal. *Applied and Environmental Microbiology*, 76(22), 7588-7597.
105. Winkler, M. K., et al., **2011**. Selective sludge removal in a segregated aerobic granular biomass system as a strategy to control PAO-GAO competition at high temperatures. *Water Research*, 45(11), 3291-3299.
106. Mino, T., et al., **1987**. Effect of phosphorus accumulation on acetate metabolism in the biological phosphorus removal process. In *Biological phosphate removal from wastewaters* (pp. 27-38). Pergamon.
107. Acevedo, B., et al., **2012**. Metabolic shift of polyphosphate-accumulating organisms with different levels of polyphosphate storage. *Water Research*, 46(6), 1889-1900.
108. Welles, L., et al., **2015**. Impact of salinity on the aerobic metabolism of phosphate-accumulating organisms. *Applied Microbiology and Biotechnology*, 99, 3659-3672.

109. Zeng, R. J., et al., **2003**. Model-based analysis of anaerobic acetate uptake by a mixed culture of polyphosphate-accumulating and glycogen-accumulating organisms. *Biotechnology and Bioengineering*, 83(3), 293-302.
110. Yuan, Z., **2021**. Combined enhanced biological phosphorus removal (EBPR) and nitrite accumulation for treating high-strength wastewater. *bioRxiv*.
111. Wang, H. G., et al., **2019**. Investigation on polyphosphate accumulation in the sulfur transformation-centric EBPR (SEBPR) process for treatment of high-temperature saline wastewater. *Water Research*, 167, 115138.
112. Carvalho, G., et al., **2007**. Denitrifying phosphorus removal: linking the process performance with the microbial community structure. *Water Research*, 41(19), 4383-4396.
113. Slater, F. R., et al., **2010**. Monitoring associations between clade-level variations, overall community structure and ecosystem function in enhanced biological phosphorus removal (EBPR) systems using terminal-restriction fragment length polymorphism (T-RFLP). *Water Research*, 44(17), 4908-4923.
114. Welles, L., et al., **2014**. Impact of salinity on the anaerobic metabolism of phosphate-accumulating organisms (PAO) and glycogen-accumulating organisms (GAO). *Applied Microbiology and Biotechnology*, 98 (12), 7609-7622.
115. Lopez, C., et al., **2006**. Endogenous processes during long-term starvation in activated sludge performing enhanced biological phosphorus removal. *Water Research*, 40(8), 1519-1530.
116. Lopez-Vazquez, C. M., et al., **2007**. Short-term temperature effects on the anaerobic metabolism of glycogen accumulating organisms. *Biotechnology and Bioengineering*, 97(3), 483-495.
117. Wan, C., et al., **2014**. Partial nitrification of wastewaters with high NaCl concentrations by aerobic granules in continuous-flow reactor. *Bioresource Technology*, 152, 1-6.
118. Bassin, J. P., et al., **2011**. Effect of elevated salt concentrations on the aerobic granular sludge process: linking microbial activity with microbial community structure. *Applied and Environmental Microbiology*. 77(22), 7942-7953.
119. Huang, W., et al., **2015**. Species and distribution of inorganic and organic phosphorus in enhanced phosphorus removal aerobic granular sludge. *Bioresource Technology*, 193, 549-552.
120. Corsino, S. F., et al., **2016**. Simultaneous nitrification-denitrification for the treatment of high-strength nitrogen in hypersaline wastewater by aerobic granular sludge. *Water Research*, 88, 329-336.
121. Corsino, S. F., et al., **2018**. A comprehensive comparison between halophilic granular and flocculent sludge in withstanding short and long-term salinity fluctuations. *Journal of Water Process Engineering*, 22, 265-275.
122. Li, X., et al., **2017**. Seawater-based wastewater accelerates development of aerobic granular sludge: a laboratory proof-of-concept. *Water Research*, 115, 210-219.
123. Wang, Z., et al., **2017**. Gradual adaptation to salt and dissolved oxygen: strategies to minimize adverse effect of salinity on aerobic granular sludge. *Water Research*, 124, 702-712.

124. Wang, Z., et al., **2015**. Effects of salinity on performance, extracellular polymeric substances and microbial community of an aerobic granular sequencing batch reactor. *Separation and Purification Technology*, 144, 223-231.
125. Wang, Z., et al., **2018**. Effect of salt on the metabolism of ‘*Candidatus Accumulibacter*’ Clade I and II. *Frontiers in Microbiology*, 9: 479.
126. Comte, J., et al., **2014**. Can marine bacteria be recruited from freshwater sources and the air? *The ISME Journal*, 8(12), 2423-2430.
127. Li, Z. H., and Wang, X. C., **2008**. Effects of salinity on the morphological characteristics of aerobic granules. *Water Science and Technology*, 58(12), 2421-2426.
128. Capodici, M., et al., **2018**. Shortcut nitrification-denitrification by means of autochthonous halophilic biomass in an SBR treating fish-canning wastewater. *Journal of Environmental Management*, 208, 142-148.
129. Corsino, S. F., et al., **2019**. Comparison between kinetics of autochthonous marine bacteria in activated sludge and granular sludge systems at different salinity and SRTs. *Water Research*, 148, 425-437.
130. Huang, J. L., et al., **2019**. Granulation of halophilic sludge inoculated with estuarine sediments for saline wastewater treatment. *Science of Total Environment*, 682, 532-540.
131. Thwaites, B. J., et al., **2018**. Ecology and performance of aerobic granular sludge treating high-saline municipal wastewater. *Water Science and Technology*, 77(4), 1107-1114.
132. He, H., et al., **2017**. Influence of salinity on microorganisms in activated sludge process: a review. *International Biodeterioration and Biodegradation*, 119, 520-527.
133. Cui, Y., et al., **2009**. Effects of salt on microbial populations and treatment performance in purifying saline sewage using the MUCT process. *Clean-Soil Air Water*, 37 (8), 649-656.
134. Chowdhury, P., et al., **2010**. Biological treatment processes for fish processing wastewater—A review. *Bioresource Technology*, 101(2), 439-449.
135. Díaz, P. A., et al., **2019**. Impacts of harmful algal blooms on the aquaculture industry: Chile as a case study. *Perspective Phycology*, 6 (1–2).
136. Hülsen, T., et al., **2019**. Saline wastewater treatment with purple phototrophic bacteria. *Water Research*, 160, 259-267
137. He, Q., et al., **2020a**. Robustness of an aerobic granular sludge sequencing batch reactor for low strength and salinity wastewater treatment at ambient to winter temperatures. *Journal of Hazardous Materials*, 384, 121454.
138. Uygur, A., and Kargı, F., **2004**. Salt inhibition on biological nutrient removal from saline wastewater in a sequencing batch reactor. *Enzyme and Microbial Technology*, 34 (3-4), 313-318.
139. Campo, R., et al., **2018**. The role of extracellular polymeric substances on aerobic granulation with stepwise increase of salinity. *Separation and Purification Technology*, 195, 12-20.
140. Zhang, L., et al., **2019**. Effects of K⁺ salinity on the sludge activity and the microbial community structure of an A2O process. *Chemosphere*, 235, 805-813.
141. de Graaff, D. R., et al., **2020**. Biological phosphorus removal in seawater-adapted aerobic granular sludge. *Water Research*, 172, 115531.

- 142.** Pronk, M., et al., **2017**. The acid soluble extracellular polymeric substance of aerobic granular sludge dominated by *Deffluviococcus* sp. *Water Research*, 122, 148-158.
- 143.** He, Q., et al., **2020b**. Elevated salinity deteriorated enhanced biological phosphorus removal in an aerobic granular sludge sequencing batch reactor performing simultaneous nitrification, denitrification and phosphorus removal. *Journal of Hazardous Materials*, 390, 121782.
- 144.** Ge, C. H., et al., **2019**. Nitritation-anammox process - a realizable and satisfactory way to remove nitrogen from high saline wastewater. *Bioresource Technology*, 275, 86-93.
- 145.** Bunce, J. T., et al., **2018**. A review of phosphorus removal technologies and their applicability to small-scale domestic wastewater treatment systems. *Frontiers in Environmental Science*, 6, 8.
- 146.** Long, B., et al., **2019**. Stability of aerobic granular sludge in a pilot scale sequencing batch reactor enhanced by granular particle size control. *Chemosphere*, 225, 460-469.
- 147.** Meng, F., et al., **2019**. Enhanced amount and quality of alginate-like exopolysaccharides in aerobic granular sludge for the treatment of salty wastewater. *BioResources*, 14(1), 139-165.

Epilogue

Appendix I

Table A 1. List of qPCR primers and condition details targeting genes involved in nitrogen metabolism used in this study

Target	Gene	Primer	Sequence (5'- 3')	Amplicon (bp)	Primer (nM)	qPCR efficiency (%)
Total eubacteria ^{A1}	16S	1055f 1392r	ATGGCTGTCGTCAGCT ACGGGCGGTGTGTAC	357	600	96±3.5
Anammox ^{A2}	<i>amx</i>	Amx694f Amx960r	GGGGAGAGTGGAACCTTCGG GCTCGCACAAAGCGGTGGAGC	300	300	95±8.5
AOB ^{A2}	<i>amoA</i>	amoA-1f amoA-2r	GGGGTTTCTACTGGTGGT CCCCTCKGSAAAGCCTTCTTC	490	300	93±5.2
Nitrobacter ^{A3}	16S	FGPS872f FGPS 1269r	TTTTTTGAGATTTGCTAG CTAAAACTCAAAGGAATTGA	388	400	95±6.2
Denitrification ^{A4}	<i>narG</i>	1960m2f 2050m2r	TA(CT)GT(GC)GGGCAGGA(AG)AAACTG CGTAGAAGSAGCTGGTGCTGTT	110	500	100±5
Denitrification ^{A5}	<i>nirS</i>	nirS1f nirS1r	CCTA(C/T)TGGCCGCC(A/G)CA(A/G)T CGTTGAACTT(A/G)CCGGT	164	500	98±5.6
Denitrification ^{A5}	<i>cnorB</i>	cnorB2f cnorB6r	GACAAGNNNTACTGGTGGT GAANCCCCANACNCCNGC	389	500	99±5.6
Denitrification ^{A6}	<i>qnorB</i>	qnorB2f qnorB2r	GGNCAYCARGGNAYGA ACCCANAGRTGNCANACCCACCA	262	500	103±2.3
Denitrification ^{A7}	<i>nosZ</i>	nosZf nosZr	AGAACGACCAGCTGATCGACA TCCATGGTGACGCCGTGGTTG	380	500	108±5.6
Nitrospira ^{A6}	16S	NSR 1113f NSR 1264r	CCTGCTTTTCAGTTGCTACCG CCTGCTTTTCAGTTGCTACCG	151	300	112±7.2

Table A 2. List of qPCR primers targeting polyphosphate accumulating organisms (PAOs) and sequences used in this study^{A8}

Clade	Primer (<i>Acc-ppk1</i>)	Sequence (5'- 3')	Amplicon	qPCR conditions		qPCR efficiency (%)
				Primer (nM)	T (°C)	
I-A	947f	TGATGCGCGACAATCTCAAATTCAA	140	400	62.1	112±5.6
	1113r	AATGATCGGATTGAAGCTCTGGTAG				
I-B	372f	TGAAGGCATTCGCTTCCT	282	400	58	98±4.5
	653r	AAGCAGTATTCGCTGTC				
I-C	362f	AGCTGGCGAGTGAAGGCATTCCG	397	350	65.5	103±10
	758r	AACAGGTTGCTGTTGCGCGTGA				
I-D	364f	TGCGACAGCGAATACAG	215	400	58.1	109±3
	848r	ACTTCGAGGCGGACG				
II-E	757f	TTCGTGGACGAGGAAGA	373	400	57.5	115±12
	1129r	ATTGTTCGAGCAACTCGATG				
II-G	410f	CCGAGCAACGCGAATGG	105	400	62	101±8.1
	514r	TGTTGAGTACGCGCGGGA				
II-H	701f	ACTCCTTCGTATTCCTCTCT	228	400	58	105±6.5
	928r	TCATCGCTTCGGAGCA				
II-I	688f	AGTGATTATGCTTTCGTCTTTC	259	400	57	98±7.8
	946r	TGAACTGTCCGAGCAGGA				

Table A 3. qPCR thermal cycle sequence used in the study

Primer	Thermal profile				
	Activation of enzyme	denaturation	annealing	extension	Additional extension
16S 1055f/1392r	95 °C /5 min	95 °C /15 s	53 °C /15 s	72 °C /40 s	72 °C /600 s
amx694f /amx960r	95 °C /3 min	95 °C /60 s	60 °C /15 s	72 °C /60 s	-do-
amoA-1f/ amoA-2r	94 °C /10 min	65 °C /30 s	50 °C /60 s	72 °C /420 s	-do-
FGPS872f/FGPS1269r	95 °C /5 min	95 °C /30 s	65 °C /30 s	72 °C /900 s	-do-
nar1960m2f/ nar2050m2r	-do-	95 °C /15 s	58 °C /15 s	72 °C /60 s	-do-
nirS1f /nirS6r	-do-	-do-	53 °C/15 s	-do-	-do-
cnorB2f/cnorB2r	-do-	-do-	-do-	-do-	-do-
qnorB2f/qnorB2r	-do-	95 °C /30 s	54 °C /45 s	72 °C /45 s	-do-
nosZf/nosZr	-do-	95 °C /15 s	53 °C /15 s	72 °C /608 s	-do-
NSR 1113f/NSR1264r	-do-	94 °C /30 s	65 °C/30 s	72 °C /90 s	-do-
<i>Acc ppk1</i>	95 °C /30 s	94 °C /5 s	xx*	72 °C /30 s	-do-

40 cycles

*xx- annealing *T* in table 2.

A1 Standard curve preparation

Total nucleic acids were extracted from 0.5 g biomass samples. DNA standards were generated by PCR amplification. The resulting amplicons were purified using PCR purification kit (QIAquick). Subsequently the concentrations were quantified using Nanodrop spectrophotometer (BioTek, Synergy H1). The standards for abundance of target genes was calculated assuming molecular mass of dsDNA (660 Da) and formula. $\text{Abundance} = 6.023 \times 10^{23} \text{ (copies mol}^{-1}\text{)} \times \text{concentration of standard (g mL}^{-1}\text{)} / \text{molecular mass (g mol}^{-1}\text{)}$. A series of dilution ranging from 10^1 to 10^7 target genes mL^{-1} was used to generate standard curve. A proper control including standards, samples, template and no-template controls were amplified in minimum of triplicate using the above primer sets. The relative fold-change values were calculated using amplification efficiencies, as described previously^{A9}.

A2 References

- A1.Harms, G., *et al.*, 2003. Real-time PCR quantification of nitrifying bacteria in a municipal wastewater treatment plant. *Environmental Science and Technology*. 37, 343–351.
- A2.Rotthauwe, J. H., *et al.*, 1997. The ammonia monooxygenase structural gene *amoA* as a functional marker: molecular fine-scale analysis of natural ammonia-oxidizing populations. *Applied Environmental and Microbiology*. 63, 4704– 4712.
- A3.Degrange, V., and Bardin, R., 1995. Detection and counting of *Nitrobacter* populations in soil by PCR. *Applied Environmental and Microbiology*. 61, 2093–2098.
- A4.Bru, D., *et al.*, 2007. Relative abundances of proteobacterial membrane-bound and periplasmic nitrate reductases in selected environments. *Applied Environmental and Microbiology*. 73(18), 5971-5974.
- A5.Braker, G., *et al.*, 1998. Development of PCR primer systems for amplification of nitrite reductase genes (*nirK* and *nirS*) to detect denitrifying bacteria in environmental samples. *Applied Environmental and Microbiology*. 64, 3769–3775.
- A6.Dionisi, H. M., *et al.*, 2002. Quantification of *Nitrosomonas oligotropha*-like ammonia-oxidizing bacteria and *Nitrospira* spp. from full-scale wastewater treatment plants by competitive PCR. *Applied Environmental and Microbiology*. 68(1), 245-253.
- A7.Chon, K., *et al.*, 2011. Abundance of denitrifying genes coding for nitrate (*narG*), nitrite (*nirS*), and nitrous oxide (*nosZ*) reductases in estuarine versus wastewater effluent-fed constructed wetlands. *Ecological Engineering*. 37, 64–69.
- A8.Zhang, A. N., *et al.*, 2016. Development of quantitative real-time PCR assays for different clades of “*Candidatus Accumulibacter*”. *Scientific Reports*. 6(1), 1-7.
- A9.Pfaffl, M. W., 2001. A new mathematical model for relative quantification in real-time RT–PCR. *Nucleic Acids Research*, 29(9), 45-45.

Appendix II

Table A 4. Composition of synthetic saline wastewater used for cultivating granular sludge from seawater microbes. *Nutrients added to seawater.

<i>Chemical</i>	<i>Value* (mg L⁻¹)</i>
Sodium acetate*	517
Ammonia-N*	30
Phosphorus- P*	11
Calcium	359
Magnesium	1189
Sulphur	11.5
Sodium	7455
Potassium	353
Strontium	6
Trace elements mix [#]	1 mL L ⁻¹
<i>Parameter</i>	<i>Value</i>
pH	8.1 ± 0.1
Salinity	34 g L ⁻¹
Turbidity	4.5 ± 0.2 NTU
Colony forming units (CFU)	4x10 ⁶ CFUs mL ⁻¹

[#] Section 2.2.2

Published papers